



Continuous Bedload Transport Measurements and Calibration Purposes using a Hydraulic Lifiable Slot Trap

by
Lukas Karl Strahlhofer

A thesis submitted to
the University of Natural Resources and Life Sciences, Vienna/ Austria
and the Lincoln University, Christchurch/ New Zealand
in partial fulfilment of the requirements for the degree of
Master of Natural Resources Management and Ecological Engineering

Supervisor:

Helmut Habersack
Ao.Univ.Prof. Dipl.-Ing. Dr.nat.techn.

Co-Supervisor:

Graeme Buchan
MSc PhD (Aberd) CPhys MInstP FRMetS FIEnvSc

Advisor:

Hugo Seitz
DI

Vienna, October 2010

Kurzfassung

Das genaue Verständnis von Geschiebetransportprozessen ist eine wesentliche Voraussetzung für nachhaltige wasserbauliche Maßnahmen in Bereichen wie Flussrevitalisierung, Sohlstabilisierung und Hochwasserschutz. Die oft aufwändige, unmittelbare Erfassung von Naturmessdaten ist auch als Basis für die Kalibrierung von Geschiebetransportgleichungen und Modellen von großer Bedeutung. Für das Geschiebemonitoring an der oberen Drau in Dellach im Drautal/Kärnten wird eine Kombination unterschiedlicher direkter und indirekter Geschiebemessmethoden sowie ergänzender Messinstrumente angewandt, um individuelle Unzulänglichkeiten zu kompensieren.

In dieser Arbeit werden die ersten Ergebnisse von direkten Geschiebemessungen an der Drau mittels einer bisher einzigartigen, hydraulisch über die Wasseroberfläche elevierbaren Geschiebefalle behandelt. Der bisherige Einsatz dieser an sich speziell für Spitzenabflüsse konzipierten hydraulischen Hubfalle fand bei verhältnismäßig niedrigen Durchflussraten zwischen 90 und 136 m³/s statt. Die Qualität der Messung konnte durch die Untersuchung der hydraulischen Effizienz der Falle und der Korngrößenverteilung des erfassten Geschiebes gewährleistet werden. Ein Schwerpunkt der weiteren Analyse lag im Vergleich der Gewichtsdaten mit den kontinuierlichen Impulsaufzeichnungen einer der Falle direkt vorgelagerten Geophonanlage. Mit einem Bestimmtheitskoeffizienten von $R^2=0,926$ lieferte die Korrelation der beiden Messmethoden ein äußerst vielversprechendes Ergebnis. Darauf basierende erste Hochrechnungen der jährlichen Geschiebefracht zeigten, dass für diesbezügliche Aussagen unbedingt weitere kombinierte Messungen bei hohen Abflüssen nötig sind. Funktionell hat die hydraulische Hubfalle bisher alle Erwartungen zuverlässig erfüllt. Während erster Wartungsarbeiten zeichnete sie sich dank des hydraulischen Hubsystems zudem durch deutlich einfachere und schnellere Erreichbarkeit und somit auch durch eine Reduktion der regelmäßigen Wartungskosten gegenüber unter Wasser fest installierten Geschiebefallen aus.

Abstract

Detailed understanding of bedload transport processes is considered as a precondition for sustainable hydraulic engineering measures related to river restoration, riverbed fixation and flood protection. For this purpose direct recordings of bedload data are furthermore an indispensable basis for the reliable calibration of bedload transport equations and models.

This thesis deals with the first results of bedload transport measurements at the Drau River using a worldwide unique version of a bedload trap. Adapted to the perennial flow conditions, this new sampler features a hydraulic system for automatic lifting of the trap above the water surface at any time. Besides, its robust construction allows for sampling during high discharges and flood peaks. The hydraulic lift trap is part of the bedload monitoring site Dellach im Drautal, where different direct and indirect measuring methods and additional instruments are combined to compensate individual shortcomings. The underlying first measurement took place at comparatively low discharge rates between 90 and 136 m³ s⁻¹. Subsequent analyses of hydraulic efficiency and grain-size distribution ensured the quality of the results. Particular emphasis of research was given on the weight increase of the trap in comparison with the continuous, indirect bedload recordings of the upstream geophone. The coefficient of determination for the correlation of both datasets already reached $R^2 = 0.926$. In this respect the outcome showed great promise for further evaluations. However, the derived calculation of the annual bedload yield revealed that additional data from floods are needed to increase the required calibration data set. As far as functionality and operation reliability of the hydraulic lift trap are concerned, all expectations were met, so far. Moreover, in contrast to ordinary bedload traps, it turned out that the hydraulic system of the lift trap enables cheaper, faster and easier access for periodic service operations.

Table of Contents

1	Introduction	9
1.1	Human impacts on alpine rivers	9
1.2	Benefits of bedload transport measurements	9
1.3	Legal background	10
1.4	Bedload monitoring in the Drau River.....	11
1.5	Objectives of the thesis	11
2	Project area.....	12
2.1	Drau River.....	12
2.2	Geology.....	14
2.2.1	Geological catchment area of the Isel.....	14
2.2.2	Geological catchment area southward of the Drau	14
3	Theory	17
3.1	Terms and definitions	17
3.2	Morphodynamics of the riverbed.....	18
3.2.1	Abrasion	18
3.2.2	Selective entrainment	19
3.3	Bedload transport.....	19
3.3.1	Initiation of motion.....	20
3.3.2	Bedload transport equations	22
3.3.3	Bedload transport measurements.....	23
3.3.4	Specifications of direct bedload measurement methods.....	24
4	Methods.....	26
4.1	Facilities of the measuring site Dellach im Drautal.....	26
4.2	Description of the measuring system peripherals	28
4.2.1	Water gauge installation	28
4.2.2	Flow velocity measurements	28
4.2.3	Discharge calculation	29
4.2.4	Trailer	29
4.2.5	Sieve shaker	30
4.2.6	Data logging	30
4.2.7	GPS-/Internet timestamp	30
4.3	Description of the bedload measuring methods.....	30
4.3.1	Large Helley-Smith Sampler (LHSS).....	31
4.3.2	Geophone device	32

4.4	Scope of applied measuring devices	33
4.4.1	Discharge-related limitations.....	34
4.4.2	Limitations regarding the grain-size	35
4.4.3	Spatio-temporal limitations	37
4.5	Combined data logging.....	39
5	The hydraulic lift trap	40
5.1	Pit trap systems	40
5.1.1	Early attempts & various developments	40
5.1.2	Slot samplers.....	41
5.2	Planning and design of the hydraulic lift trap	42
5.2.1	Trap dimensioning.....	43
5.2.2	Hydraulic actuator	44
5.2.3	Load cells.....	47
5.2.4	Flow resistance	48
5.2.5	Statics	49
5.2.6	Slot door mechanism	49
5.2.7	Handling of suspended load	50
5.3	Mode of operation.....	51
5.4	Maintenance.....	51
6	Results	53
6.1	Hydraulic efficiency of the lift trap	53
6.2	Sedimentation analysis.....	55
6.3	Data correlation.....	58
6.3.1	Correlation between discharge and weight increase.....	58
6.3.2	Correlation between discharge and geophone impulses	59
6.3.3	Correlation between weight increase and geophone impulses	60
6.4	Calculation of bedload transport yield.....	65
7	Discussion.....	67
7.1	Hydraulic efficiency: comparison with former slot trap.....	67
7.2	Design modifications	68
7.2.1	Slot door	68
7.2.2	Side doors	69
7.2.3	Load cells.....	70
7.3	Texture and grain-size analysis.....	71
7.4	Correlation results.....	73
7.5	Annual bedload yield calculation.....	75

Consideration of expenditures.....	76
8 Conclusions	78

Figures

Figure 1: Location of the project area	12
Figure 2: Geology of the Drau catchment area (University of Innsbruck, 1980)	15
Figure 3: Stress-induced change of transport behaviour.....	17
Figure 4: Hjulström curve	20
Figure 5: Shields diagram for dimensionless critical shear stress (COE 1994).....	22
Figure 6: Draft of the integrated measuring system Dellach im Drautal	27
Figure 7: Principle of the bedload measuring system Dellach im Drautal	28
Figure 8: OTT-radar sensor	29
Figure 9: Determined rating curve in Dellach im Drautal	29
Figure 10: Sieve Shaker	30
Figure 11: Large HS sampler & trailer with mounted cable winch.....	31
Figure 12: Geophone device installation	32
Figure 13: Display of the pulse signal recording.....	33
Figure 14: Application areas of the applied measuring devices	34
Figure 15: Grain-size related limits of the Large Helley-Smith Sampler.....	35
Figure 16: Grain-size related limits of the bedload slot traps.....	36
Figure 17: Grain-size related limits of the geophones.....	36
Figure 18: Spatiotemporal distribution of bedload flux at the cross-section in Dellach im Drautal.....	37
Figure 19: Annual distribution of geophone impulses at the cross-section	37
Figure 20: Location of lift trap in relation to geophone device	39
Figure 21: The hydraulic lift trap before installation.....	43
Figure 22: Longitudinal section of the lift trap (Seitz et al., 2009)	44
Figure 23: Horizontal projection of the lift trap (Seitz et al., 2009)	44
Figure 24: Hydraulic plungers and cylinders	45
Figure 25: Installed hydraulics	45
Figure 26: Manual control.....	45
Figure 27: Underwater video surveillance system.....	45
Figure 28: Diagram of the hydraulic actuator	46
Figure 29: Wheatstone bridge circuit (McGraw-Hill, 2005)	47
Figure 30: AutoCAD drawing of the load cell type SB4.....	48
Figure 31: Close-up view of deployed load cell.....	48
Figure 32: Arrangement of load cells in fixed slot trap.....	48
Figure 33: Roll guides	49

Figure 34: Tilting test.....	49
Figure 35: View of the under-side mechanism of the slot door.....	50
Figure 36: Close-up view of the gap sealing	50
Figure 37: Conduct of sampling procedure	51
Figure 38: Worn out M16 screw nut after one-year operation	52
Figure 39: Removal of sediment accumulations using an airlift pump	52
Figure 40: Measurements performed from a bucket.....	53
Figure 41: Results of the flow measurements in and around the trap.....	54
Figure 42: View through trap side-door.....	55
Figure 43: Documentation of stratification	55
Figure 44: Scheme of the sampled sediment layers.....	56
Figure 45: Scheme of the grain-size distribution within the sample container (armour layer excluded)	57
Figure 46: Total grain-size distribution (30 -31 July 2009).....	58
Figure 47: Cumulative weight increase compared to discharge	59
Figure 48: Sum of geophone impulses per minute compared to discharge	60
Figure 49: Cumulative curve of mass compared to cumulative curve of impulses	60
Figure 50: Course of impulses compared to course of weight increase (moving average of 15 minutes).....	62
Figure 51: Linear correlation at different filling levels (moving average of 15 min).....	63
Figure 52: Linear correlation under exclusion of grain-sizes smaller than 20 mm.....	64
Figure 53: Impulse distribution at the cross-section from July 30 to July 31, 2009 (14 hours)	65
Figure 54: Annual impulse distribution at the cross section Dellach/Drautal in 2008	66
Figure 55: Annual impulse distribution at the cross section in Dellach/Drautal in 2009	66
Figure 56: Changing hydraulic efficiency with filling level (Habersack et al., 2001).....	67
Figure 57: Mechanism of slot cover (Bergman et al., 2007) compared to mechanism of trap door.....	69
Figure 58: Faulty removal of the trap side door.....	70
Figure 59: Acrylic glass window (Kuhnle, 1992)	70
Figure 60: Uniform pressure distribution by scissor cradle (Sear et al., 2000)	71
Figure 61: Disproportional amount of fine grain-sizes displayed in the graph	74
Figure 62: Basket trapping bedload sample (Rickenmann et al., 2010)	75
Figure 63: Relation between discharge and bedload transport (adapted from Kreisler, 2010).....	76
Figure 64: Maintenance operation at hydraulic lift trap (August 2009)	77
Figure 65: Maintenance operation at fixed slot samplers (April 2010)	77

Tables

Table 1: Hydrological data of the measuring site in Dellach im Drautal (Seitz et al., 2009)	13
Table 2: Bedload classification (adapted from Garcia, 2008)	18
Table 3: Abrasion coefficients (adapted from Malcherek, 2009)	19
Table 4: Discussion on integrated measurement techniques (Habersack, 2010)	24
Table 5: Comparison between selected grain-size percentiles in different slot samplers	71

Formulas

Equation 1: Limiting grain-size diameter after Kresser (1964)	17
Equation 2: Abrasion coefficient	18
Equation 3: Critical Shields parameter, Froude number	21
Equation 4: Reynolds number, kinematic viscosity	21
Equation 5: Drag force.....	24
Equation 6: Hydraulic efficiency	25
Equation 7: Sampling efficiency.....	25
Equation 8: Bedload yield for measuring period	64

1 Introduction

1.1 Human impacts on alpine rivers

Until the end of the 19th century most alpine rivers formed braided, aggrading channel systems as a result of their originally enormous supply of sediments. Then the prevalent goals of flood protection and land reclamation for intensified agriculture and new settlement areas led to engineering measures, which were focussing on increased bed shear stress and diminished sediment supply, bank fixations, straightening, meander cut-off and the reduction of channel width (Habersack & Nachtnebel, 1994). Moreover, in the 20th century many alpine valleys became particularly attractive in terms of energy production. In the last decades the utilisation of this naturally occurring potential has ensured a great deal of the Austrian electricity supply, but the construction of numerous hydropower plants also implicated severe interference on the natural regime of rivers in the form of diversions, surge effects and the disruption of the bedload transport continuum. Last but not least, the bedload balance of many streams was often affected by gravel mining in addition to the above-mentioned stresses. Altogether, in the 1990s only 10 % of the river regimes in the alpine region have retained their natural character (Muhar et al., 2008).

In addition to the negative impacts on riverine ecosystems and their associated floodplain wetlands, this array of area-wide severe alterations has also caused the development of more than expected, hard to impede self-dynamics.

A serious problem in this context is the gradual bed degradation in many alpine rivers as a result of bedload deficiency, leading to frequently observed adverse effects such as scouring and erosion of regulative and protective hydraulic constructions (Habersack & Nachtnebel, 1994). In the worst case the gradual degradation even leads to complete intersection of the riverbed, followed by sudden and vast vertical erosion, completely changed flow conditions and declining ground water levels.

Barrages of hydropower stations cause increased aggradations and a surplus of solid particles in reservoirs. Even if the reduction of storage capacity in the alpine region is mostly not alarming so far (Habersack, 1996), possible adverse effects include diminished flood protection, stability problems of barrages and reduced water quality as a result of accumulated heavy metals.

1.2 Benefits of bedload transport measurements

Counteractive engineering measures undertaken after adverse effects have already occurred usually implicate rough and cost-intensive interventions (Habersack, 2009). Bedload transport equations and models provide a basis for well-timed redevelopment measures with regard to the sustainable

improvement of bedload balance and river morphology. But for their reliable calibration it is essential to know the actual situation in river sections concerned, as well as the individual cause-and-effect chain of determined bedload deficiencies.

For these purposes, data from in-situ bedload transport measurements are indispensable. These direct data can improve the understanding of bedload transport processes in terms of quantitative amounts (bedload flux, transport, yield), as well as the spatiotemporal distribution of bedload transport. Thereby it also enables the calibration of indirect measuring techniques. Apart from the use as a calibration standard, in-situ measurements also play an important role in planning and decision-making of different stakeholders involved. In this regard, direct data about bedload transport is the basis for:

- integrative flood protection; including active as well as passive measures
- documentation of flood events
- revitalisation measures
- reservoir management
- monitoring of hydraulic engineering projects

1.3 Legal background

Direct measurements of sediment transport are legally required in consequence of the establishment of the EU Water Framework Directive (2000/60/EC) and its transformation into national Austrian law. The main environmental objectives of the WFD are to

- achieve a good ecological and chemical status of all surface waters and ground waters throughout the EU territory by 2015
- prevent deterioration of the quality status of each water body and to preserve high water quality where it still exists.

Even if the WFD does not specifically deal with sediments, conditions needed to achieve a good ecological status include amongst biological and chemical criteria also hydro-morphological aspects in terms of water balance, structural variation and connectivity and continuity of biota and sediments. Thereby, the implementation of the directive and its incorporation in Austrian law shifted the scope from local sediment management to river basin scale. The EU Floods Directive (2007/60/EC) is another, more anthropocentric directive on river basin management, which also involves sediment measurements. According to Article 6 (5d), Member States thereby shall prepare flood hazard maps and flood risk maps, which include information about areas where floods with a high content of transported sediments can occur.

In 2003, the amendment of the Austrian Federal Water Act (FWA) says in § 59c (3) that the investigation of the water balance including surface waters, ground waters, springs, precipitation,

evaporation and solid particles in waters shall refer to their distribution in terms of amount and duration.

Furthermore, the *Wasserkreislaufferhebungsverordnung 2006 (WKEV)*, a legal order to investigate the water balance in Austria, concretises under § 12 that bedload transport and bedload yield shall be determined at defined measuring sites.

1.4 Bedload monitoring in the Drau River

Quantitative and qualitative recording of bedload transport is essential for planning and decision-making in river engineering. This applies for purposes of river restoration as well as flood protection and is therefore also required by law.

The Institute of Water Management, Hydrology and Hydraulic Engineering at the University of Natural Resources and Life Sciences Vienna (BOKU) started the first bedload transport measurements in the Drau River near Dellach im Drautal in 1994. Thereby, sampling was carried out using a Large Helley-Smith Sampler.

One year later, the Drau was the first large gravel-bed river where a slot trap was installed and deployed under perennial conditions (Habersack et al., 2001).

Since 2006, an integrative bedload monitoring network consisting of the measuring site in Dellach im Drautal/Carinthia and two sampling locations upstream in Lienz/Eastern Tyrol enables the comprehensive recording of bedload transport in the upper Drau River. At the moment each site is equipped with mobile samplers, geophone installations and supplementary measuring instruments. For the purpose of continuous direct bedload measurements, the location in Dellach im Drautal is additionally provided with two fix installed slot traps and one hydraulic liftable slot trap, which was first deployed in 2009. The main idea behind this combined application of different measuring devices is the compensation of individual shortcomings (Habersack et al., 2010).

1.5 Objectives of the thesis

The purposes of this thesis are:

- First data correlation between geophone device and adjacent hydraulic lift trap; two complementary measuring installations in Dellach im Drautal
- Calculation of bedload yields on the basis of data achieved by the lift trap in combination with recordings of the geophones
- Qualitative analysis of the trapped material and textural interpretation
- Analysis of the functionality and applicability of the lift trap

2 Project area

The project area displayed in figure 1 encompasses the catchment areas of the rivers Drau and Isel in Eastern Tyrol and a 68 km long free flowing section of the Drau in Carinthia between the frontier and a hydropower plant in Paternion.

2.1 Drau River

The Drau rises in Puster Valley/Southern Tyrol near Toblach and flows 748 km eastward through Carinthia (212 km), northeast Slovenia and northern Croatia before it discharges into the Danube Stream near Osijek. Altogether, the river drains an area of 41 000 km², the catchment area upstream of Dellach im Drautal encompasses 2131 km². Thereby, 1198.7 km² are allocated to the main tributary, the Isel River. Before it disembogues into the Drau in Lienz/ Eastern Tyrol, the glacier-fed Isel is with a mean discharge of 38.7 m³ s⁻¹ actually the larger of the two rivers. Strongly influenced by its main tributary, the Drau in Dellach im Drautal shows a nivo-glacial regime: During winter, when precipitation is bounded in form of ice and snow, flow rates are very low, whereas in the summer months the largest share of annual rainfall in addition to the glacial melt water entails the maximum discharge (Seitz et al., 2009).

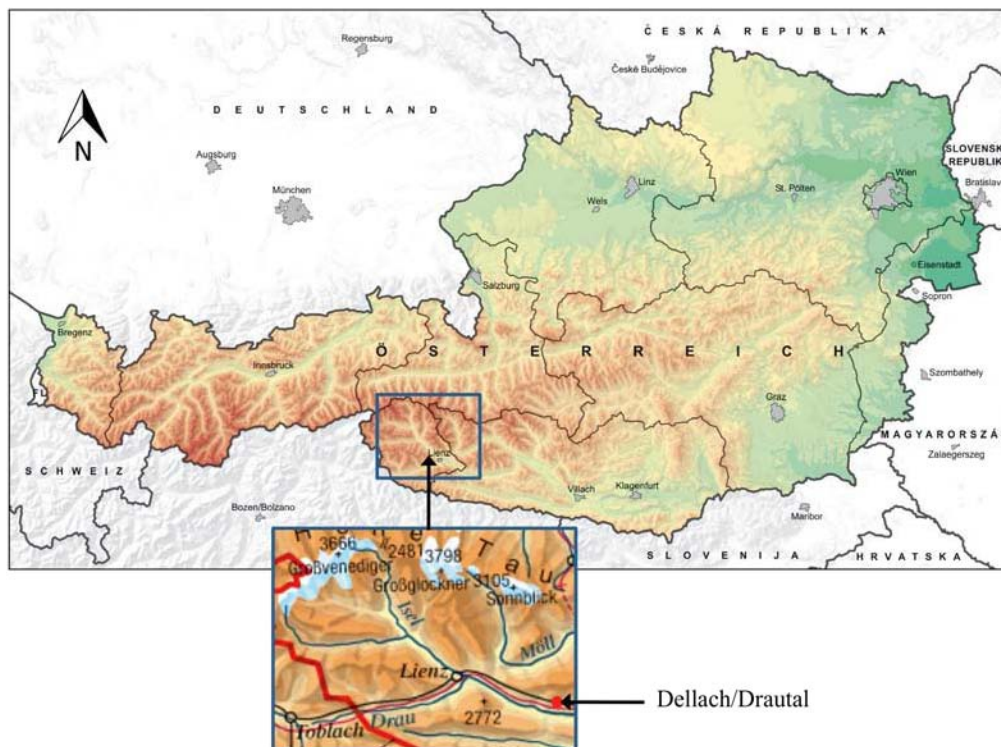


Figure 1: Location of the project area

Table 1: Hydrological data of the measuring site in Dellach im Drautal (Seitz et al., 2009)

Hydrological data of the measuring site in Dellach im Drautal	
River kilometre [km]	202.34
Catchment area [km ²]	2131
Regime	perennial
Slope [m m ⁻¹]	0.0019
Bed width [m]	50
Altitude [m AMSL]	606.04
MQ [m ³ s ⁻¹]	69.2
Q _{max} [m ³ s ⁻¹] / Date (2004 – 2008)	325 / 30.06.2008
Q _{min} [m ³ s ⁻¹] / Date (2004 – 2008)	13.7 / 16.01.2007

One hundred years ago the upper Drau River still formed a free flowing, alluvial river. The annual flood dynamics of the branching river created a landscape characterised by gravel bars, floodplain forests and spacious marsh area. These conditions only allowed for extensive forms of land use. First river training occurred in the context of railway construction around 1868. Subsequent to thereby performed riverbed fixations, the engineering measures in the following years also included bank fixations, straightening and meander cut-off for purposes of flood protection and land reclamation. Dykes were not constructed, however (Pichler, 2003). Consequently, in the nineties of the last century the free flowing section of the Drau encompassed only 27 % of the river length on Austrian territory (Habersack, 1996). The dramatically increased channelization of the river resulted in loss of gravel bars and branches and the abolition of habitats involved. Moreover, an additional problem arose after two once-in-hundred-years flood events in the 1960s: Bedload transport deficiencies as a result of gravel digging, riverbank fixations and torrential barriers at the upper Drau in combination with increased shear stress induced by straightening led to riverbed degradation and declining groundwater tables. Besides, regulative and protective constructions became threatened by erosion (Petutschnig et al. 1991).

Against this background, in the early nineties a river management concept was commissioned to find appropriate measures against the stated problems concerning ecology and flood protection (Michor et al., 1993). First revitalisations occurred in 1991, extensive actions were taken within the frame of the LIFE-project “Upper Drau”, initiated in 1998. Overall target of the project was the revitalisation of riverbanks, including large-scale river widening, planting of floodplain forests and the resettlement of endangered flora and fauna within a Natura 2000 - area of 68 km river-length. Due to the fact that there are only few dykes at the upper Drau and the flood regulation at the

section is mostly built for mean discharge, flood events with a probability of reoccurrence of 5 to 10 years periodically inundate the floodplains (Pichler, 2003).

2.2 Geology

The orogenesis of the Eastern Alps as a part of the young alpidic Mediterranean mountain system was induced by the collision of the Euroasiatic plate with the northward moving African plate during the Cretaceous and the Tertiary. Today, the structure of the range exhibits a distinctive nappe system, which can be subdivided relative to age and rate of metamorphosis in Helvetic Zone, Flysch Zone, Upper Austro-Alpine, Middle Austro-Alpine, Lower Austro-Alpine and the Penninic Zone (Tollmann, 1980).

As shown in figure 2, the upper Drau River separates two dominant geological units: The main tributary in the area, the Isel River rises in the crystalline (gneiss, granite) of the Central Alps in the north, where nappes of the Penninic zone, the Lower and the Middle Austro-Alpine can be found. In contrast, the south of the Drau is dominated by the Southern Limestone Alps and Dolomites, which are part of the Upper Austro-Alpine.

2.2.1 Geological catchment area of the Isel

The drainage basin of the Isel River encompasses the Tauern Window with Matreier Zone, the Schober Range and the Deferegger Mountains.

As the largest geological window in Austria, the Tauern Window enables insight into the deepest tectonic units of the Eastern Alps. Initially, the Austro-Alpine units superposed this Penninic Zone during the Alpidic orogenesis in the late Cretaceous 90 million years ago. During this first metamorphosis, melted granitic mass intruded into the crystalline substratum was transformed into the so-called central gneiss. The second phase of metamorphosis occurred in the Lower Tertiary, when compensating tectonic movements led to bulging and lifting of the Tauern Window (Krainer, 1994). Consequently, the Austroalpine units slid and constitute the frame around the window today (Tollmann, 1980).

The Matrei Zone originates from rocks accumulated in the southern part of the Penninic ocean, which were then affected by further metamorphism during the subduction of the of the Penninic ocean below the Austro-Alpine continental margin (McCann, 2008).

The Schober Range and the Deferegger Mountains, which are mainly formed of micaceous schist, paragneiss and quartz phyllite, belong to the Middle Austro-Alpine (Krenmayr, 1999).

2.2.2 Geological catchment area southward of the Drau

The drainage basin in the south is formed of limestone and dolomite. The Drauzug was separated by tectonic movement from the Limestone Alps north of the Tauern Window and belongs to the

Upper Austro-Alpine unit. The orogenesis occurred by sediment accumulations in the Tethys. Due to the fact that most of the younger sediments from Jurassic to Tertiary are already eroded, carbonates from Trias are prevalent today (McCann, 2008; Krenmayr, 1999).

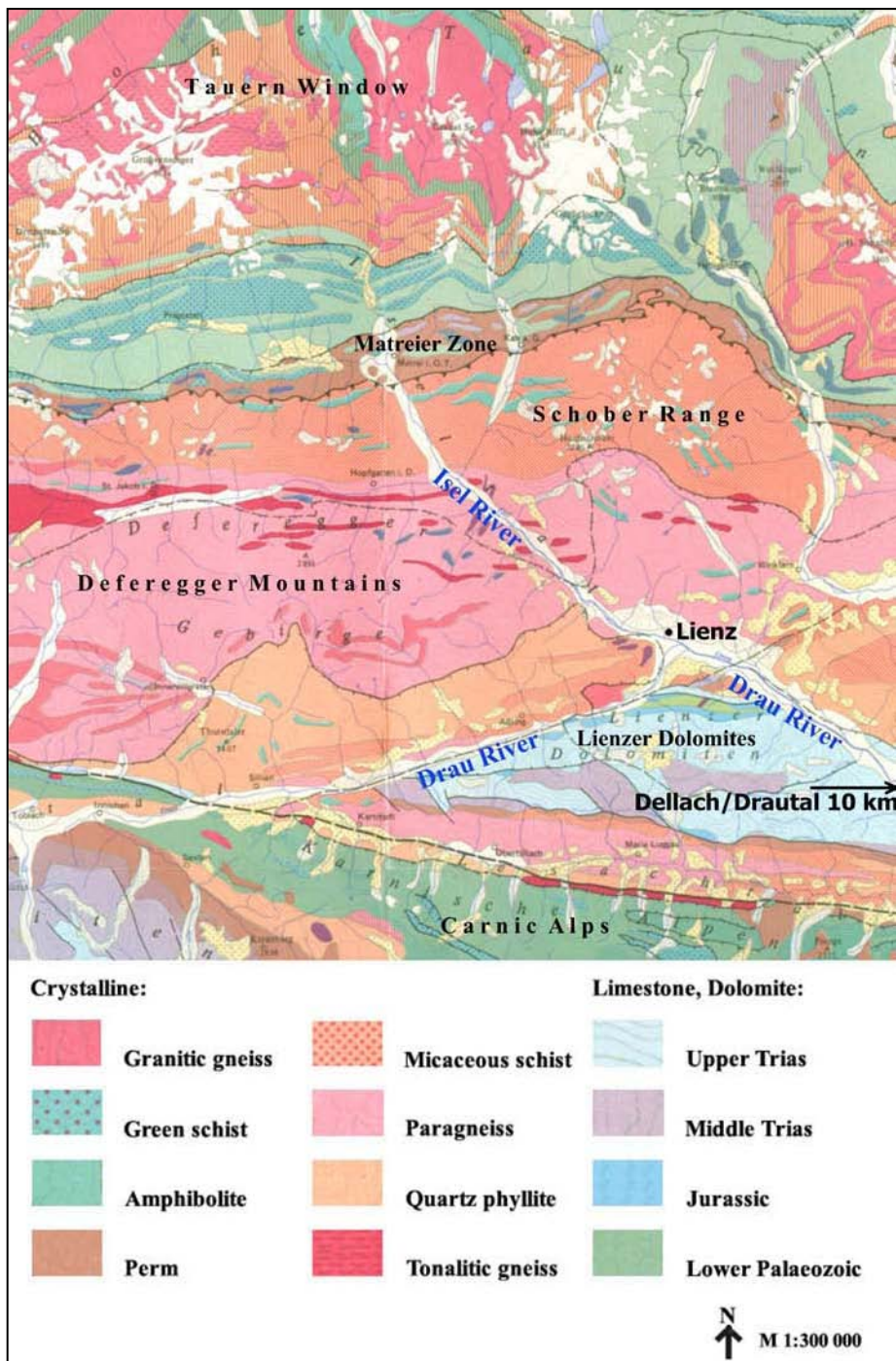


Figure 2: Geology of the Drau catchment area (University of Innsbruck, 1980)

The Drau upstream of Lienz is actually characterised by huge amounts of bedload input from several mountain torrents, but a hydropower plant 25 km west of Lienz reduces the transport capacity downstream of the weir. Nonetheless, a petrographic analysis of bedload performed by Kreisler (2007) in Dellach/Drautal revealed that more than 50 % of the trapped material at the site

is of carbonatic origin from the Limestone Alps. Because there do not exist any nameable torrents between Lienz and Dellach, the carbonatic bedload must come from the river section upstream of Lienz. It seems as if the enormous supply with new bed material in this stretch outweighs the reduced transport capacity (Kreisler, 2007).

3 Theory

3.1 Terms and definitions

The following basic appellations are defined according to the Austrian Standard Institute's ÖNORM B 2400:

- *Solid particles* describe the entirety of bedload, suspended load and floating particles
- *Sediment* describes solid particles, which settle in a standing water body
- *Bedload* means solid particles, which slide, roll or bounce along a streambed
- *Suspended load* describes fine, solid particles, which travel in more or less uniform distribution with stream water
- *Floating particles* encompass all solid particles, which swim at the water surface (e. g. driftwood), excluding ice

The smooth transition between bedload and suspended load is reflected in the flow-dependent change of solid particle movement. When the movement starts, at low stresses the particles roll or slide discontinuously and slower than the stream water, short distanced may also be travelled by saltation. At further increased flow, the movement occurs in several layers (sheet flow) before at high stresses smaller grain-sizes change into suspension (Gao, 2008).

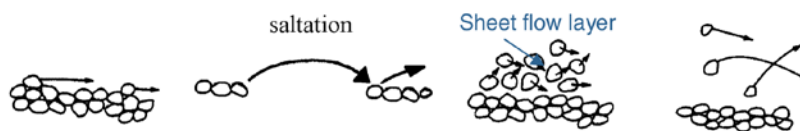


Figure 3: Stress-induced change of transport behaviour

To find a boundary between the solids that are part of the bedload and solids that are transported in suspension, Kresser (1964) defined a limiting diameter d_{gr} [mm] for a particle subject to the average flow velocity v [$m\ s^{-1}$]:

$$d_{gr} = \frac{v^2}{360 * g} \quad (\text{Equation 1})$$

With regard to suspended load, it can be distinguished in detail between floating channel-borne particles and so-called *wash load*, which originates from the floodplain (Habersack, 1997). Bedload is subdivided in different categories depending on the respective grain-size. In this thesis the analysed material was classified according to Garcia (2008):

Table 2: Bedload classification (adapted from Garcia, 2008)

Class Name	Millimetres
Cobbles	256 ~ 64
Very coarse gravel	64 ~ 32
Coarse gravel	32 ~ 16
Medium gravel	16 ~ 8
Fine gravel	8 ~ 4
Very fine gravel	4 ~ 2

From the spatiotemporal point of view, further differentiations can be made in terms of the bedload movement. Accordingly, *bedload flux* describes the transported bedload in kg per unit time at a defined section of a river cross-profile. Whereas the sum of all cross-sectional bedload fluxes shows the *bedload transport* (kg s^{-1}), which, when added up for a specific period, results in the *bedload yield* (kg) (Zanke, 2002).

3.2 Morphodynamics of the riverbed

Generally, in alluvial gravel-bed rivers the bedload grain-sizes tend to decrease in flow direction. Moreover, even if bedload is the dominant factor in riverbed formation, its proportion of the annual solid particle yield in lowland rivers accounts for not more than 10 to 15% (ATV-DVWK, 2000). Two processes can explain this downstream fining of characteristic grain-sizes and the decline in bedload fraction: *abrasion* and *selective entrainment* (Garcia, 2008).

3.2.1 Abrasion

Abrasion by gradual degradation results from the clash of single grains and their contact with the riverbed during fluvial transport (Habersack, 1997). Thereby, the impact energy increases with particle weight, which therefore is proportional to the rate of abrasion. This gradual wear is quantified in terms of an abrasion coefficient α_v , defined as the fractional loss in volume respectively weight per unit distance travelled (Garcia, 2008):

$$\alpha_v = -\frac{1}{V_p} \frac{dV_p}{ds} \quad (\text{Equation 2})$$

where V_p [cm^3] describes the particle volume and s [km] is the distance of travel. The rate of abrasion and size distribution is strongly related to lithological properties of the bedrocks (Kodama, 1994). Malcherek (2009) determined the abrasion coefficients of different rocks via roll testing:

Table 3: Abrasion coefficients (adapted from Malcherek, 2009)

Rock type	Abrasion Coefficient α in km^{-1}
Trias limestone	0.003 – 0.005
Marble (Treuchtlingen)	0.006 – 0.008
Limestone (Flysch)	0.003 – 0.006
Sandstone (Flysch)	0.004 – 0.009
Dolomite	0.003 – 0.012
Quartzite (rough surface)	0.002 – 0.004

3.2.2 Selective entrainment

Selective entrainment results from the fact that finer particles are more susceptible to increased flow conditions than coarse material. Due to the selective non-entrainment and slower transport of coarse grains, perennial streambeds develop a two-layer format, which is sorted according to size and weight. Eventually, a relatively coarse armour layer compacted with interstitial material covers a finer sublayer. The thickness of the armour layer usually equates to the maximum grain-size diameter (Laronne et al., 1994; Habersack, 1997).

3.3 Bedload transport

Apart from deterministic factors including gravity and lift and drag forces on specific particles, many effects on bedload transport are of random nature, such as grain placement and turbulence. According to Habersack (2001), following processes of bedload transport are influenced by stochastic elements:

- initiation of motion
- transport path
- transport rates
- river morphology
- sediment budgets and catchment-wide aspects

Due to the lack of possibilities to make reliable observations of all underlying physics, most assumptions about stochastic processes are only based on laboratory studies and methods of probability theory (Habersack, 2001).

3.3.1 Initiation of motion

The initiation of movement of each single grain is dependent on a variety of factors, such as flow velocity, grain-size and shape (DVWK, 1992). The boundary conditions for this stochastic process can be determined by critical shear stress, critical flow, critical depth and critical slope (Zanke, 2002). Thereby, coarser grains have a higher flow resistance, but they are also more exposed to the flow. In contrast, small particles are more susceptible to the flow, but in return they are often covered and protected by larger ones. The consequence of this so-called *Hiding-effect* is that several grain-size fractions start to move simultaneously. Taking this into consideration, the designation of a standard grain-size in calculations is quite according to natural conditions (Patt et al., 2004). In the following, two basic approaches for determining the initiation of motion are discussed in more detail:

Hjulström (1935) described the relationship between different grain-sizes and mean flow velocities required to entrain, transport and deposit them (see figure 4). The curve with double logarithmic scale shows that generally lower velocities are needed for transport than for erosion of each size-category. Each grain-size is deposited again when the velocity falls below a certain critical minimum level. Furthermore, the run of the upper curve reveals that higher velocities are needed to entrain clay than sand. This is due to intense cohesive forces existing between the particles in the size-range of clay and silt.

Disadvantageous in terms of practicability is that the curve is only tolerable for flow depths between 1 and 5 m and a sediment density of $\rho_s = 2.65 \text{ t m}^{-3}$ (Zanke, 2002). Besides, it only can be applied for loosely packed bed material with uniform grain-size distribution. Consequently, the diagram should not be used for more than a rough estimation of the initiation of motion (Hütte, 2000).

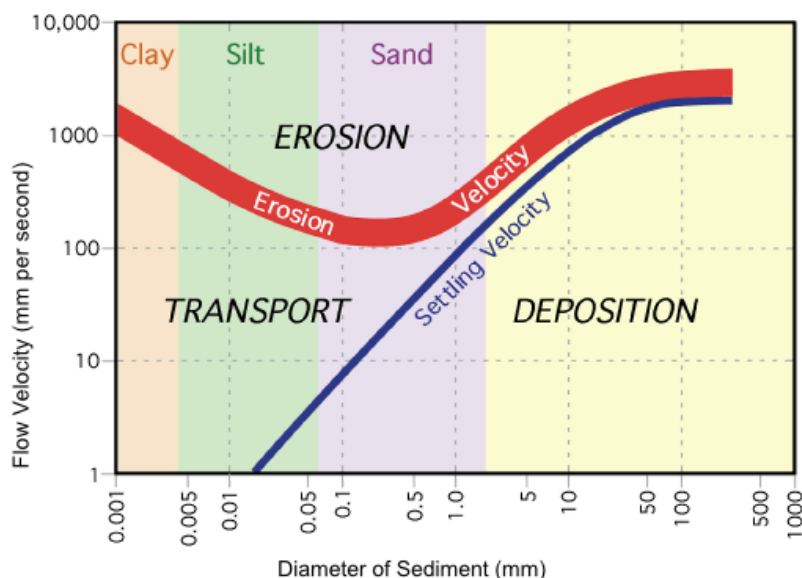


Figure 4: Hjulström curve

In contrast to the Hjulström curve, the *Shields diagram* visualises the initiation of motion under the conditions of variable densities of sediments and fluids at any depth (see figure 5). For this purpose, Shields (1936) formulated the terms of equilibrium between rising shear stress and the respective forces of resistance by the use of a wide range of experimental data. The derived dimensionless critical Shields parameter θ_c , as an alternative often also displayed as the Froude number Fr^* of the grain, describes the critical condition required for incipient motion of sediment (El Kadi Abderrezzak, 2009; Cao et al., 2006):

$$\theta_c = \frac{\tau_c}{(\rho_s - \rho_w)gd} = Fr^* = \frac{u_*^2}{sgd} \quad (\text{Equation 3})$$

With:

τ_c = critical bed shear stress [N m^{-2}]

ρ_s, ρ_w = densities of fluid and sediment, respectively [kg m^{-3}]

g = gravitational acceleration [m s^{-2}]

D = sediment particle diameter [mm]

$s = \rho_s / \rho_w - 1$ = submerged specific weight of sediment

u_* = bed shear velocity [m s^{-1}]

$$u_*^2 = \frac{\tau}{\rho_w} = ghI$$

h = water depth [m]

I = inclination

In the diagram the dimensionless critical Shields parameter on the y-axis is put in relation to the shear Reynolds number R_e^* on the x-axis:

$$R_e^* = \frac{u_* D}{\nu} \quad (\text{Equation 4})$$

where ν describes the kinematic viscosity [$\text{m}^2 \text{s}^{-1}$] of the fluid.

For defined fluid and sediment conditions, it is only possible to find the critical bed shear stress by some sort of trial and error method or iterations, however. In spite of many inconsistencies and misconceptions revealed in terms of the original measurements (Buffington, 1999; Buffington & Montgomery, 1997), as well as significant deviations from reliable and actual measurements (Habersack et al., 2001), the Shields diagram still remains the most commonly applied criterion for initiation of motion, nowadays (Cao et al., 2006).

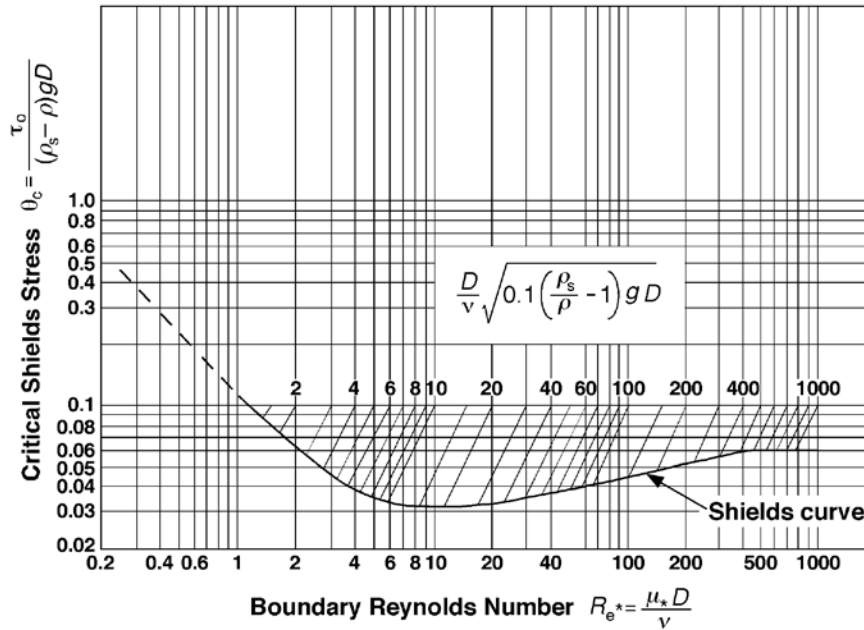


Figure 5: Shields diagram for dimensionless critical shear stress (COE 1994)

3.3.2 Bedload transport equations

In forecasting of bedload transport it can be distinguished between two main approaches (Environmental Protection Agency, 2008):

- Calculation by power
- Calculation by force

Predictions calculated by power act on the assumption of normal discharge and maximum bedload supply. Laboratory conditions for definitions are plane riverbeds without armour and enough bedload supply.

Calculations by force focus on the actual bedload transport in consideration of losses. Therefore, basic data originate from direct measurements in rivers or near to laboratory conditions with shaped riverbed, formation of armour layer and unsteady supply.

This broad differentiation can be sub-classified in further approaches, whose exact number is a matter of opinion, however. While Yang (1996) distinguishes the criteria shear stress, energy slope, discharge, velocity, bed form, probabilistic, stochastic, regression and equal mobility, Graf (1984) mentions only three essential approaches, differing in respect of their main focussing on:

- shear stress (*du Boys*-type equations)
- discharge (*Schoklitsch*-type equations)
- stochastic lift forces (*Einstein*-type equations)

Defined relations between sedimentological and hydraulic parameters for computing sediment transport depend on specific basic conditions in the formulation. The application of any equation

requires enough understanding of its individual constraints and assumptions, as well as sufficient measured data to properly calibrate the model (Environmental Protection Agency, 2008). With regard to the frequently reported significant deviation of calculated results from direct measurements in nature (Habersack et al., 2001), the need for the latter has to be accentuated, in particular. In-situ bedload transport measurements are essential for validation and calibration of existing models and the development of new formulas.

3.3.3 Bedload transport measurements

Nowadays, various methods to measure sediment transport in rivers have already been successfully approved. Presently applied bedload measuring techniques in natural channels can be classified in four groups (e.g. Rickenmann and McArdell, 2007; Turowsky et al, 2008):

- Capture of sediment in a retention basin or calculation of river delta growth
- Tracking and assessment of bedload movement by tracer stones
- Collection of moving particles in the river bed, including temporary methods such as pressure-difference basket samplers (Delft Hydraulics, 2006) and other portable devices (Bunte et al., 2004), but also such continuous measurement methods as slot trap systems (Habersack et al, 2001)
- Measurement of transport intensities using indirect methods, such as the recording of vibrations via geophones

Thereby it is worth mentioning that a particular widespread accepted standard method for monitoring bedload does not exist, so far. The reasons are individual deficiencies of each technique in terms of applicability and costs. For example, the main drawback of tracer stones and mobile bedload samplers is that they usually provide only discontinuous measurements in time and space. Continuous measurement devices such as geophones and slot traps on the other hand are often expensive in construction, operation and maintenance (Habersack et al., 2010). Furthermore, in this context it can also be differentiated by stream type tolerance, ease of use, the disruption of flow fields, flow resistance, or the potential use as calibration standard (Ryan et al, 2005; Bunte et al., 2004; Habersack et al., 2010). However, most of the devices described already have provided useful data in combined arrangement.

Table 4: Discussion on integrated measurement techniques (Habersack et al., 2010)

Method	Flow disturbance	Mobility/flexibility	Sample duration	Hydraulic and sampling efficiency	Grain size determination	Transport path	Auto-mation	Costs
Basket sampler	---	+++ ¹	-- ⁶	--	+++	---	---	-
Trap	+ ⁻¹	--- ⁷	++	+++	++	---	++	--
Radiotracer	+ ⁻⁴	+++	++	+ ⁻	+++	+++	++	-
Geophones	-	---	+++	+ ⁻	---	---	+++	---
Sonar	- ⁵	++ ²	+++	+ ⁻	---	+ ³	+	-

¹ +++	significantly positive. high	⁵ -	slightly negative. low. low costs
² ++	positive. high	⁶ --	negative. low. medium costs
³ +	slightly positive. high	⁷ ---	significantly negative. low. high costs
⁴ + ⁻	neutral. no effect. unknown		

3.3.4 Specifications of direct bedload measurement methods

Direct bedload measuring techniques, such as basket samplers and slot trap systems are not only used to determine bedload yields and transport rates, but they also enable qualitative analyses of the trapped material. To provide reliable data, each method has to meet some basic requirements.

An important criterion in this regard is flow resistance. To allow for sampling also at high discharge rates and to minimise thereby the disruption of natural flow fields, the working area of the measuring device has to be as small as possible. Moreover, in case of permanent installations, a more hydrodynamic shape can avert scouring processes. The drag force F_d , the force component in direction of the flow velocity, is defined as:

$$F_d = \frac{1}{2} \rho v^2 C_w A \quad (\text{Equation 5})$$

where $\rho = 1$ is the mass density of water in g/cm^3 at 4°C , v describes the flow velocity, c_w is the dimensionless drag coefficient and A is the reference area.

Another precondition in terms of reliable sampling results and the use of the measuring system as calibration standard for other measuring devices is sufficient trap efficiency. In general, total trap efficiency is composed of hydraulic efficiency and sampling efficiency. Thereby, a first informative basis about the sampling efficiency can be obtained by knowledge of the hydraulic efficiency α_H , expressed as the ratio of trapped bedload flux to bedload flux in nature.

It is defined as:

$$\alpha_H = 1 - \frac{v_i}{v_o} \quad (\text{Equation 6})$$

with v_i as the mean flow velocity inside the sample container and v_o as mean flow velocity on the riverbed outside the measuring device.

The measurement data required for the calculation of the hydraulic efficiency of the lift trap was collected using a bi-axial electromagnetic E-40 probe combined with a P-EMS control unit (programmable four-quadrant electromagnetic liquid velocity meter; Delft Hydraulics, 2010). By generating an electromagnetic field, the flow velocity measuring is based on Faraday's electromagnetic induction law. The application area of the sensor thereby ranges from 0 – 5 m s⁻¹, with an accuracy of ± 0.01 m s⁻¹ or 1%.

The sampling efficiency α_s is expressed as following ratio:

$$\alpha_s = \frac{m_t}{m_n} \quad (\text{Equation 7})$$

with m_t as the trapped bedload flux and m_n as the bedload flux occurring in nature.

4 Methods

With regard to the above-mentioned measuring technique classification, the gauging station in Dellach im Drautal as part of the integrative measuring system Drau-Isel applies methods of nearly every group described (see figure 6). By combining various sediment measuring devices and other instruments, the aim is to achieve meaningful findings in terms of bedload quality and quantity. Individual shortcomings are compensated by complementary assembly and combined measurements.

4.1 Facilities of the measuring site Dellach im Drautal

In 2010, the measuring system in Dellach consists of the following components:

- geophone installation
- 2 fixed bedload traps with electronic load cells
- hydraulic liftable bedload trap with four electronic load cells
- radar sensor for continuous surface water flow velocity measurements
- turbidity sensor
- temperature sensor
- automated ISCO suspended load sampler
- pressure gauge for continuous water level measurements
- trailer for
 - Large Helley-Smith bedload sampler (LHSS)
 - flow velocity measuring via Ott-current-meter
 - suspended load sampling
- radio clock for time levelling
- Remote transmission of data via GPRS modem

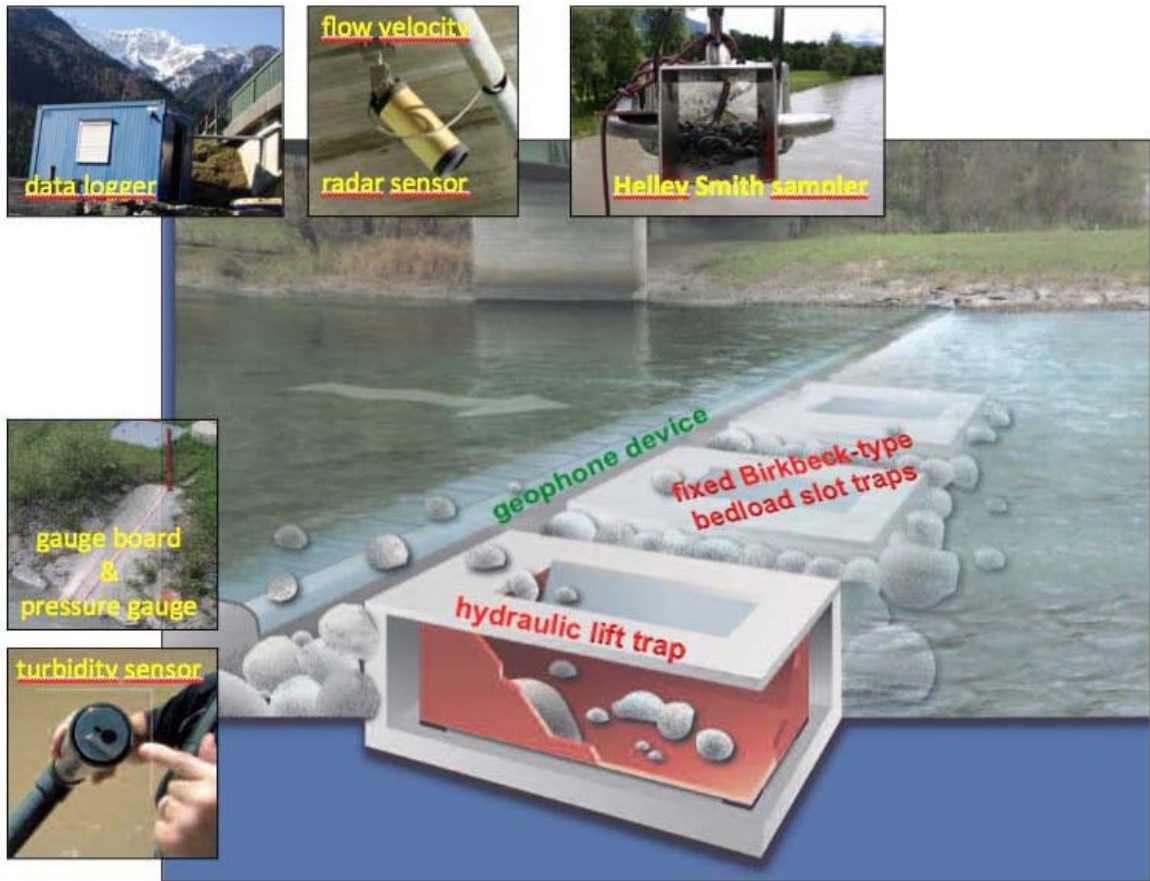


Figure 6: Draft of the integrated measuring system Dellach im Drautal

According to the following figure 7, the system arrangement is composed of three branches:

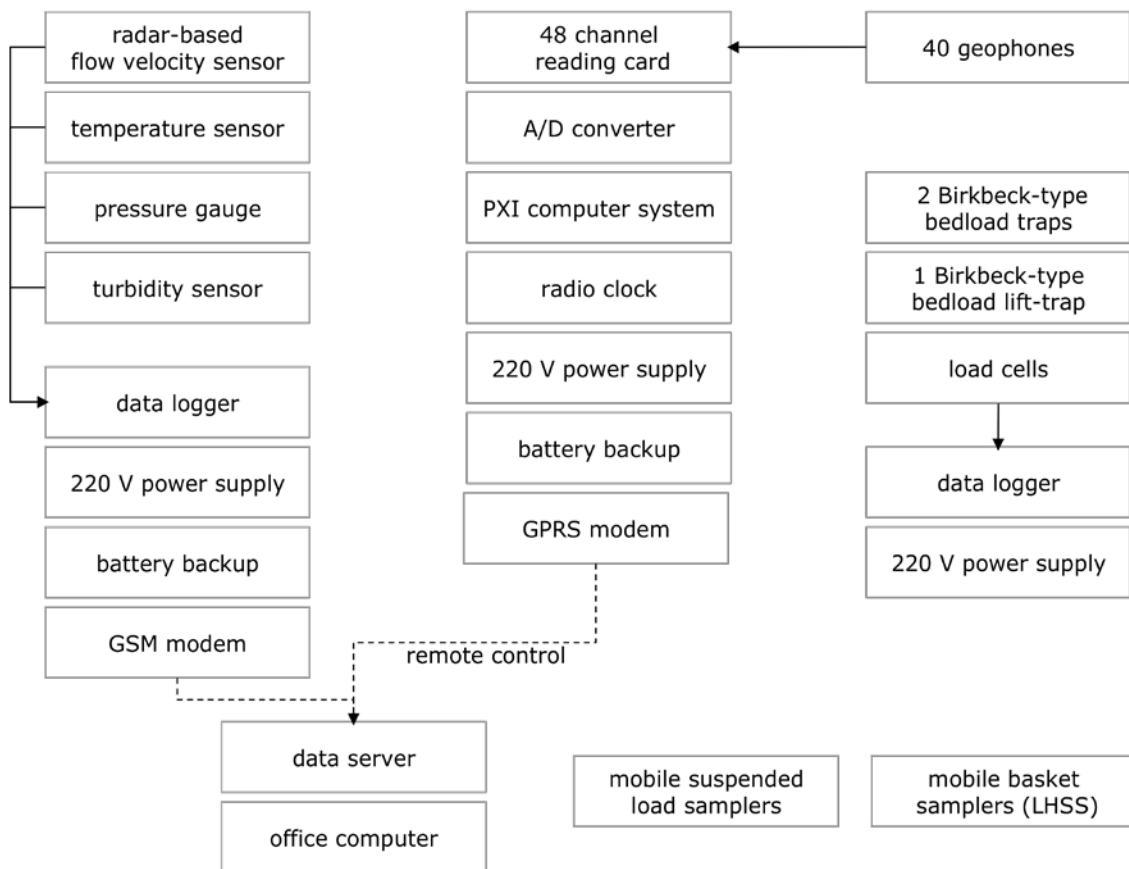


Figure 7: Principle of the bedload measuring system Dellach im Drautal

4.2 Description of the measuring system peripherals

The most important secondary components of the integrated measuring system in Dellach are as follows.

4.2.1 Water gauge installation

The water level trend is recorded fully automated using a pressure sensor of Ott Kempton Inc (Nimbus) and displayed in 15-minute values. The bubble sensor of the pressure gauge (600,04 m AMSL) is installed 14 cm above the lowest level of the measuring system (599,90 m AMSL; constant for two-thirds of the cross-section).

4.2.2 Flow velocity measurements

So far the discharge was calculated in certain positions down from a bridge proximately upstream of the measuring site. For this purpose, an ACM measuring probe (until 2000), an OTT-current-meter and a Delft 2D inductive sensor were deployed. Furthermore, the Hydrographical Service of

Carinthia mounted an OTT-radar sensor beneath the bridge, which allows for continuous flow velocity measurements and discharge calculations, even during flood events (see figure 8).



Figure 8: OTT-radar sensor

4.2.3 Discharge calculation

The long-term flow velocimetries with diverse 1D, 2D and 3D (current-meter, Delft, ADCP) measurement instruments enabled the analysis of the correlation between water level and discharge at the measuring site and the calculation of a rating curve (see figure 9). By fixing the cross-profile with a shallow weir in 2006, the operating expense for any extensions of the rating curve was reduced to complementary flow velocity measurements. Additional measurements would be particularly useful in the events of low flow and flood, where the rating curve has still some deficiencies.

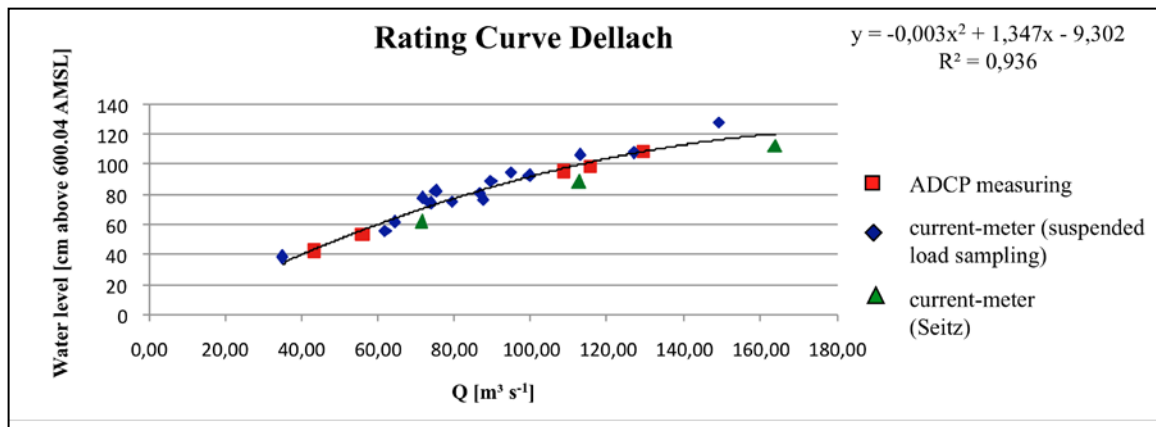


Figure 9: Determined rating curve in Dellach im Drautal

4.2.4 Trailer

A trailer with mounted cable winch ensures the standardised procedure of research operations at the bridge adjacent to the gauging station, such as the analysis of bedload transport via LHSS, suspended load sampling, or flow velocity measurements via current-meter.

4.2.5 Sieve shaker

After sun drying the trapped bedload gets put in a sieve shaker (see figure 10) with sequenced square mesh widths of 150 mm, 125 mm, 90 mm, 63 mm, 56 mm, 31.5 mm, 22.4 mm, 16 mm, 11.2 mm, 8 mm, 4 mm, 2.5 mm, 2 mm and 1 mm. Then the individual sieve fractions get weighed for further data evaluation.



Figure 10: Sieve Shaker

4.2.6 Data logging

The transmission of data occurs via data cable to a PortakabinTM at the riverbank. Equipped with a personal computer with adapted graphical user interface (LabVIEW), this cabin acts not only as data collection centre, but also as a first control station. Moreover, a GSM connection enables real-time monitoring of up-to-date measuring data.

4.2.7 GPS-/Internet timestamp

Previous measurements revealed the internal clocks of single measuring devices as potential weak points of the combined system. Therefore a timestamp for the whole data was installed. Using long wave radio signals from the radio clock in Frankfurt/Germany in combination with a Meinberg-time recording device, the measuring system is updated every second since then.

4.3 Description of the bedload measuring methods

Apart from the hydraulic bedload lift-trap which will be specified in chapter 5, all other applied sampling and measuring devices of the research station Dellach in Drava Valley are briefly described in the following.

4.3.1 Large Helley-Smith Sampler (LHSS)

The Helley-Smith bedload sampler basically consists of a square entrance nozzle, a sample bag made of mesh polyester and an aluminium frame. This most widely used mobile pressure-difference basket sampler with a standard square entrance nozzle of 76.2 x 76.2 mm was principally designed to trap grain sizes between 0.5-16 mm. The main advantages of the HS sampler are the easy handling and its extensive calibration, which is based on about 10.000 samples in a laboratory flume (Emmet, 1980; Delft Hydraulics, 2006). However, experience revealed its calibration factor to be unreliable, particularly in fine-textured riverbeds the device tends towards oversampling (Delft Hydraulics, 2006; Rijn, 2007; Schober, 1999). The surveying precision of the sampler is significantly affected by design and mode of operation, as well as prevailing bedload grain size and bed material (Habersack et al., 2010). Due to different field conditions, there exist several adapted types of the sampler, variable in nozzle width, mesh width and weight.

In accordance with the prevailing coarse gravel bed, the Large Helley-Smith sampler used in Dellach im Drautal has a 152 mm intake and a mesh width of usually 0.5 mm (depends on flow velocity). Regarding its mode of operation, the trailer with mounted cable winch is situated at defined measurement position on the bridge and the LHSS is connected to a suspension cable (see figure 11). While the cable winch lowers the sampler to the streambed, a tether line connected between the sampler and the bridge fixes the position of the LHSS. The line is also used to impede downstream drift of the sampler and scooping of sediments by the entrance nozzle during placement and retrieval. The optimal testing time is defined through the filling level of the sampler determined in a first test measurement.



Figure 11: Large HS sampler & trailer with mounted cable winch

4.3.2 Geophone device

The geophone installations are an indispensable component of the integral bedload measuring system Dellach.

Predominantly used in seismic technology, geophones measure surface vibrations. The measuring device basically consists of a coil suspended by springs in a magnetic field, encased in a steel housing. While any kind of vibration can move the housing, inertia keeps the encased coil stationary. The external movement of the case related to the stationary coil is only in the range of nano-meters. Nevertheless, this motion induces electrical voltage, which is proportional to the velocity of the housing in relation to the coil (Sensor, 2008).

For acting as continuous indirect bedload measuring method, the geophones are screwed at the rear side of stainless steel plates, which cover a waterproof box (see figure 12). After the box in turn is embedded in a concrete trough along the river cross-section, the steel plates are flush with the riverbed. In order to avoid the chain of steel plates getting buried, a site without predicted bedload accumulation should be chosen. An example therefore is the edge of a weir. Every time a bedload grain bounces against one of the steel plates with mounted geophone, the caused vibrations induce electrical voltage. A rubber membrane between the box and the plates thereby avoids the potential cross-transmission of vibrations from adjacent steel plates. When the induced and afterwards amplified electrical voltage exceeds a predefined threshold (see figure 13), a pulse signal is recorded (Habersack et al., 2010; Turowsky et al., 2008). Hence, the number of impulses per unit time can be understood as bedload transport intensity at a certain river cross-section (Rickenmann and McArdell, 2007).

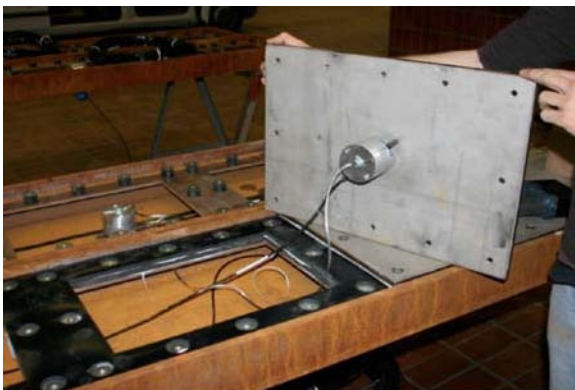


Figure 12: Geophone device installation

The geophone installation in Dellach consists of 40 geophones mounted beneath steel plates of 50 cm length and 36 cm width. For data processing all pulse signals are recorded in cumulative values per minute. To avoid the recording of ambient noise, the response threshold is set to a minimum grain size of 2 cm.

An additional feature is the registration of maximum amplitudes and integrals on magnitudes for calculating the energy input. However, the analysis of this information requires further in situ- and laboratory tests. Future findings of measurements taken with the hydraulic lift trap may play an important role in this regard.

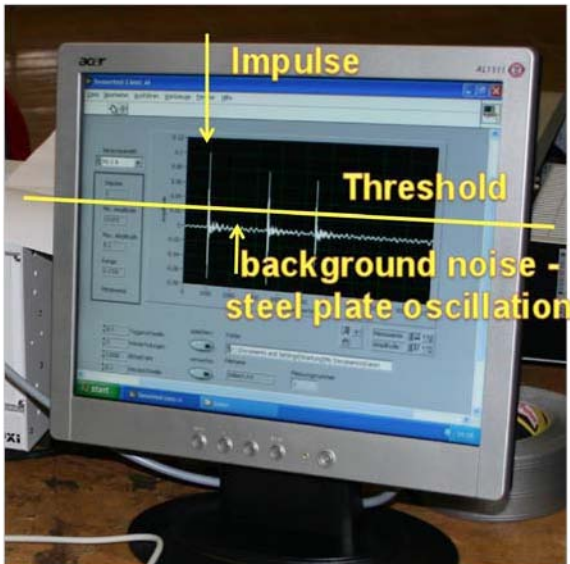


Figure 13: Display of the pulse signal recording

Main advantage of the geophone installation is the continuous spatiotemporal coverage of the entire cross-section. Therefore, the device is very suitable for determining the start of bedload motion, as well. Furthermore, in terms of practical application, its robustness, easy handling and flood resistance can be emphasised (Habersack et al., 2009). Disadvantageous on the other hand are the high costs, the lack of flexibility and the extensive development efforts with regard to programming and calibration measurements involved.

4.4 Scope of applied measuring devices

The main idea behind the integrative measuring system described is the identification of relations between geophone impulses, discharge and actual bedload samples in order to get meaningful conclusions about bedload transport intensities. A precondition therefore is correlation analysis of the used measuring devices. In doing so, it is of course necessary to apply various measuring methods simultaneously, or at least under similar conditions. However, due to individual design limitations, the possible application areas do not always overlap. Correlation hence becomes more complicated. In the following, particular discharge- and grain size-related limitations of the measuring devices applied in Dellach/ Drava Valley are described in more detail.

4.4.1 Discharge-related limitations

While some devices are applicable for the entire hydrograph, other methods only cover a certain range:

- The LHS sampler is used for calibration of the measuring system during average and slightly increased discharge.
- The measurement range of the geophones spans the entire hydrograph.
- In principle, the two fixed slot samplers are applicable for the entire hydrograph. Due to their heavy weight, the possibilities to install and empty them are restricted to low water conditions during winter, however. Their practicability for bedload sampling under perennial flow conditions is therefore limited by the stream flow, too.
- Due to its hydraulic plungers and cylinders, the lift trap enables the year-round sampling of bedload at any discharge.

The different discharge-dependent application areas of the applied measuring devices are displayed in figure 14:

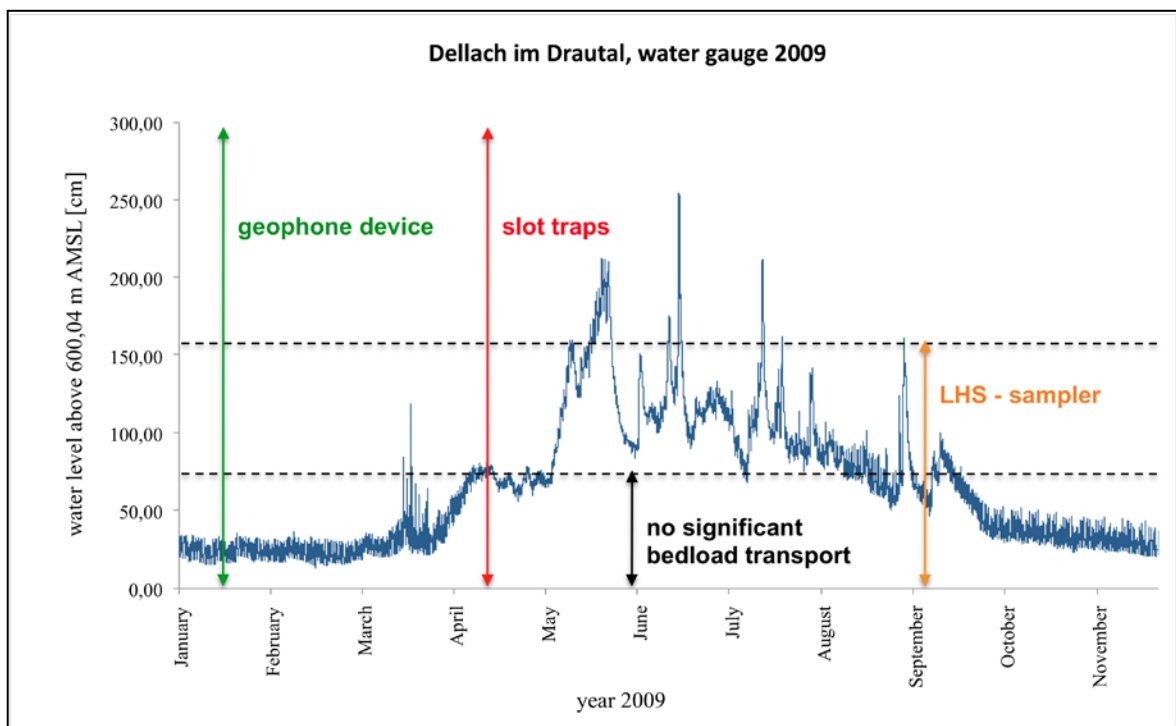


Figure 14: Application areas of the applied measuring devices

4.4.2 Limitations regarding the grain-size

Individual design limitations impede the complete sampling of the occurring grain-size spectrum:

Large Helley-Smith Sampler

The application area of the LHS sampler has clearly defined upper and lower limits in terms of grain-size distribution (see figure 15). The square entrance nozzle of 15.2 x 15.2 cm defines the upper limit, whereas the minimum grain-size sample depends on the polyester mesh width.

Thereby, the in Dellach usually chosen mesh width of 0.5 mm is due to flow velocity; assuming a flow velocity of 2 m/s and a mesh width of 0.5 mm, the pressure difference based LHS sampler behaves neutral to flow fields up to a filling level of 2/3 (Schober, 1999). In this regard the filling level is significant for functionality, too.

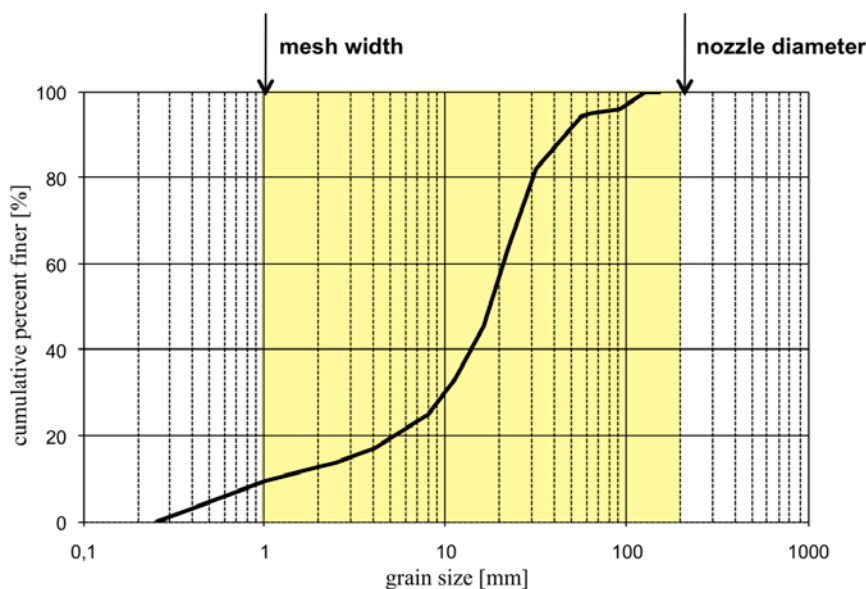


Figure 15: Grain-size related limits of the Large Helley-Smith Sampler

Bedload slot traps

The grain-size related application area of the trap-type systems is mainly defined by their slot diameters. In contrast to the two fixed traps, which are able to sample bedload grain with a b-axis up to 25 cm, the special design of the hydraulic lift trap for operating during flood peaks implicates a larger slot width of 50 cm (see figure 16). At the other end of the scale, the slot traps in principle have no lower grain size limit. With a volumetric capacity of 1.46 m³ the traps have enough space to capture a representative amount of bedload even at high discharges.

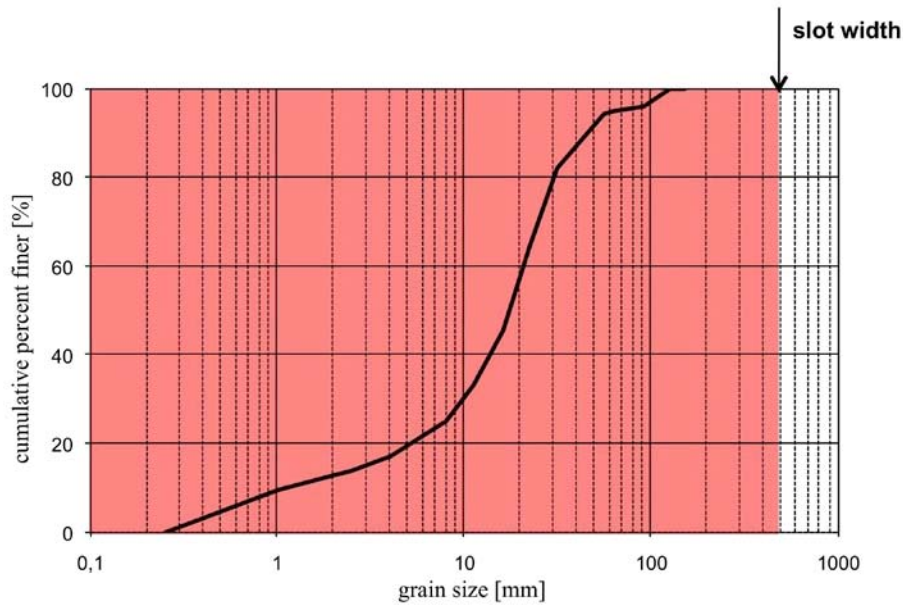


Figure 16: Grain-size related limits of the bedload slot traps

Geophones

The response threshold of the geophones is set to a minimum grain size of 2 cm in order to avoid the recording of ambient noise. The upper limit of the system is reached only during most extreme flood events, when highly concentrated bedload charge makes the detection of single grains impossible (see figure 17).

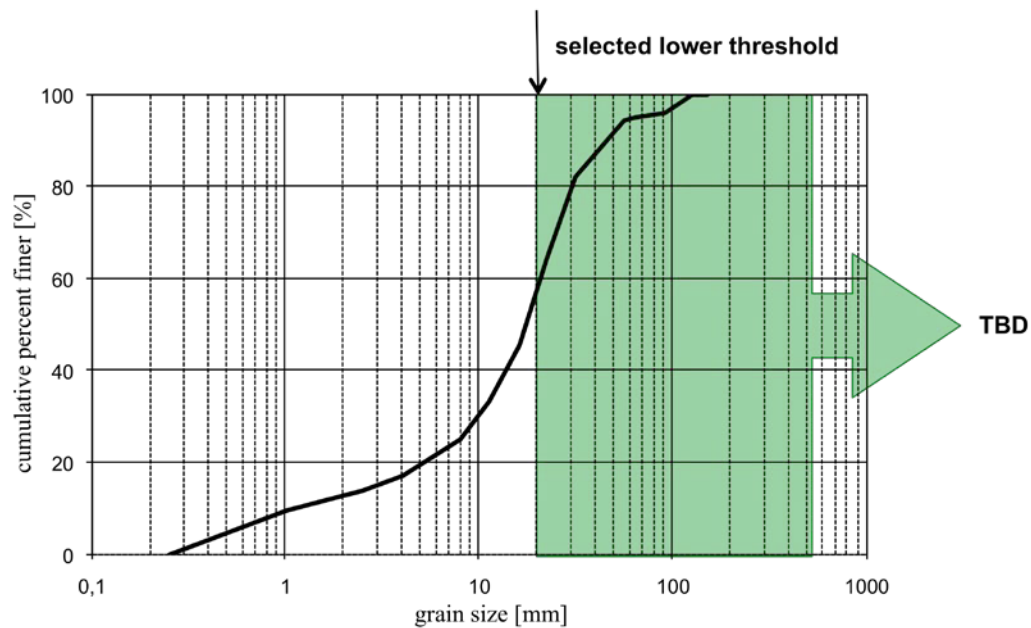


Figure 17: Grain-size related limits of the geophones

4.4.3 Spatio-temporal limitations

The applied measuring devices also show different spatial and temporal spectrums in bedload recording.

Geophone device

The geophone device certainly has the largest spatiotemporal spectrum in measuring bedload transport (see figure 18). It not only enables the year-round recording of bedload flux (at least when grain-sizes are larger than 20 mm), the arrangement of 40 geophones also covers the entire river width (see figure 19). Even if thereby in fact just every second steel plate of 50 cm length is equipped with one geophone, their regular distribution easily allows for extrapolation to the entire cross-section. The comprehensive coverage over time reveals spatiotemporal fluctuations of the bedload flux at the study site, which cannot be clearly identified by other measuring techniques. However, geophones provide only indirect data about bedload. In this respect the method will always depend on direct and independent measuring techniques, such as slot trap systems.

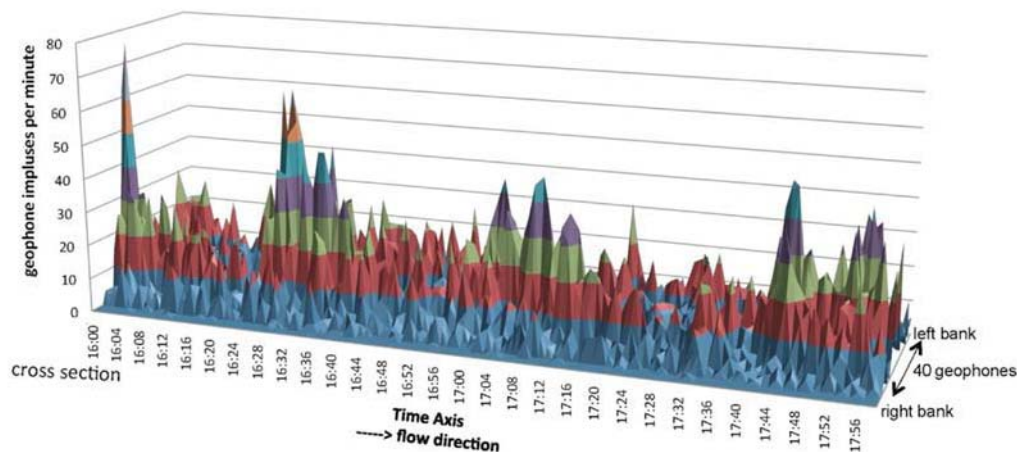


Figure 18: Spatiotemporal distribution of bedload flux at the cross-section in Dellach im Drautal

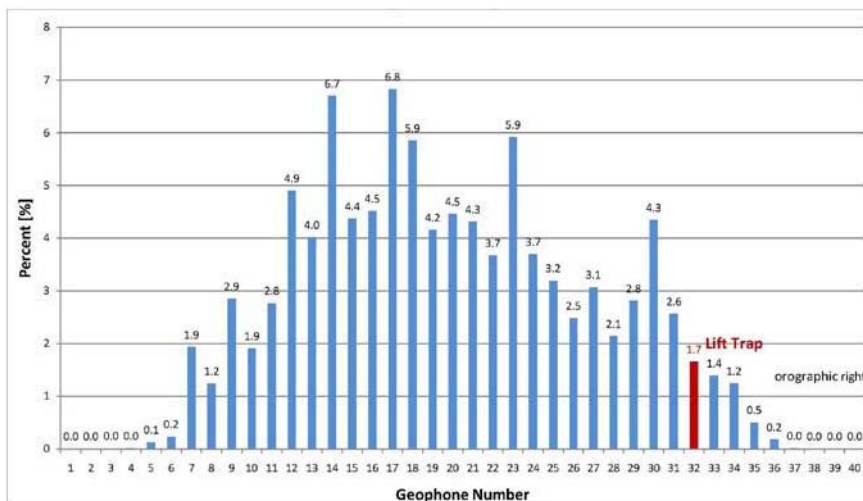


Figure 19: Annual distribution of geophone impulses at the cross-section (2009)

Bedload slot traps

Depending on the slot width, the spatial bedload recording spectrum of bedload traps is restricted to predefined sections of the river cross-profile. As far as the two fixed slot traps are concerned, their respective spatial bandwidth is 25 cm, whereas the hydraulic lift-trap with its slot width of 50 cm covers 1 % of the entire cross-section.

Measurements with slot samplers last in principle long enough to enable the identification of temporal bedload flux fluctuations during a certain period of time. However, due to their limited capacity, a year-round bedload recording (in contrast to geophones) is not possible. Instead, for each measurement campaign certain flood conditions have to be chosen in order to cover in the long run the entire discharge hydrograph. The use of fixed slot traps is thereby much more time-limited than the operation of the hydraulic lift-trap, because fixed systems under perennial conditions can only be emptied and replaced during low water conditions in winter.

Large Helley-Smith Sampler

Mobile basket samplers are used to determine discharge-dependent bedload flux at selected sections of the river cross-profile. As a mobile basket sampler, the LHS sampler has a flexible spatial application area. However, at any one time just one position can be sampled and individual sampling lasts only around one minute, depending on the prevailing bedload flux. Thus, the data achieved by taken measurements is very selective. As a result, LHS samplers are hardly able to identify the short-term temporal variability of bedload flux. This unknown impact of spatiotemporal transport fluctuations makes the method susceptible to wrong assumption. According to Kreisler (2010), the comparison of individual samples with contemporaneous recorded data from adjacent geophones and slot traps is problematic, too. The reasons are relatively long distances between the devices of about 3 to 4 m and the fact that LHS sampling may cause strong interference of the natural flow.

Lots of labour-intensive samplings have to be performed for minimising uncertainties.

Furthermore, in terms of better calibration results, Kreisler (2010) recommends the use of the LHS sampler directly downstream of the geophone device.

4.5 Combined data logging

Taking into consideration their complementary areas of application, combined measurements by the hydraulic lift trap and the geophone device are possibly of great importance for the comprehensive quantitative determination of bedload transport (see figure 20). While the hydraulic lift trap has actually no grain-size related limitations for bedload recording, the geophones are only able to detect stones with a minimum grain-size of 20 mm. The geophone device in turn enables the year-round recording of bedload flux at the entire river cross-section, while the application of the lift trap is restricted to a section of 50 cm, adjacent to one single geophone. One big advantage both methods share together is their ability for continuous measurements. In this regard, a proved high data correlation between recorded weight increase and geophone impulses can be seen as a precondition for a comprehensive quantitative determination of bedload transport.



Figure 20: Location of lift trap in relation to geophone device

5 The hydraulic lift trap

The following chapter first describes the development of pit trap systems in general, followed by the explanation of slot sampler systems in particular. Afterwards, the planning and design, the mode of operation and the maintenance of the hydraulic lift trap at the Drau River will be discussed in detail.

5.1 Pit trap systems

Against the background of the tremendous temporal and spatial variability of bedload transport in natural channels, bedload analysis using simply portable devices or temporary installations have always been prone to large sampling errors. Moreover, such methods often tend to over- or under-sampling bed material and inevitably disturb the flow field (Bunte et al., 2004; Bergman et al., 2007). To get more accurate and reliable results, pit traps and enhanced slot samplers were designed to allow for automatic and continuous recording of bedload transport behaviour without affecting the flow. The development thereby ranges from simple containers to complicated weighing and recording instruments.

5.1.1 Early attempts & various developments

The earliest documented apparatus was used in the alpine River Inn, Tyrol/Austria (Mühlhofer, 1933). Six pit traps of 1 m depth were installed at the gravel bank along the river cross-section during the low water period in winter 1928/29. The main intention was the analysis of the bedload grain-size distribution and stratification.

Another sampler first used by Einstein (1944) in Mountain Creek, South Carolina and modified later on by Hubbell (1964) was semi-portable and easy to install in low-velocity streams. Thereby, a pump continuously pumped the sediment and water slurry as it accumulated in the trap to a weighing tank on the riverbank, from where it returned to the stream again. Because this procedure would not work in case of coarse bed material, its application is restricted to sand-bedded, low-velocity streams.

Leopold and Emmett (1976) designed a very elaborate, but also cost-intensive conveyor belt slot system at East Fork River, Wyoming. Regarding its assembly, a concrete trough installed along the river cross-section was covered by a row of eight hydraulic controlled gates. Opening and closing these doors separately allowed the sampling of different locations along the cross-profile. A conveyor belt at the bottom of the trough routed the trapped bedload sideways to a weighing hopper, where the values were recorded every minute (Lewis, 1991).

The function of the vortex-tube bedload trap is based on a discharge-induced vortex, which carries trapped bedload in a trough diagonal to the riverbank (Lewis, 1991). Even if this system does not enable sectional determinations of bedload transport rates along the river cross-section, at least at steep sloped rivers it has been a quite popular measuring technique in the past. The simple construction and possible coverage of the whole river cross-section entailed the application of the vortex-tube trap in different locations worldwide. So the system was applied in Oak Creek, Oregon (Milhous, 1973), in the Torlesse Stream, New Zealand (Hayward and Sutherland, 1974) and in Virginio Creek, Italy (Taconni and Billi, 1987).

5.1.2 Slot samplers

The slot sampler describes a weighing slot system, which enables continuous bedload measurements at predefined locations within a cross-section (Reid et al., 1980). The trap consists of a sample container, covered by a slotted plate and inserted in a formed concrete pit in the riverbed. The moving stones fall through the slot, get trapped and automatically weighed within the container.

Even it does not allow for measuring the whole cross-section, the unique advantage of this relatively low cost method is that the bedload does not need to be removed from the channel for weighing (Lewis, 1991). The sampling thereby occurs without the need for personnel to be present. This has considerable benefits, particularly in remote areas with unpredictable flood events (Sear et al., 2000). Slot samplers in general proved to be very reliable regarding their sampling efficiency, too (Habersack et al., 2001). Their embedded installation prevents over-sampling and the fact that mobile grains “line up” at the slot for getting trapped, in turn minimises under-sampling of coarser grain-sizes (Bergmann et al., 2007). Moreover, because the channel flow is separated from the water column within the trap, slot traps sample only bedload, but exclude suspended load (Laronne et al., 2003).

According to Habersack et al. (2001), the slot sampler system has so far been applied in Goodwin Creek, Mississippi (Kuhnle et al., 1988), in several locations in Israel (Laronne et al., 1992; Powell et al., 1998; Laronne and Cohen, 1998), in the Rio La Todera in Spain (Garcia et al., 2000), as well as under perennial conditions in the River Drau in Austria (Habersack et al., 1998).

For weighing, the original slot sampler uses a water-filled pressure pillow beneath the sample container. The pillow thereby responds to the accumulating bedload and overlying water column by changing hydraulic pressure, which then gets transmitted to a pressure-bulb transducer, followed by a chart recorder. Lewis (1991) describes an advanced version, where the pressure pillow and complex mechanical and hydraulic linkages were replaced with an electronic load cell and an electronic data logger. Some main reasons therefore were a higher precision and stability, reduced operating problems and elimination of the temperature effects found in pressure pillow

systems (Lewis, 1991 and Sear et al., 2000). The present weighing slot trap system including the hydraulic lift trap in the river Drau is based on this enhanced weighing method, as well. Apart from the weighing principle, the slot sampler has experienced some other design modifications, mainly because of disparities in field conditions and exploratory intentions. Lewis (1991) and Sear et al. (2000) erected low-profile fences along the cover plate slots to prevent lateral ingress of bedload. Bergman et al. (2007) describe design modifications to bedload samplers deployed in an ephemeral gravel-bed channel in Israel. One amendment thereby was the installation of a slot cover, which can be opened at later stages of a flood event. For opening, two spring-loaded catches have to be released via manually pulling a cable. The two other modifications included slots, whose widths are adjustable post-installation; and a side door at the sample container that allows documentation of the stratification and textural changes within the accumulated bedload.

The slot sampler deployed by Habersack in 1995 in the river Drau was the first to be installed in a large perennial gravel-bed river. It was equipped with a slot cover and side doors. The greater minimum flow depth and velocity compared to previous application areas necessitated a larger sampling capacity and the complete data-logging unit to be waterproof (Habersack et al., 1998). However, due to the perennial conditions it was only possible to withdraw and reinsert the sample container during low water in winter, and if done so, it was still complicated. The two present fixed bedload traps in the river Drau are affected by the same problem. The unsatisfactory situation gave rise to careful considerations about possible technical improvements. Finally the idea of using hydraulics to enable the lifting of the trap above the water surface at any time of the year was born.

5.2 Planning and design of the hydraulic lift trap

In spring 2008, the installation of the hydraulic bedload lift trap in Dellach im Drautal marked an important keystone in the completion of the integrative measuring system in Eastern Tyrol and Carinthia. The whole development process of this system took nearly 15 years, so far. Lead-managed by Habersack from BOKU Vienna, the hydraulic lift trap was developed by Seitz (BOKU). Project partners for realisation were the hydraulics company *Kohyd* in Mödling/Lower Austria and the steel construction company *Wöss marine engineering* in Zwentendorf/Lower Austria.

Apart from the restricted budget, various technical aspects in planning and design of the hydraulic lift trap have been challenging.

5.2.1 Trap dimensioning

Derived from previous findings by Habersack et al. (2001) and with regard to its projected field of application during flood peaks, the chosen slot width and slot length of the lift trap were 500 mm and 1600 mm, respectively.

The sample container has a width and depth of 900 mm and a length of 1800 mm, resulting in a reservoir capacity of 1.46 m³. Assuming that the density of wet gravel is 2 tons/m³, the filled container weighs 3 t. In general, the reservoir capacity of the trap had to strike a balance between:

- embedding depth of the formed concrete pit below the channel bed
- capacity of the container resting within the formed concrete pit, which should be as high as possible to maximise sample quantity and sampling time
- handling of the sample using heavy equipment
- lifting capacities of hydraulic shovels and heavy-duty cranes, which are limited to 4 tons



Figure 21: The hydraulic lift trap before installation

The lift trap including the loaded container in total weighs 5 tons. The single components of the construction are:

- trap enclosure
- cover of enclosure
- container housing
- sample container
- trap cover
- trap door
- two hydraulic plungers and cylinders
- four load cells

Thereby, the liftable steel components weigh 2 t (see figure 21). Adding the filled container with 3 t, the needed lifting capacity for each of the two hydraulic plungers and cylinders so would be 2.5 t. But due to the fact that about 2/3 of the construction is buoyancy-assisted, the actual lifting capacity is reduced to 1.7 t (Seitz et al., 2009).

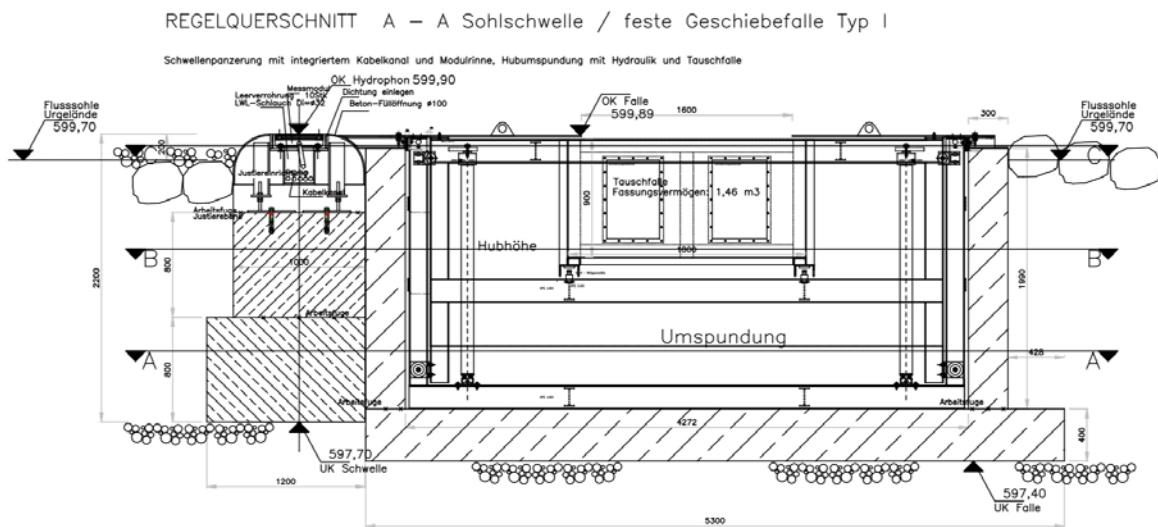


Figure 22: Longitudinal section of the lift trap (Seitz et al., 2009)

Grundriss feste Geschiebefalle Typ I, Schnitt C-C
M 1 : 20

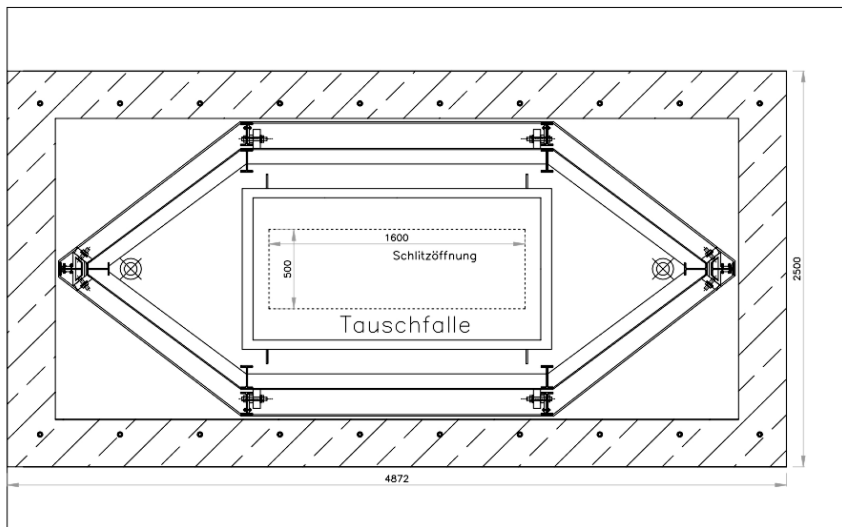


Figure 23: Horizontal projection of the lift trap (Seitz et al., 2009)

5.2.2 Hydraulic actuator

Particular attention was paid to the design and construction of the hydraulic actuator, which represents the core of the bedload lift trap (see figure 28). The main challenge thereby has been the selection and design of adequate hydraulic system components in consideration of its submerged

application and the aquatic environment. With the exception of the manual control (see figure 26) and the pump, all other components therefore are made of stainless steel. Due to reasonable ecological concerns regarding the utilisation of oil as hydraulic medium in an aquatic ecosystem, for this purpose water is used instead. This requirement has even more complicated the synchronisation of the two hydraulic cylinders, however (see figures 24 and 25). The original synchronisation concept based on a flow divider has had to be revised, because the device was not available for water as hydraulic medium. The alternative idea of controlling the synchronous run electronically using a spirit level has been discarded for financial reasons and reasons of underwater operating reliability.

Finally, a video surveillance system has been realised. Two underwater cameras simultaneously sight measuring scales at the rear and the front of the lift trap (see figure 27). Flow meters implemented in the feed pipes enable additional monitoring of the motional process.



Figure 24: Hydraulic plungers and cylinders



Figure 25: Installed hydraulics



Figure 26: Manual control

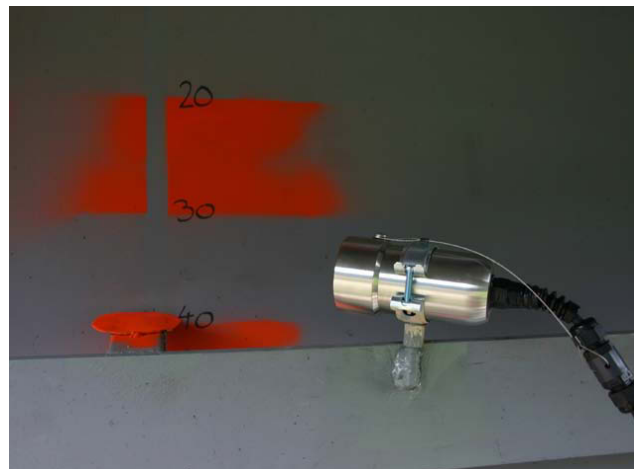


Figure 27: Underwater video surveillance system

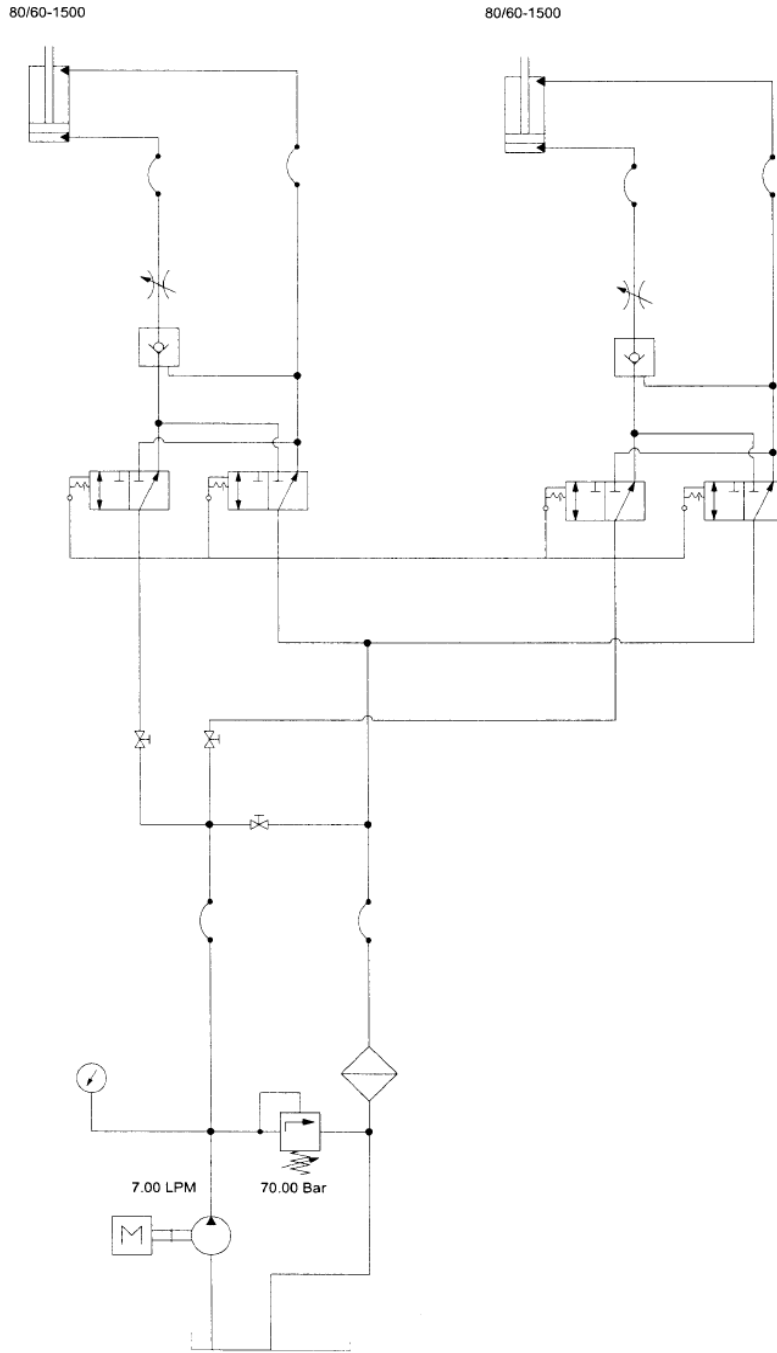


Figure 28: Diagram of the hydraulic actuator

5.2.3 Load cells

The load cells are the most important part of the slot trap weighing system. According to Omega Engineering, Inc. (2010), „a load cell is a transducer that converts a load acting on it into an analogue electrical signal. This conversion is achieved by the physical deformation of strain gages which are bonded into the load cell beam and wired into a wheatstone bridge configuration“.

A Wheatstone bridge is a circuit consisting of four interconnected resistors. The device is used to determine the electrical resistance of one resistor when the other three resistances are known. R_{CD} in figure 29 describes the one resistor, whose varying resistance due to deformation is measured by comparing it with the known standard resistances of R_{AB} , R_{BC} and R_{AD} . For recording, usually a highly sensitive galvanometer is deployed (McGraw-Hill, 2005).

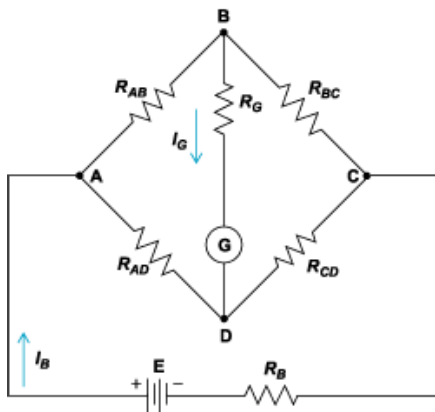


Figure 29: Wheatstone bridge circuit (McGraw-Hill, 2005)

Nowadays, the most commonly used types of load cells are based on strain gages. Depending on the used measurement principle, strain gage load cells can be subdivided in bending-, shear- or compression-types (Omega Engineering, Inc., 2010).

With regard to the extreme operating conditions in Dellach im Drautal, the focus in type-selection was on trouble-free operation and maximum robustness. Due to its simple stainless steel construction and complete hermetic sealing, the deployed bending beam type load cell SB4 (see figure 30) is specially designed for the use in harsh environments, such as submerged riverbeds. The type in general is available for capacities from 5 kN to 100 kN. Load cells used in Dellach im Drautal have a range from 5 kN to 20 kN (which equals 510 kg to 2039 kg) and offer an accuracy of 0.03 % (Flintec, 2005). Each sample container rests on four load cells, which are mounted on two cross beams near the ground of the trap housing (see figures 31 and 32). By connecting the load cells in parallel, the output is a single voltage that is proportional to the weight increase.

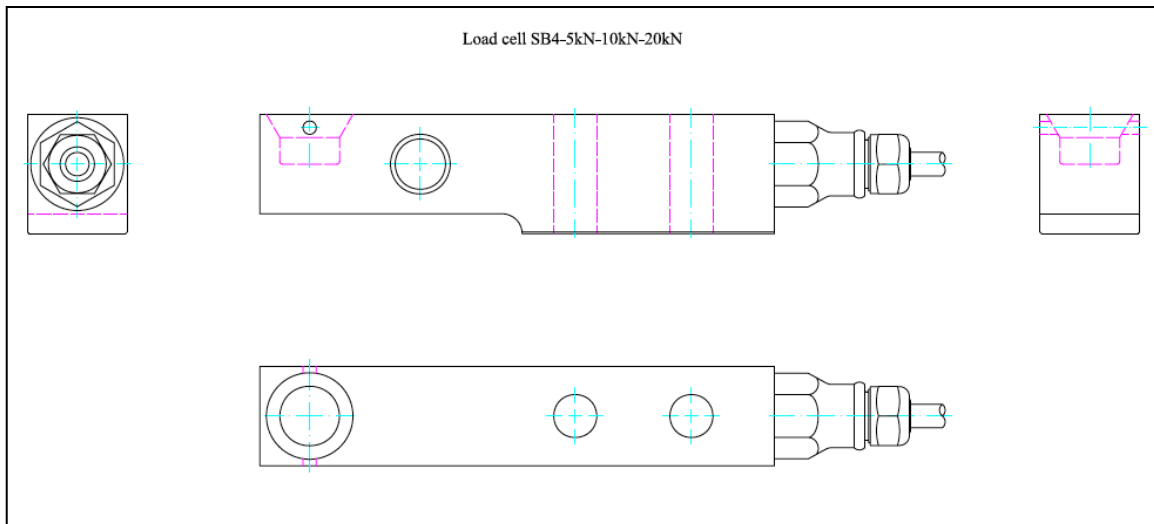


Figure 30: AutoCAD drawing of the load cell type SB4



Figure 31: Close-up view of deployed load cell



Figure 32: Arrangement of load cells in fixed slot trap

5.2.4 Flow resistance

The underlying assumption for the determined drag force has been a flat upright wall of 1 m height and 1.7 m length, perpendicular to flow. This would imply a drag coefficient c_w around 1 (Bengtson, 2010). However, the streamlined construction of the trap enclosure in fact reduces the flow pressure; when the trap is lifted, the actual c_w -value is assumed to be around 0.3.

5.2.5 Statics

With regard to stability and longevity, the construction was consciously over-dimensioned and arranged as simple as possible.

An important point was the adequate embedding depth of the roll guides (see figure 33). On the one hand, the roll guides should be situated deep enough to avoid tilting caused by flow pressure or irregular lifting of the hydraulic cylinders. On the other hand, there should remain enough headspace underneath the container in order to prevent early blocking of the roll guides by fine sediments, which inevitably accumulate within the construction over the years.

Lifting the trap 1000 mm, there still remain 860 mm embedding depth of the roll guides. Previous tests as shown in figure 34 have demonstrated that the construction in general tolerates a tilt of about 10 %.

With regard to the suspended load accumulation within the construction, the operational experience in the last two years has shown that more headspace underneath the container is recommendable in terms of service intervals.



Figure 33: Roll guides



Figure 34: Tilting test

5.2.6 Slot door mechanism

The slot door mechanism of the hydraulic lift trap differs from previous deployed slot covers in Nahal Eshtemoa, Israel (Bergmann et al., 2007) and in the river Drau (Habersack et al., 2001). In contrast to the hitherto complete removal of the cover by pulling a cable, the slot door of the lift trap swings open inwardly (see figure 35). Two interlock bolts retain the door in place until they get pushed away hydraulically, at which point the door swings open, allowing sampling to commence.



Figure 35: View of the under-side mechanism of the slot door

5.2.7 Handling of suspended load

As a result of glacier-meltwater and the abrasion of bedload, the river Drau carries in particular during summer huge amounts of suspended particles with concentrations up to 300 mg per litre. Projected for a year, this means approximately 1 million tons of suspended load (Habersack et al., 2009).

A complete sealing of the construction is not possible, because the fine particles easily ingress through the smallest gap. In order to minimise the suspended load input, rubber seals tighten all gaps of the trap enclosure and the slot door (see figure 36). An additional method is projected, but not realised, so far: Groundwater pumped from a well on the riverbank into the trap causes light hyperbaric conditions inside, what impede the infiltration of fine particles from outside.



Figure 36: Close-up view of the gap sealing

5.3 Mode of operation

Figure 37 describes the conduct of the bedload sampling procedure using the hydraulic lift trap. In rest position the trap is situated beneath the channel bed, while the slot is closed and flush with the bed. In the event of an approaching bedload wave, the trap door gets opened hydraulically via manual control and the balance starts recording the mass increase within the trap. When the trap is completely filled up with bedload, the slot remains open. After the water level goes below a meter depth, hydraulic plungers and cylinders lift the construction above the water surface. To be able to analyse the trapped bedload, a crane withdraws the filled container and disembarks it on the riverbank. Afterwards the crane reinserts the container and the cover with closed slot gets screwed on. Finally, the trap is lowered to rest position again.

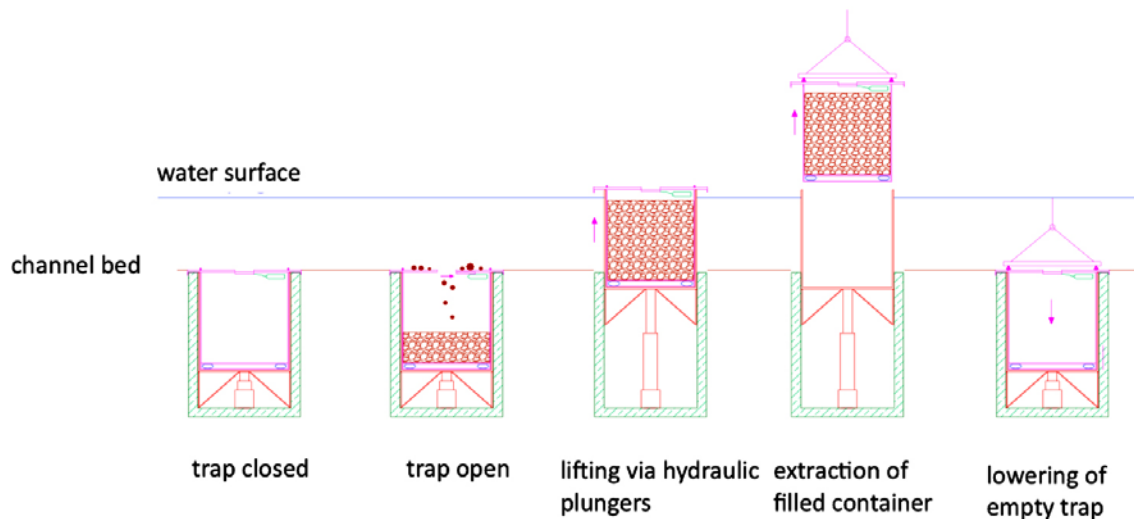


Figure 37: Conduct of sampling procedure

5.4 Maintenance

A well-performed maintenance of the hydraulic slot trap system is crucial in terms of costs, operating reliability and continuity of sampling. As already aforementioned, the river Drau carries high concentrations of suspended particles. The consequential need for regular servicing focuses particularly on two areas of the hydraulic lift trap:

- The stainless screw nuts, which affix the cover onto the trap enclosure, are most exposed to the abrasive forces of water and solid particle flux and so need to be replaced once a year.
- Because a complete sealing of the construction is not feasible, fine particles accumulate over time underneath the inner container and as a consequence need to be removed roughly once in two years. The service interval thereby also depends on the time span the slot has been left open after sampling without lifting the trap above the water surface.

Lewis (1980) has used a suction dredge in an assembly commonly used by placer gold-miners to empty slot trap sample containers in Caspar Creek during storms without removing them from their

position. However, this system is not applicable to the local conditions of the large Drau River, least of all during flood events.

Because of the easier and more sensitive handling within the trap enclosure and the already existing compressor of the hydraulic system, an airlift pump is used for the removal of sediments instead (see figure 39).

As far as the abrasion of the screw nuts is concerned, previous experience has shown that the use of larger screw sizes (e.g. M24) in future trap constructions instead of the presently applied M16 screws would retard intense abrasion and thereby extend the service interval (see figure 38).

Besides, it is recommended to grease waterproof adhesive lubricant between the nuts and the screws to ease the later replacement of worn out nuts.

With regard to the submerged conditions within the trap enclosure during servicing and the complex operating system, the operation and maintenance of the hydraulic lift trap requires well-trained personnel. However, due to the enabled lifting above water surface, respectively the choked flow within the lifted trap enclosure, the conditions are much more comfortable compared to the complicated and laborious servicing of fixed slot samplers in perennial rivers.



Figure 38: Worn out M16 screw nut after one-year operation



Figure 39: Removal of sediment accumulations using an airlift pump

6 Results

6.1 Hydraulic efficiency of the lift trap

When performing the hydraulic efficiency measurements, the trap has been empty, the flow depth of the river was about 40 cm and the flow velocity was approximating 1.3 m s^{-1} . Individual measurements lasted 1 minute and were undertaken from a bucket, which was directed above the measuring positions in and around the slot. In doing so, it was possible to exclude any disturbance of natural flow conditions (see figure 40).



Figure 40: Measurements performed from a bucket

According to previous measurements undertaken by Habersack et al. (2001), the five verticals for current metering were chosen 1 m upstream of the slot, at the upstream end of the slot, at the centre of the slot, at the downstream end of the slot and 1 m downstream of the slot. At the two verticals around the slot, currents were measured 10 cm below the water surface, in the middle of the water level and 3 cm above the riverbed. At the three verticals inside the trap, they were measured 3 cm below the slot entrance, in the middle of the empty sample container and 3 cm above the container base. Figure 41 displays the results of the bi-axial flow velocity measurements in vector products. While the flow velocity on the riverbed at the given instant was around 1 m s^{-1} , at the base of the sample container it never has exceeded 0.05 m s^{-1} . Only at the pit centre close to the slot it reached up to 0.4 m s^{-1} .

Calculations based on the measurement data reveal a high hydraulic efficiency of 97 % near the container bottom. However, current metering was not performed at different stages of filling, yet.

Flow velocity measurements ($m s^{-1}$) in and around the empty trap (08/04/2010)

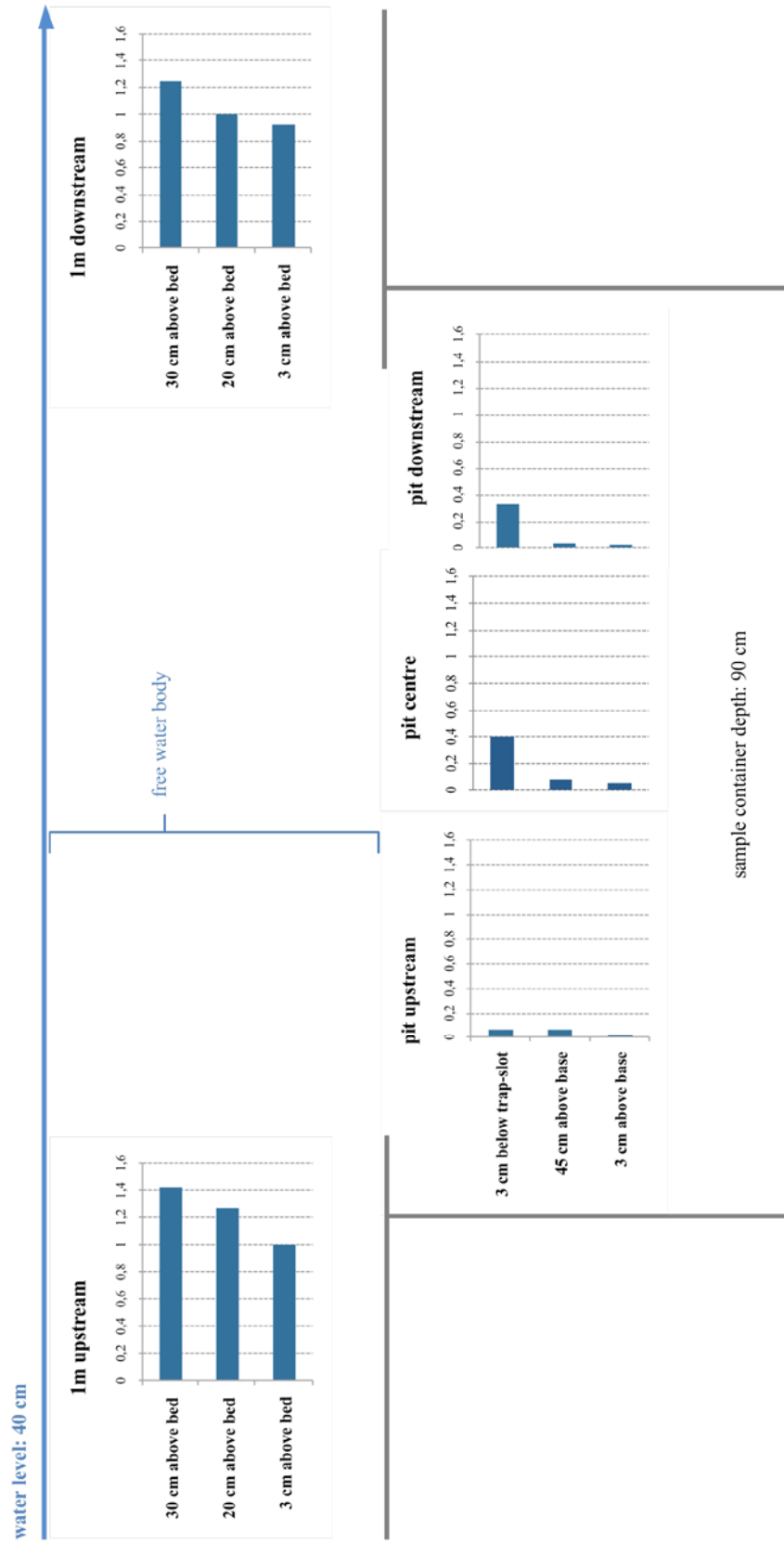


Figure 41: Results of the flow measurements in and around the trap

6.2 Sedimentation analysis

Analysis of the sedimentation within the sample container facilitates the understanding of varying mass increase rates during the measurement period. Particularly in combination with data from discharge- and geophone impulse measurements, it provides not only information about the grain size distribution at different stages of the flood event, but also about deposition behaviour within the bedload wave.

After the sample box was disembarked on the riverbank, the side doors of the container enabled the documentation of bedload stratification (see figures 42 and 43). What thereby became particularly obvious was a sharply bounded change of grain-sizes in the upper fourth, approximately 20 cm below the container edge. Quite coarse gravel was suddenly succeeded by material with a high proportion of fine sand. The distinctive armour layer on top was excluded from further analysis.



Figure 42: View through trap side-door



Figure 43: Documentation of stratification

For the purpose of determining the grain-size distribution at different filling levels, a sieve analysis was performed. Therefore, sieve samples were taken from the armour layer on the top, from different sediment layers in depths of 30 cm, 45 cm, 70 cm, as well as from the bottom layer (see figure 44) The sun-dried material was put in a sieve shaker with sequenced square mesh widths of 150 mm, 125 mm, 90 mm, 63 mm, 56 mm, 31.5 mm, 22.4 mm, 16 mm, 11.2 mm, 8 mm, 4 mm, 2.5 mm, 2 mm and 1 mm. In data evaluation the individual sieve fractions of the samples were displayed in kg and percentage. In further analysis, the $d_{\max b}$ and standard grain-size diameters, as well as different grain-size distribution percentiles (d_{10} , d_{16} , d_{20} - d_{80} , d_{84} , d_{90}) of each sample were determined. The detailed single results of the sieve analysis are displayed in Appendix 1.

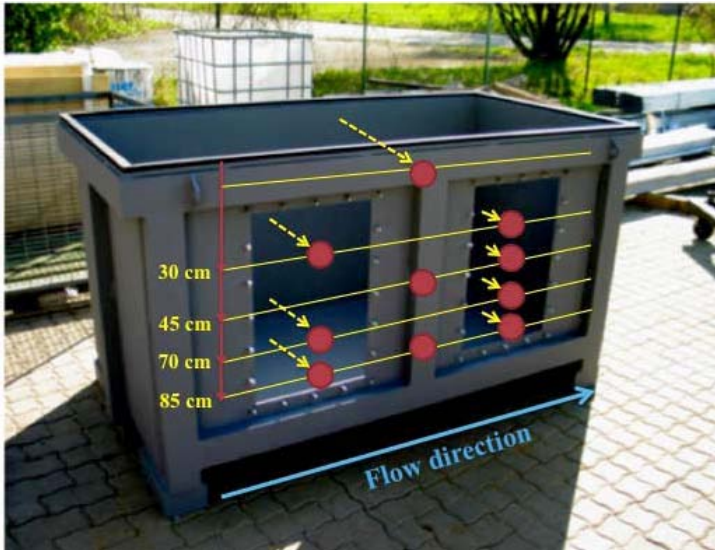


Figure 44: Scheme of the sampled sediment layers

The sieve results displayed as longitudinal cross profile of the sample container show textural variations not only in vertical, but also in horizontal direction (see figure 45). Taking into account the small absolute flow velocities ($< 0.1 \text{ m}^3 \text{ s}^{-1}$) measured within the trap, up to 80 % fill (Habersack et al., 2001) any secondary flow cells would only have a negligible effect on sediment mobilisation. So it can be concluded that bedload deposition itself does not occur in uniform horizontal layers, but with varying angle in stratification. Taking this into account, a more cone-shaped morphology of accumulation could be assumed with rising fill, particularly below the upstream slot edge. At further increased charging, the steepened slope of the cone would eventually slide towards the downstream container wall so that the gravel layers would become more horizontal again.

One supportive indicator for this theory is the significant higher concentration of coarse material at a filling level of 15 cm near the downstream slot end: This location is inconsistent with respective measurements from discharge, weight cells and geophones, which concordantly reflect a significant rise in shear stress not until the second half of filling time, after one third of the total load increase. A plausible explanation for the surprising location of these cobbles might be that they were deposited actually later near the upstream end on top of a quite steep sloped gravel cone, but glided off afterwards due to their comparably higher kinetic energy. Another evidence is the observed tendency to more uniform horizontal grain-size distribution at higher filling levels, where, according to this theory, the gravel cone would be flattened.

However, due to the lack of possibilities for observing the sedimentation process in-situ, so far only assumptions can be made on the basis of combined data from sieve analysis and measurements of discharge, weight increase and geophone impulses. Absolute certainty about deposition behaviour can only be gained by simulation tests under laboratory conditions.

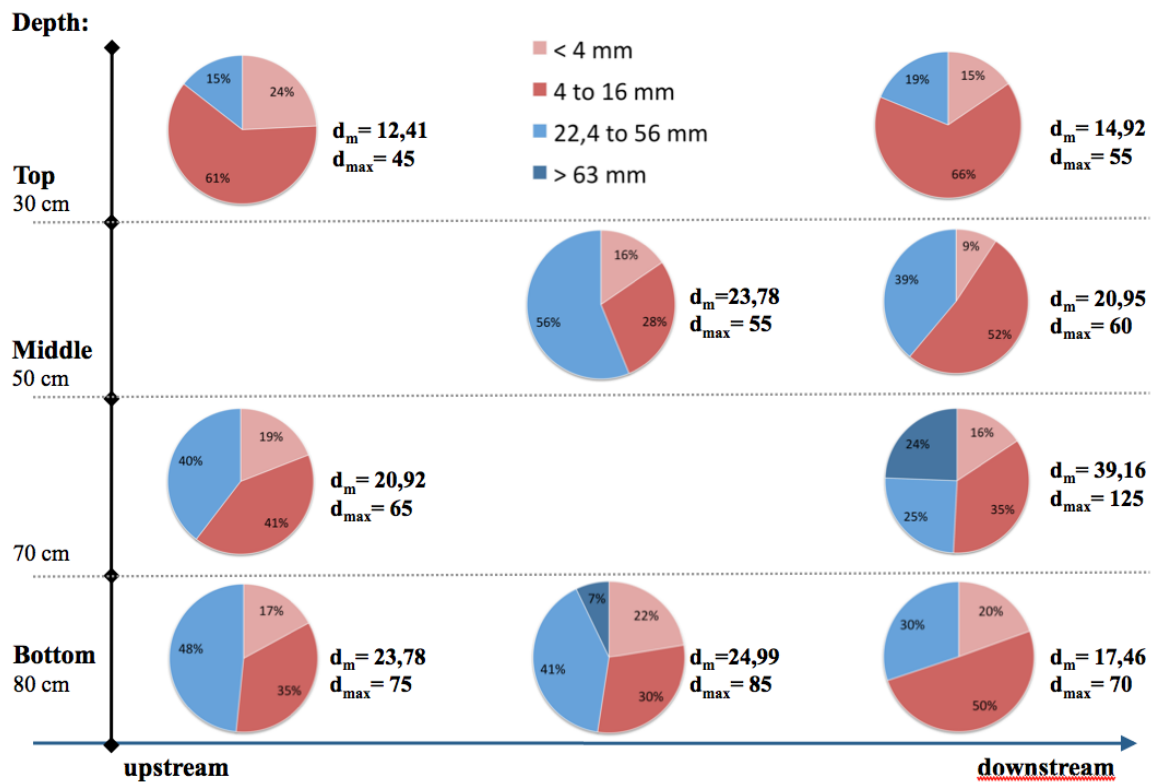


Figure 45: Scheme of the grain-size distribution within the sample container (armour layer excluded)

Definitely obvious is the high amount of small grain-sizes below 16 mm in each of the taken sieve samples. The proportion varied between 44 % and 85 %. Evaluation of the total grain-size distribution revealed that 54 % of the analysed bedload is smaller than 20 mm (see figure 46).

Considering the assumed minimum threshold of 20 mm, more than 50% of the trapped material was not recorded by the geophones.

The sharply bounded textural change in the upper fourth of the trap container, which has already been detected and documented through the container side door, was evaluated in detail by sieve analyses. Thereby, approximately 30 % more fine sediments were found in the nearly horizontal layer in 20 cm depth than in the adjacent layer below. However, while the load cells very well record the disproportionate sudden increase of fine fractions, it cannot be detected by the geophones. If this fact might influence the correlation between load increase and geophone impulses, will be discussed in the next section.

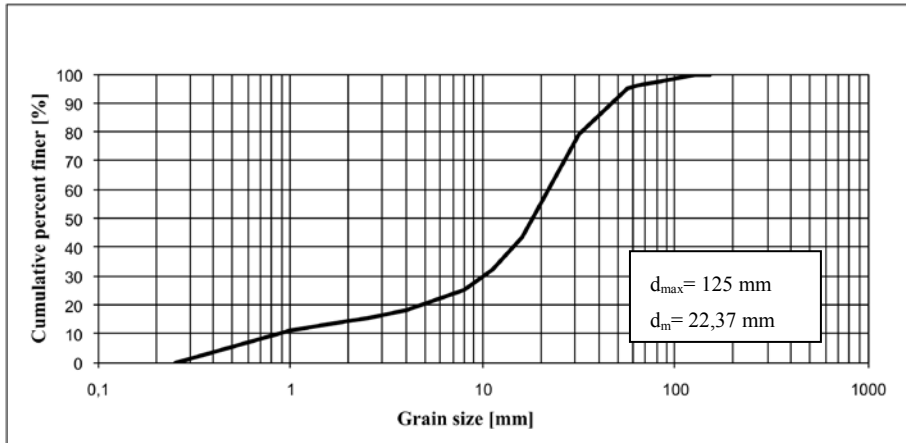


Figure 46: Total grain-size distribution (30 -31 July 2009)

6.3 Data correlation

In the following, at first the relations between discharge rates, weight increase within the sample container and geophone impulses will be described. Then the correlation between weight increase and geophone impulses will be discussed in detail. Finally, the impact of the aforementioned high disproportionate amount of fine fractions on the correlation will be analysed.

6.3.1 Correlation between discharge and weight increase

In 2009, it was the first time the hydraulic lift trap was used for automatic recording of bedload discharge. The filling of the trap thereby took place between July 30 and July 31, during a period of around 15 hours. All in all 2530 kg of bedload were sampled until the container was full. Figure 47 shows the mass increase within the trap compared to the respective discharge, which varied between $90 \text{ m}^3 \text{ s}^{-1}$ and $136 \text{ m}^3 \text{ s}^{-1}$. In this regard the flow discharge has already been too high to detect the initiation of motion. According to previous measurements undertaken by Habersack et al. (2001), $47 \text{ m}^3 \text{ s}^{-1}$ is the lowest discharge when bedload transport was observed with a slot trap in the River Drau. For the first third of the trap filling, during a comparably long time span of 10 hours, a quite steady weight increase can be observed. The meanwhile small discharge variations of $\pm 10 \text{ m}^3 \text{ s}^{-1}$ are probably due to surge effects caused by a water power plant located around 40 km upstream of the measuring site. Most filling obviously occurred during a short period of 4 hours at increased discharge, in which the highest gain in weight per unit time can be observed shortly after the flood peak.

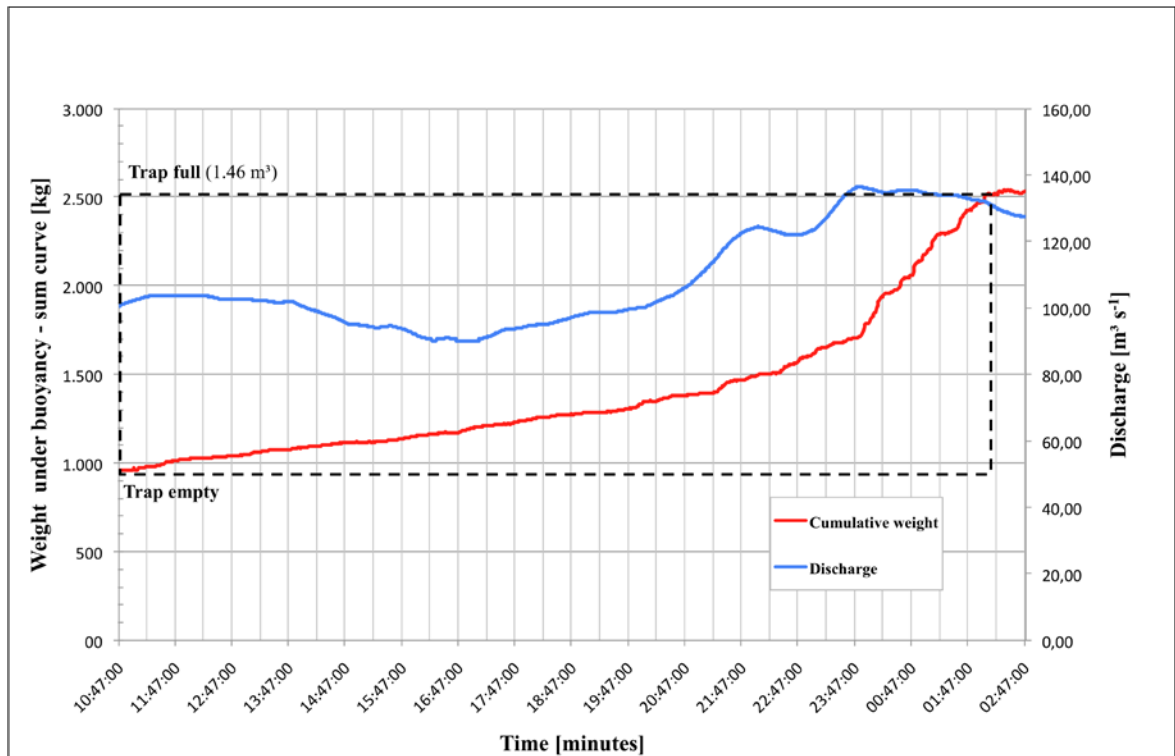


Figure 47: Cumulative weight increase compared to discharge

6.3.2 Correlation between discharge and geophone impulses

In comparison with the trend of the cumulative weight curve, the recorded geophone impulses in relation to discharge show a very similar run. In the first ten hours of the respective measurement period, the impulses show a quite constant distribution, too. Only when the discharge increased, more impulses per minute were counted, in which the largest peak in counted impulses was also recorded a few minutes after the flood peak. Moreover, figure 48 displays the temporal variability of bedload flux over a period of 15 hours. Thereby, distinct peaks of bedload waves can be observed. To be able to make definitive statements about the periodicity of these peaks, not only the temporal, but also the spatial variability of bedload flux along the river cross-section has to be considered. This purpose requires detailed data analysis including the total array of geophones. With regard to the focus of this work, only recordings of geophone number 32 were utilised, however.

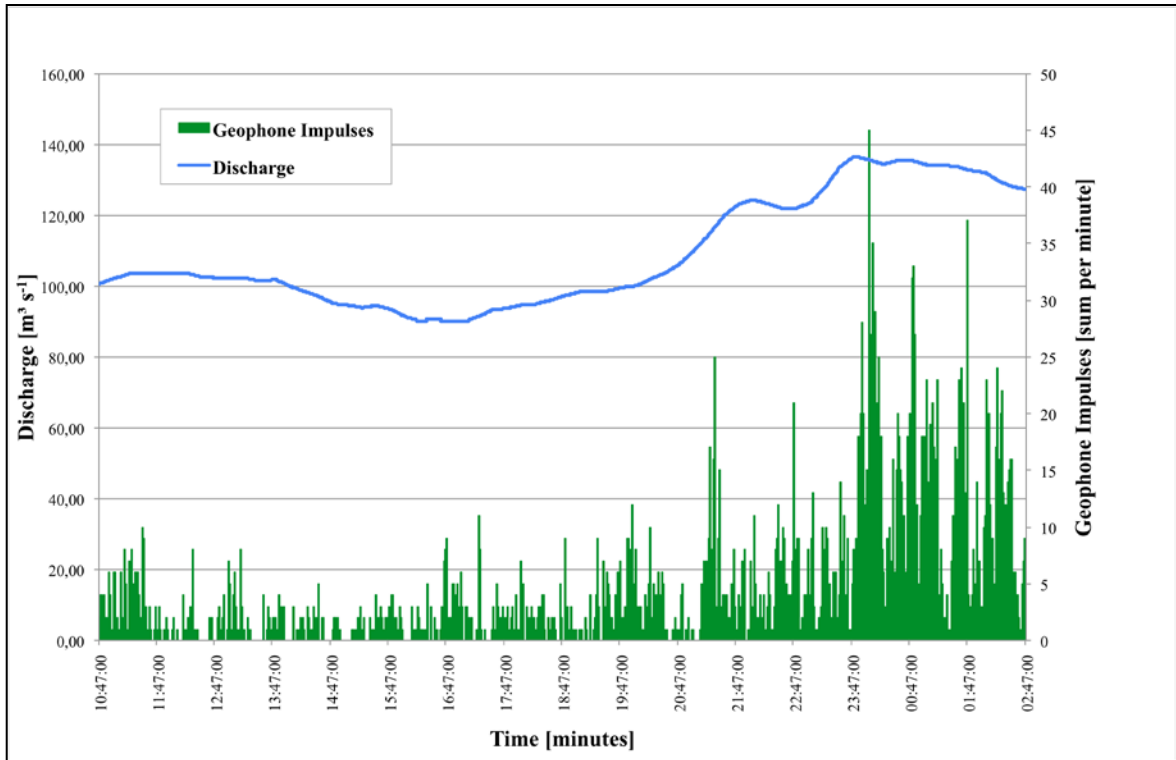


Figure 48: Sum of geophone impulses per minute compared to discharge

6.3.3 Correlation between weight increase and geophone impulses

Also the direct comparison of the cumulative weight curve and the cumulative curve of impulses shows a very similar temporal course (see figure 49):

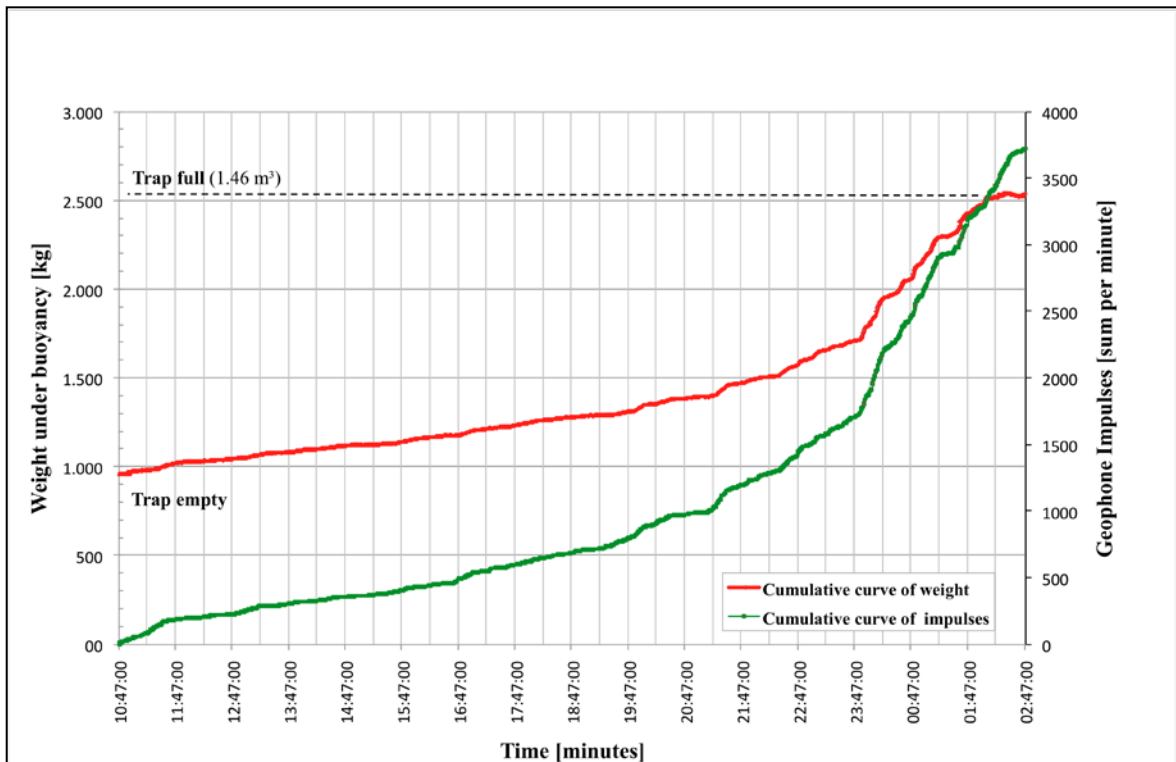


Figure 49: Cumulative curve of mass compared to cumulative curve of impulses

The comparably flat cumulative weight curve can be explained by relatively low discharge rates during the trap filling. The present grain-size analysis shows that only 5 % of the trapped material is larger than 56 mm, in which the biggest stone is 125 mm in b-axis diameter.

What is particularly interesting with regard to the observed high amount of small grain-sizes below 20 mm is that the course of the cumulative weight curve seems to incline proportional to the cumulative pulse curve. In this respect it can be assumed that the proportion of fine fractions is distributed fairly equal among the total recording period. Otherwise, in case of excessive sectional deposition of fine material, the weight curve would occasionally show disproportional steeper increases.

Nevertheless, the sedimentation analysis revealed one period, when around 30 % higher accumulations of small grain-sizes occurred. In order to assess if this may have any negative effects on correlation, the quantitative amount and moment of disproportionate deposition was estimated. Calculating the weight at a filling level of 70 cm enabled the determination of the time when the respective layer was deposited. Despite some uncertainties in terms of density and porosity of the accumulated bedload, it was possible to locate the potential time of deposition in the last stage of filling between 1:00 and 2:20 in the morning. The in-depth evaluation of data revealed that the largest ratios of weight increase and geophone impulses per minute in fact can be observed at 1:37, with 17,2 kg compared to only one impulse. One minute later, the ratio was 24.7 kg opposite to two counted pulses. Taking into account that the average ratio for the whole measurement period was 0.4 kg per impulse, the surplus increase in grain-sizes below 20 mm in only these two minutes was about 40 kg.

Figure 50 allows for more detailed comparison between the geophone graph and the load curve. In this way a first evaluation of the detected disproportionate deposition can be done. Using a moving average of 15 minutes to smooth out short-term fluctuations and highlight the longer-term trend, at first sight the curves seem to have a very similar, proportional temporal course, comparable to the trend already shown in figure 49. Nevertheless, on closer inspection the figure reveals increasing differences between the graphs from about 1:00 onwards, thus exactly in the period where excessive accumulation of fine fractions was detected in the analysis of sedimentation.

Experiments undertaken on a previous slot trap type (Habersack et al., 2001) disclosed a significant decrease in hydraulic and sampling efficiency from 80 % fill onwards; when winnowing processes caused by eddies that enter the trap become more common. Back-calculating the total load of approximating 2530 kg to a weight level of 80% enabled the time determination of the respective filling. In doing so, 80 % fill was reached between 1:05 and 1:09. In this respect the observed increasing difference between the curves and the disproportionate deposition of fine grain-sizes refer to those last 20 % of charging, where trap efficiency is said to be insufficient.

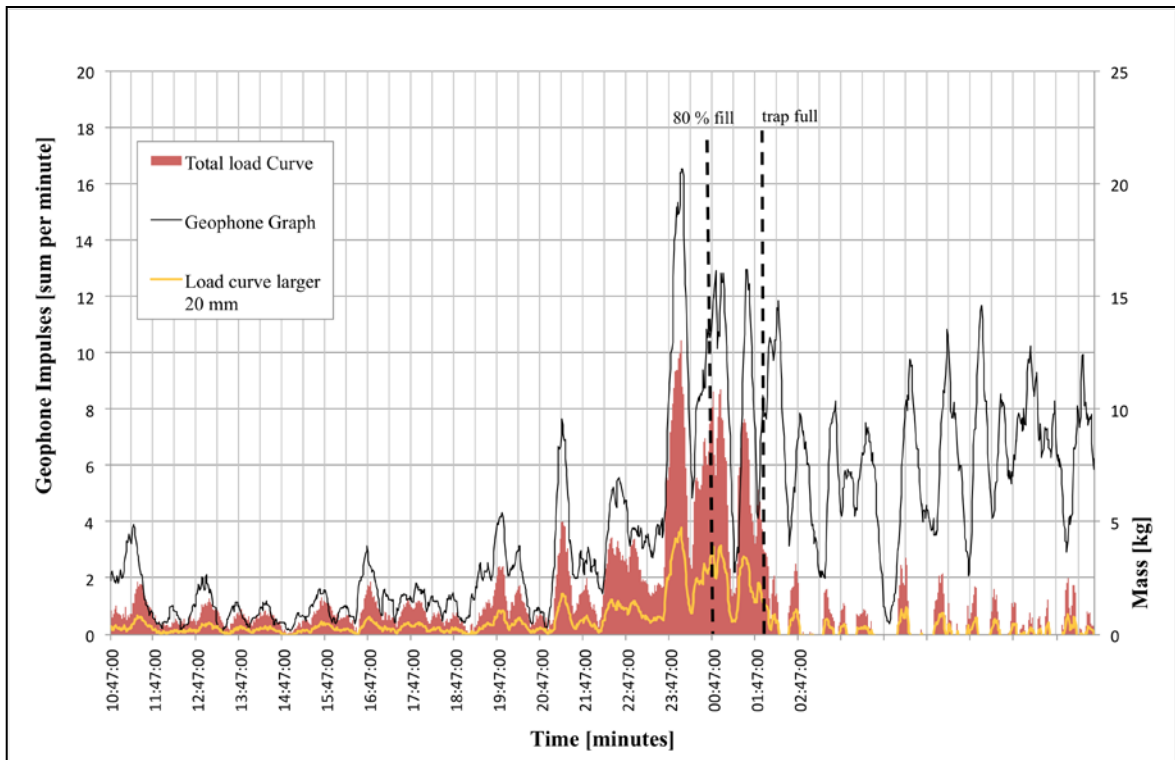


Figure 50: Course of impulses compared to course of weight increase (moving average of 15 minutes)

Taking this all into consideration finally allowed for quantifying the relation between hydraulic lift trap and geophone device. Therefore, the linear correlation between the geophone impulses per minute and the weight increase per minute was calculated deploying a moving average of 15 minutes. Regarding the excessive accumulation of fine sediments in the last 20 %, the influence of this deviation on the correlation was analysed first. Figure 51 displays the correlation between the mass of trapped material at 70 %, 80 % and 100 % filling level and the respective counted impulses per minute. Despite numerous iterative shifts upwards and downwards, the 80 % fill at 1:07 a.m. showed clearly the best correlation results.

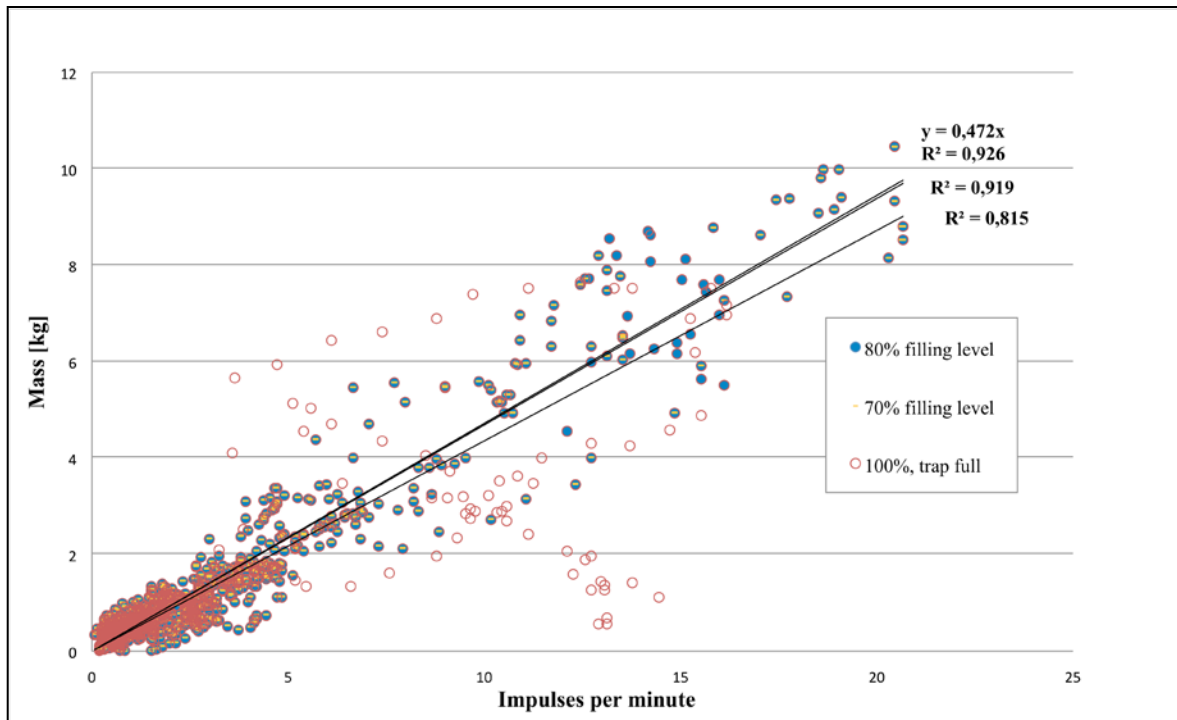


Figure 51: Linear correlation at different filling levels (moving average of 15 min)

One step later the impact of the general high proportion of fine sediment smaller than 20 mm was assessed. Based on the aforementioned findings, for this purpose only data concerning an 80 % - fill was used. Subtracting from each value the proportion of grain-sizes smaller than 20 mm related to the total grain-size distribution of the trapped material, the correlation coefficient is still the same as the coefficient of the correlation including the entire grain-size spectrum. However, the coefficient of determination changes when the detected shift of grain-size distribution with rising filling level is considered. The problem thereby is that deposition behaviour within the trap will never be completely understandable, in other words it is difficult to “draw a line” between different layers of sediment within the trap. Nevertheless, by virtue of data achieved from sedimentation analysis and the continuous recording of weight increase it was possible to create scenarios on deposition. Two scenarios of gradual filling are displayed in figure 52.

The first is based on the assumption of horizontal filling. According to figure 47, the first third of charging occurred at low discharges during a comparably long time span of 10 hours until 22:42. Defining this as phase 1 of horizontal deposition, the samples to determine the respective proportion of sediments smaller than 20 mm encompassed the layers in 80 and 70 cm depth. The calculated percentage of sediment smaller than 20 mm thereby was 50.6 %. Phase 2, in which samples from the layer in 50 cm depth represented the basis for the calculated percentage of 43.3 %, referred to the rest of the period until 80 % charging.

The second scenario was created on the assumption of cone-shaped deposition. Phase 1 until 22:42 encompassed altogether three samples from the upstream half of the trap container; two of them were taken from 80 cm and one from 70 cm depth. The percentage of fine sediment smaller than

20 mm in this area was 47.5 %, in phase 2 (until 80 % fill) it was 50.4 %. Finally, both scenarios showed only small differences regarding their correlation coefficient. While gradual horizontal exclusion of fine sediments marginally decreased the underlying correlation coefficient of 0.926, subtraction based on the assumption of cone-shaped deposition marginally improved it even more to 0.927. Numerous further scenarios including shifted thresholds of minimum grain diameters (16, 18, 22 mm) did not achieve this coefficient, anymore. Beyond doubt the correlation is good enough to provide a basis for more accurate predictions of bedload yields at the study site.

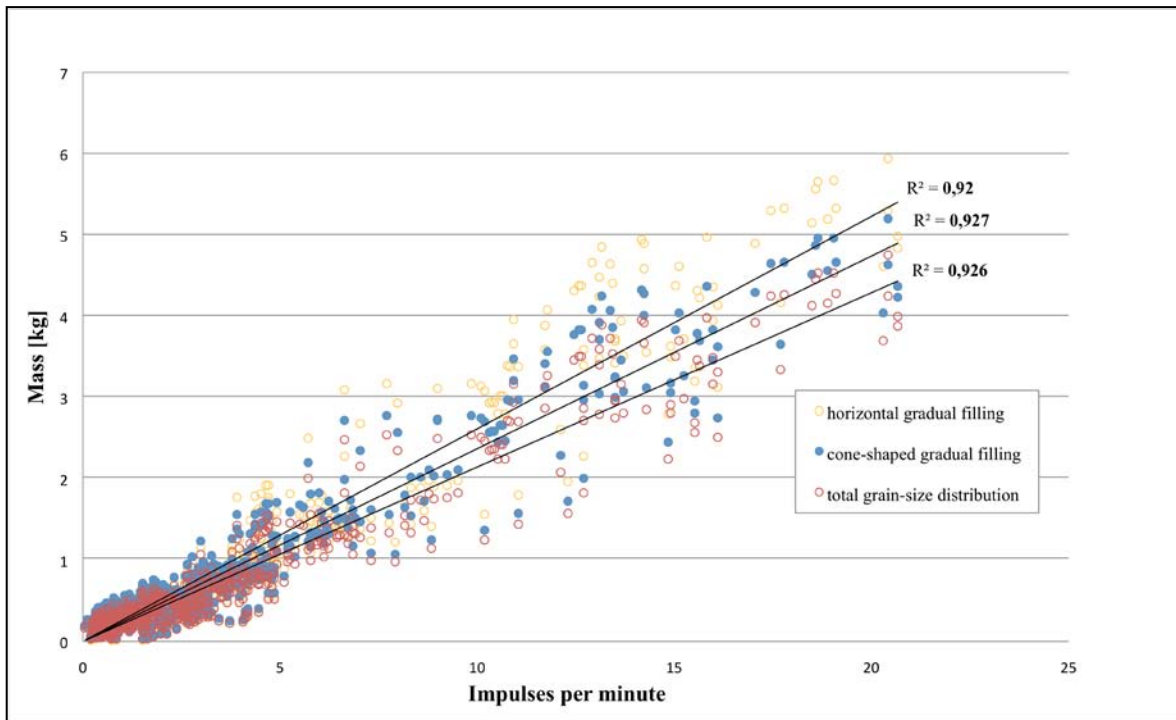


Figure 52: Linear correlation under exclusion of grain-sizes smaller than 20 mm

6.4 Calculation of bedload transport yield

The formula obtained by linear regression at 80 % filling level (including all grain-sizes) in combination with the entire cross-sectional geophone impulses recorded simultaneously to the measuring period of the lift trap enables the calculation of the total bedload yield in Dellach/Drautal for the respective time span from July 30 to July 31 2009. Regarding the spatial cross-sectional percentage of recorded impulses between 10:42 p.m. and 01:07 a.m., the geophone number 32 in orographic right position, which is directly upstream of the lift trap, has a proportion of 4.3 % (see figure 52). Altogether, 48 480 impulses were counted within a period of 14 hours.

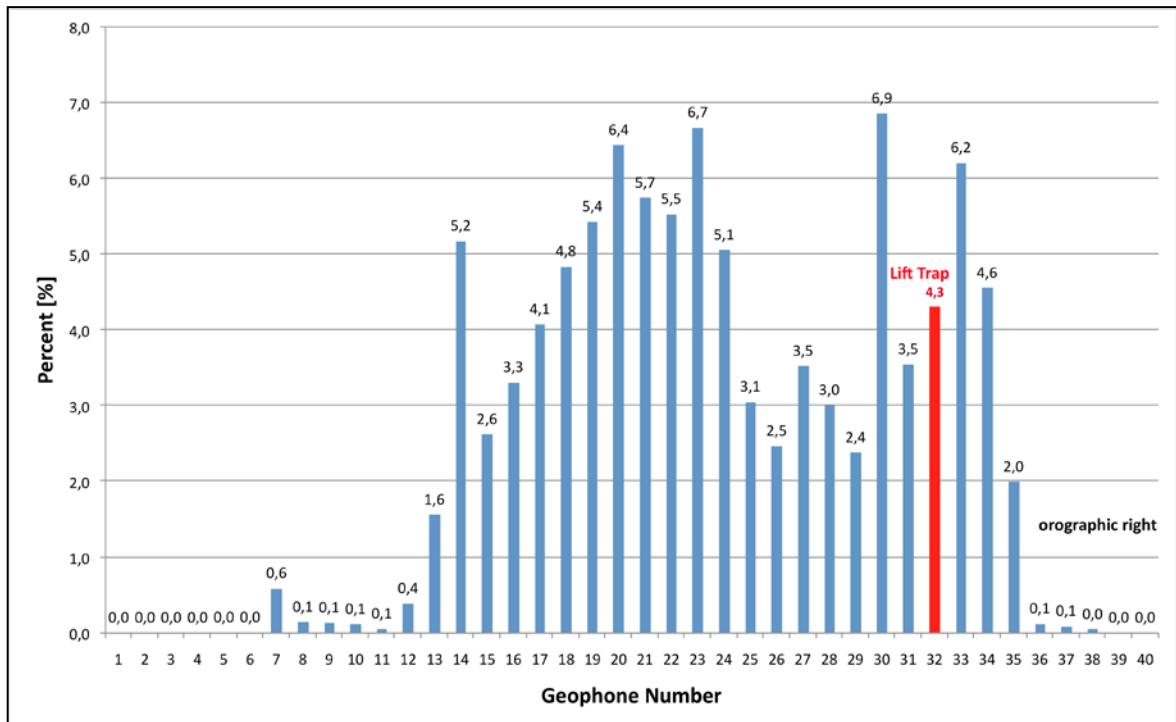


Figure 53: Impulse distribution at the cross-section from July 30 to July 31, 2009 (14 hours)

Derived from the correlation analysis in figure 51, the equation for the total bedload yield in Dellach/Drautal for the 16 hours - measuring period from July 30 to July 31 is:

$$\frac{100\%}{2,15\%} * 0,472 * \sum_{i=0}^{n \leq \text{trap full}} x_i \quad (\text{Equation 8})$$

where $x_i = 2088$ is the sum of impulses per minute and $2,15\% = \text{half of } 4,3\%$, considering only every second steel plate of the geophone device to be actually equipped with a geophone underneath.

Consequently, the in this way calculated bedload yield constitutes 45 839 kg, approximating 46 t within a period of 14 hours at discharge rates between $90 \text{ m}^3 \text{ s}^{-1}$ and $136 \text{ m}^3 \text{ s}^{-1}$.

For calculating the annual bedload yield, data of the total annual impulse distribution within the cross-section was deployed. Figure 53 and figure 54 reveal that in 2008, as well as in 2009 the proportion of yearly recorded impulses at geophone number 32 was about 2%.

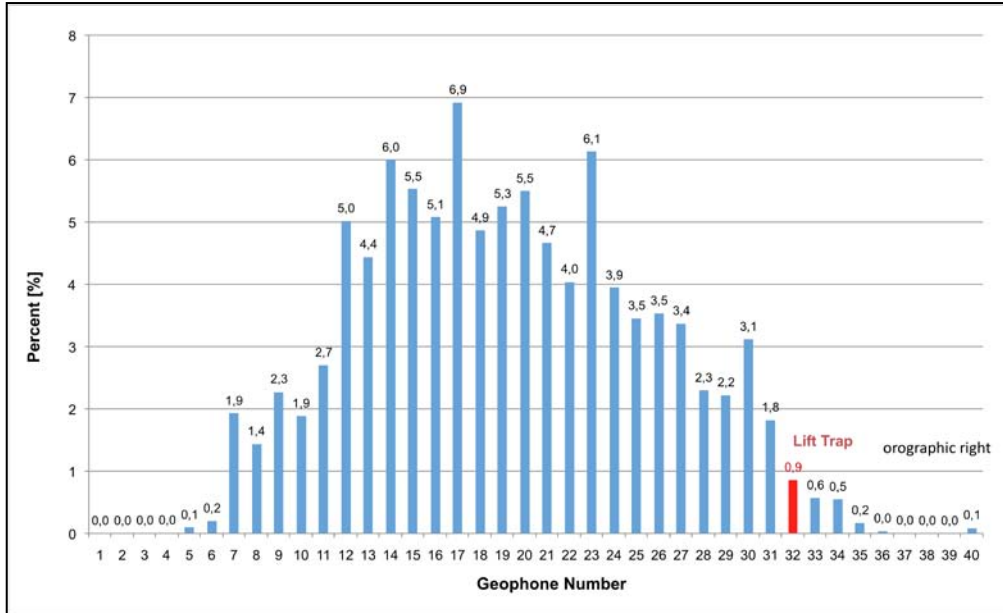


Figure 54: Annual impulse distribution at the cross section Dellach/Drautal in 2008

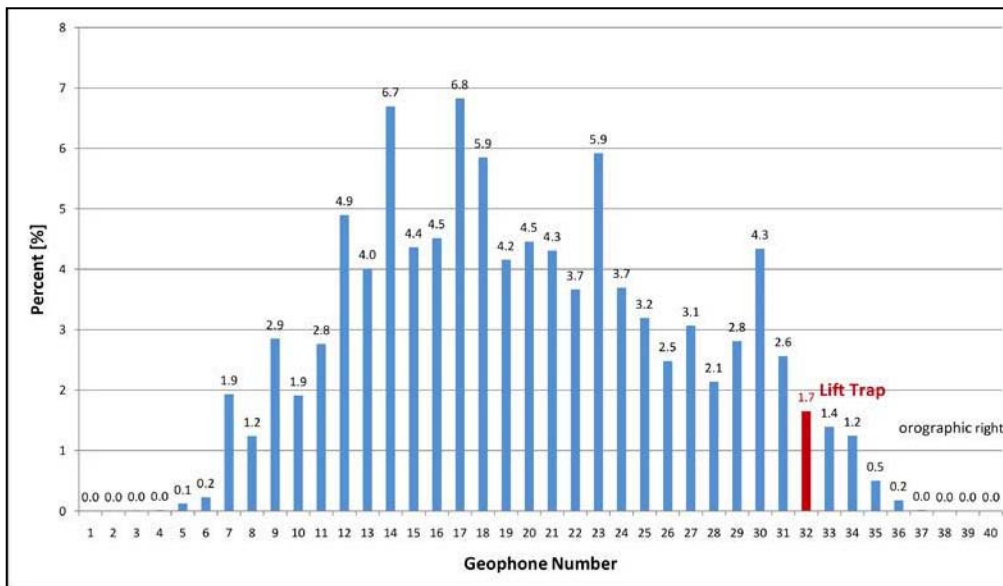


Figure 55: Annual impulse distribution at the cross section in Dellach/Drautal in 2009

A total of 52 042 259 impulses were recorded in 2009. Applying all these data to the equation derived from the measurement of July 2009, the computed annual bedload yield is 49 127 t. The amount computed by Kreisler (2010) on the basis of Helley-Smith measurements added up to 62 000 t per year. This significant divergence will be discussed in detail later on.

7 Discussion

7.1 Hydraulic efficiency: comparison with former slot trap

For better comparability, the horizontal and vertical current metering positions related to hydraulic efficiency determination were defined according to the measuring setup already applied in case of the first automatic slot trap system in Dellach im Drautal (Habersack et al., 2001).

Compared to the hydraulic lift trap, the at that time applied system consisted of a concrete tube of 2 m diameter and 1.5 m depth, a wooden cover and a slot width of 150 mm. Regardless of these differences in design, the hydraulic efficiencies of both traps were nearly 100% in cases of no fill.

While further current metering has not been undertaken at different filling levels within the new trap, Habersack et al. (2001) determined the hydraulic efficiency of their slot trap at stages of 20, 40, 60, 80 and 100% fill (see figure 55). Thereby it has to be mentioned that the first automated slot sampler at the study-site was operated, when directly comparable, continuous data from the geophone device did not exist. According to Bergmann et al. (2007), decreased sampling efficiency can be identified by a spontaneous decrease in the rate of filling regardless of the prevailing discharge conditions. Considering the identified increasing divergence between geophone graph and load curve from 80 % fill onwards, data comparison and correlation between weight increase and geophone impulses per minute can provide a good informative basis about the trap efficiency. With regard to the high correlation achieved at 80 % filling level, the measured high hydraulic efficiency of 97 % near the container bottom, general low flow velocities below 0.05 m s^{-1} within the sample container, the sampling efficiency and trap performance is assumed to be similar to the good results achieved by Habersack et al. (2001) on the first trap type.

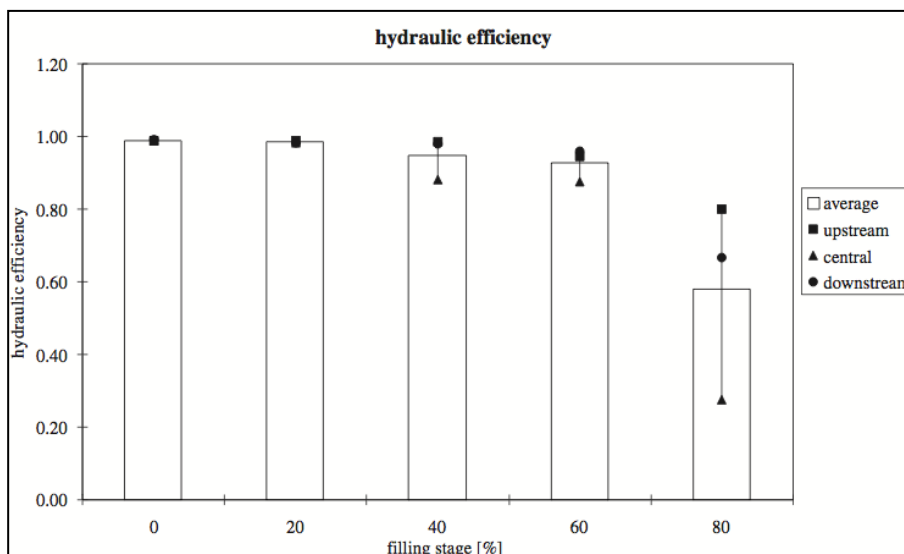


Figure 56: Changing hydraulic efficiency with filling level (Habersack et al., 2001)

However, this does not mean at all that under the present conditions further hydraulic efficiency measurements are dispensable. In particular the supposed increasing processes of scouring and winnowing from 80 % fill onwards should rather be tested on the hydraulic lift trap, as well.

7.2 Design modifications

So far, the hydraulic lift system proved to be very satisfying and promising in terms of functionality, trouble-free operation and handling. Except the unique hydraulic system, other features of the lift trap in Dellach can be compared directly with slot trap designs applied in other areas.

7.2.1 Slot door

By delaying the accumulation of bedload, removable slot covers provide the opportunity to sample defined stages of flood events. In combined arrangements of several samplers, sampling periods can be extended to the entire hydrograph (Bergman et al., 2007).

With regard to the mode of operation, the slot doors of the presently applied slot samplers in Dellach im Drautal are completely different to previous deployed slot covers in Nahal Eshtemoa, Israel (Bergman et al., 2007) and in the Drau River (Habersack et al., 2001).

In contrast to the hitherto complete removal of the cover, the hydraulic trap doors swing open inwardly and so remain a fixed part of the system (see figure 57).

Besides, the slot cover deployed in Israel is detached manually by pulling a steel cable. This cable is carried by two small pulleys and connected to a pair of spring-loaded catches, which hold the cover in position until the operator decides to activate sampling (Bergmann et al., 2007).

In case of the lift trap, two interlock bolts retain the door in place until they get pushed away hydraulically, at which point the door swings open, exposing the slot and allowing sampling to commence. The opening mechanism of the slot door is also triggered manually, but via remote control located in the PortakabinTM on the riverbank. Regarding the proposed main application area of the lift trap, in this position it is theoretically possible to perform sampling during flood events of HQ₁₀₀ without any risk for the operating person.

The main threat for the operational reliability of both opening systems is fine sediment. Bergmann et al. (2007) report an event in Nahal Eshtemoa, Israel, where floating organic debris yanked the cable of the slot cover. Even if the slot thereby was opened just partially, fine sediment entered the slot inadvertently and so anticipated the actual sampling. It could be assumed that this would not have happened in case of hydraulic trap doors, because in contrast they do not include any free-floating constituent parts. However, since their installation in 2006, the two fixed bedload slot traps unfortunately were not able to come into operation, yet, because their hydraulic opening system became also blocked by unintended massive fine sediment accumulation within the inner trap. The

assumed reason for malfunction is insufficient sealing of the trap covers; this problem can only be fixed at the general overhaul next winter.

Due to the fact that the hydraulic lift trap in contrast can be lifted almost any time above the water surface, the rubber seals of its trap door and the stiffness of the door itself were immediately improved after problem identification, trouble-free operation could easily be ensured.



Figure 57: Mechanism of slot cover (Bergman et al., 2007) compared to mechanism of trap door

7.2.2 Side doors

According to previous applied slot trap sampling systems (Habersack et al., 2001; Bergmann et al., 2007), also the lift trap is equipped with two container sidewall doors to be able to study the sediment stratification and textural changes within the trap. Thereby obtained information about the variation in grain-sizes and texture can afterwards be compared with data from the hydrograph and the geophones.

However, if not performed in the cautious way of slightly inclining the dewatered sample container backwards when the doors get opened, the loose material most likely slips out immediately. As a result, the analysis of stratification becomes very complicated. This was the case when one of the container doors of the lift trap in Dellach got opened (see figure 58). A possible design modification in this regard could be an incorporated acrylic glass window in the container wall, what already has been successfully deployed by Kuhnle (1992) in a slot sampler installed in Goodwin Creek (see figure 59). As another alternative the author recommends the use of a removable mesh-wire fence (mesh-width about 5 mm) behind the container side doors.



Figure 58: Faulty removal of the trap side door



Figure 59: Acrylic glass window (Kuhnle, 1992)

7.2.3 Load cells

On the strength of higher precision and stability, reduced operating troubles, independence of water stage and elimination of temperature effects (Lewis, 1991 and Sear et al., 2000), the actual weighing system is based on load cells instead of previous commonly applied pressure pillow systems. Thereby, instead of using one single, centrally placed load cell (Lewis, 1991), each sample container in Dellach rests on four load cells to ensure stability in the event of uneven filling. Besides, the load increase in this way is transmitted completely and directly to the strain gages. Taking into account the considerable expenditures of around 10.000 € for the present weighing system of the traps in Dellach, a possible alternative in terms of costs is provided by Sear et al. (2000): They deployed just a single load cell on the bottom of a sample container of 0.27 m², whereas the pressure was distributed uniformly on the strain gage by utilising a specially designed stainless steel scissor cradle (see figure 60). Before applying this system to the weighing system in the Drau River, it should be considered that for a container bottom area of 1.44 m² the cradle would need to be considerably larger. Besides, the cradle is a mechanical system, which needs regular servicing (Sear et al., 2000). With regard to the already quite high work input in Dellach, additional efforts are not desirable.

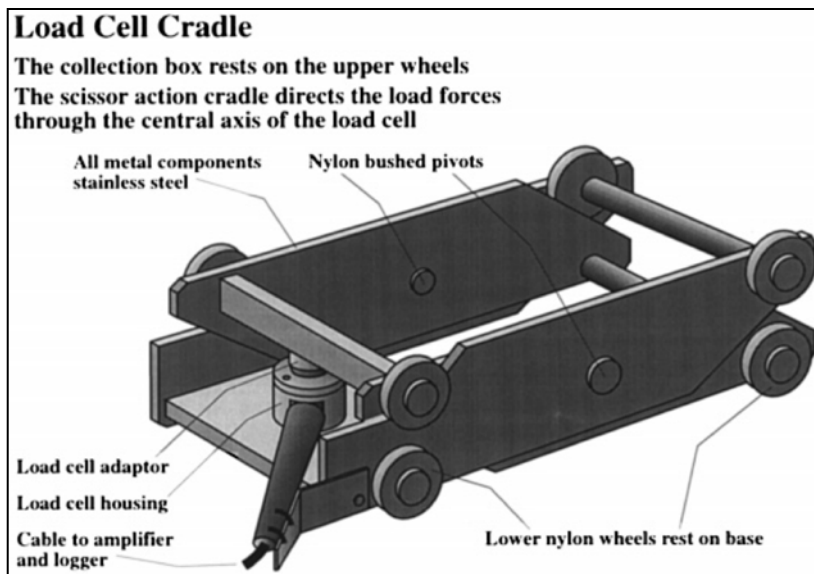


Figure 60: Uniform pressure distribution by scissor cradle (Sear et al., 2000)

7.3 Texture and grain-size analysis

Comparing the morphology and texture of deposited bedload within the lift trap with bedload accumulations already observed and documented in other slot samplers, some differences become obvious: Bedload depositions in the first slot trap deployed in the Drau have shown a higher concentration of large grain-sizes in the centre of the sample container (Habersack et al., 2001). In contrast, analyses by Laronne et al. (2003) in an ephemeral gravel-bed channel in the Rahaf and Qana'im in Israel have revealed a distinct and quite symmetric sideways increase in texture. As a reason for this the authors give variations in the angle of stratification, respectively an asynchronous accumulation of bedload in horizontally sliced samples. The grain-size distribution in the lift trap for now shows a trend to larger textures at the downstream end of the box. However, it has to be admitted that comparably few samples have been taken from horizontal layers of the lift trap, so far. Of each slice two to three representative samples were taken in longitudinal direction, but sideways differentiation was omitted. In this regard the need for more detailed stratification analyses in future samplings would have to be pointed out.

Nevertheless, the quite symmetric sideways increase in texture and varying angle of stratification found by Laronne et al. (2003) might also be supportive for the case of cone-shaped accumulation within the lift trap. Assumptions about the moment of deposition of single sediment layers and the accumulation behaviour in general so far have been based on comparison between sample textures and data from discharge, weight increase and geophone impulses. To achieve even better certainty in this regard, more detailed stratification samples should be taken and also be compared with results from Helley-Smith samplings performed under comparable hydraulic conditions.

The sieve analysis revealed that more than 50 % of the trapped material was smaller than 20 mm; the standard grain-size diameter d_m of the bulk sediment trapped was not more than 22.37 mm. Interestingly, the comparison of four selected grain-size percentiles (D_{50} , D_{84} , D_{90} and $D_{maxb} = D_{100}$) of the respective bulk sediment trapped by five slot samplers in Nahal Eshtemoa, Israel (Bergmann et al., 2007) and the present data from the lift trap shows great similarity (see table 5), despite completely different environmental conditions. Apart from distinctions in terms of bed morphology, vegetation cover and specific density of bed material, the major difference is the lack of channel-bed armouring in ephemeral channels. Due to quickly subsiding, intense flash floods occurring in desert regions, the bed has little time to reorganise itself by selective non-entrainment and the formation of an armour layer consisting of coarse material. As a result, the ungraded bed material becomes highly mobile at comparative low fluid shear stress (Laronne et al., 1994). Nevertheless, the single grain-size percentiles of the trapped material of both study sites exhibit quite similar diameters.

Another distinctive feature all displayed grain-size percentiles have in common is that D_{90} is always much less than half of the respective measured maximum b-axis diameters. According to Bergmann et al. (2007), D_{max} tends to be erratic and its large distance to D_{90} demonstrates the frequently reported randomness concerning the size of the single largest grain (Wilcock, 1992).

Table 5: Comparison between selected grain-size percentiles in different trap samplers

	Nahal Eshtemoa, Israel (Bergmann et al., 2001) Grain size, b-axis, mm, in sampler (slot width, mm)					Drau
Grain-size percentiles	Sampler L (165)	Sampler LC (110)	Sampler C (110)	Sampler RC (165)	Sampler R (110)	Lift trap (500)
D_{50}	12	13	14	13	11	18
D_{84}	32	36	40	35	37	38
D_{90}	41	43	51	44	48	47
D_{maxb}	102	123	106	150	130	125

7.4 Correlation results

The comparison of the cumulative weight curve with the related discharge shows a very similar trend. Also the curve of geophone impulses per minute develops in accordance with the hydrograph; a first sudden increase in impulses was recorded when the discharge exceeded $110 \text{ m}^3 \text{ s}^{-1}$, highest impulse rates were counted proximately to the peak discharge. This accordance is surprising and cannot be taken for granted, however. According to Turowski et al. (2008), often observed independence of bedload transport rates from discharge may have several reasons:

- displayed in distinct peaks of geophone impulses (Habersack et al., 2001), bedload transport usually occurs in waves
- fluctuation of channel-borne bedload supply during measurement periods
- small tributaries and landslides from riverbanks provide additional bed material at unchanged discharge rates

With regard to fluctuating bedload flux, the raw data recorded by geophones and load cells requires editing before reliable correlation results can be achieved. First, this involves the application of a moving average of 15 minutes in order to smooth out short-term fluctuations and highlight the longer-term trend. Afterwards, the direct comparison between the time dependent curve of impulses and the chronological trend of weight increase enables the visual identification of significant divergences. In combination with findings from the sedimentation analysis in this way it was possible to reveal the filling from 1:07 onwards to be faulty. The standard grain-size diameter d_m in this layer was only 13,6 mm, compared to 22,4 mm in the adjacent layer below. By ignoring the last 20 % of charging the correlation coefficient was consequently improved from 0.815 to 0.926. The geophone device in this regard turned out to be very supportive for trap efficiency control. Besides, in combined use a basis for more accurate predictions of bedload yields at the study site was provided.

On the other hand, it was not possible to verify the proper calibration of the geophones and their minimum threshold of 20 mm just on basis of trap data, so far. Reasons therefore are the quite uniform distribution of fine sediments over the entire sampling period until 80 % fill, or rather the for this purpose small number of samples taken from the container. Subtracting grain-sizes smaller than 20 mm stepwise according to their mean proportion at different filling levels resulted only in minor changes of the correlation coefficient, in which the procedure in consideration of a cone-shaped filling showed the best value of $R^2 = 0.927$. Also iterative shifting of the threshold upwards and downwards 20 mm did not improve the correlation, but has only shown small decreases. Using just data from the trap, the presumed threshold of 20 mm for geophone recordings can still only be assumed. For improved certainty in this regard, combined calibration measurements of a geophone and a directly adjacent LHSS could be more suitable.

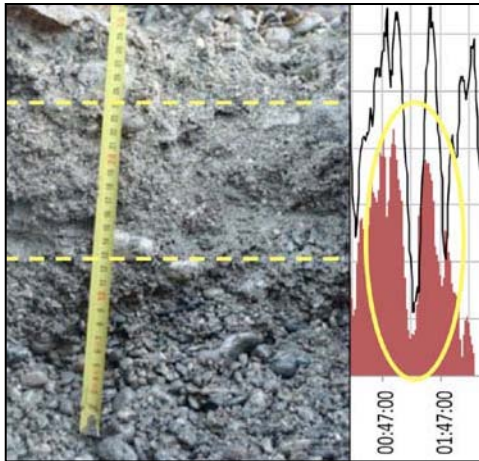


Figure 61: Disproportional amount of fine grain-sizes displayed in the graph

Due to the worldwide unique combination of the two measuring devices in a large alpine gravel-bed river, direct comparison with data from somewhere else is not possible, so far. Other research projects with related focussing were based on extensive calibration measurements with piezoelectric impact sensors and geophones in several torrents in Switzerland and Austria (e.g. Turowski et al., 2008; Rickenmann and McArdell, 2007). In the Pitzbach torrent in Tyrol, Rickenmann and McArdell (2007) analysed the correlation between sensor impulses and weight increase in the settling basin of a weir. Over short period there was a large scatter between number of impulses and bedload weight, but when they deployed moving averages from 15 minutes upwards, a linear correlation became obvious. Using a resolution of 15 minutes, the coefficient of determination was 0.56; with daily values a coefficient of even 0.91 could be achieved (Rickenmann and McArdell, 2007).

Recently, geophone installations in the Erlenbach mountain torrent in Switzerland have been supplemented by an automatic and continuous bedload sampling system, too (Rickenmann et al. 2010). For the purpose of combined data logging, movable, slot-type cubic baskets were mounted on a rail at the wall of a large check dam downstream of the geophone device (see figure 62). Compared to large gravel-bed rivers, such as the Drau, the small channel of the Erlenbach thereby allows for sampling of the entire cross-section. First measurement results of this alternative system were quite promising in terms of correlation. Additionally, the slot-type cubic baskets also enable the short-term monitoring of discharge-related grain-size distributions. But by reason of a wire mesh width of 10 mm, smaller sizes cannot be detected. Besides, while slot samplers usually feature quite good stratifications within, deposition in case of the basket system is assumed to occur more erratically, because the interior in contrast is not separated from the natural flow. Nevertheless, even if both systems show significant differences in areas of application and construction, the comparison of future results at least might help to improve the calibration of geophones in general.



Figure 62: Basket trapping bedload sample (Rickenmann et al., 2010)

7.5 Annual bedload yield calculation

On the strength of the directly underlying data obtained from geophones, lift trap and water gauge, the calculated bedload yield of 46 t during the reference measurement (July 30 – July 31) is quite reasonable, even if other comparable results do not exist so far.

This is not the case with regard to the predicted annual bedload transport yield: Comparing the results of 49 000 t per year versus 62 000 t per year, there is a significant difference between the calculated bedload yield with data from the lift trap and the previous calculation by Kreisler (2010), which was based on Helley-Smith measurements. While for the purpose of calculation the data from the lift trap were just correlated to the counted geophone impulses per year, the latter were related to the respective values of the annual discharge hydrograph. For more realistic and reliable results, the initial function derived from HS samplings and discharge rates was adapted to a sigma-function, which, instead of rising exponentially with increasing discharge, visually approximates an asymptote in the data areas of minimum and maximum bedload flux. With defined boundary values on the basis of local conditions it was possible to extend the sigma-curve to areas, where for high discharges data was missing (Kreisler, 2010).

Figure 63 displays the so far available measuring results of the lift trap (in yellow) in relation to the functions generated by Kreisler (2010). Thereby, it becomes obvious that the information gathered from the lift trap covers only a comparably small section of the (sigma-) function, namely in the discharge range from 90 to 136 m³ s⁻¹. Taking this into consideration, it is too early to make reliable statements regarding the annual bedload yield just on the basis of the present data. For this purpose and also in order to verify the run of the sigma-function generated by Kreisler (2010), more measurements are essential, in particular at high rates of discharge.

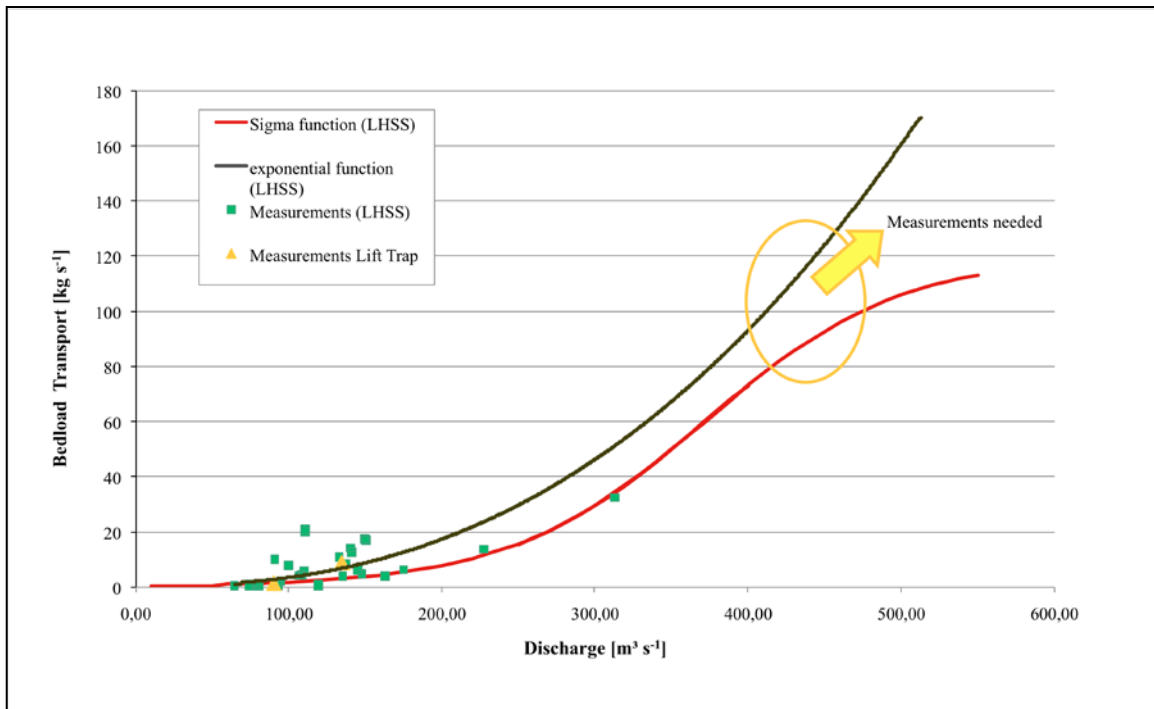


Figure 63: Relation between discharge and bedload transport (adapted from Kreisler, 2010)

Consideration of expenditures

Due to the included hydraulic system, the lift-trap certainly caused higher costs for material and construction than the two fixed bedload traps at the study site. But after one year of practical application it already became obvious that this improved adaption to perennial conditions significantly contributes to reduced expenditures on servicing and labour. By simply lifting the trap above water surface, in particular regular maintenance work, such as the replacement of scuffed nuts and the removal of fine sediments can be performed comparatively effortless (see figure 64). In contrast, figure 65 displays that for any regular servicing at the fixed slot traps a provisional dam needs to be built around by a bucket digger. Moreover, this procedure can only be undertaken during low water in winter and even if done so, some water always ingresses inevitably through the gravel dam. As a consequence of the to some extent unavoidable submerged conditions and the prevalent turbidity, servicing of the fixed traps turned out to be very laborious and was often likely to fail. Apart from the high lease costs for the bucket digger of 1000 € per day and the permanent risk of failure, the required deployment of heavy equipment also implies a regular, severe disturbance of aquatic ecosystem at the study site. In this regard, the hydraulic lift trap is not only suitable in terms of periodic maintenance and labour costs, but also for application in sensitive environments, such as the Drau River.



Figure 64: Maintenance operation at hydraulic lift trap (August 2009)



Figure 65: Maintenance operation at fixed slot samplers (April 2010)

8 Conclusions

Bedload transport measurements are essential for detailed understanding of bedload regimes and provide a basis for reliable calibration of bedload transport equations. In this regard, they describe an important element in planning and design of modern hydraulic engineering measures related to river restoration, riverbed fixation and flood protection.

The combined use of direct and indirect measuring techniques proved to be most promising for comprehensive recording of bedload transport processes, because only in this way it is possible to compensate individual shortcomings. A widely accepted standard method for monitoring bedload does not exist, so far.

In the last three decades, automated slot trap systems have been deployed for direct and continuous bedload sampling under various hydraulic conditions in several areas of the world. This independent measuring method mostly features robustness, high trap efficiency and minor impacts on natural flow conditions; attributes, which also make it perfect for a combined use with other bedload measuring systems.

The hydraulic lift trap installed in the Drau River is the latest version of a slot sampler. Equipped with two hydraulic plungers and cylinders and a hydrodynamic housing, its special adjustment for the year-round operation under perennial hydraulic conditions is worldwide unique.

Aforementioned general strengths of trap-type sampling systems can also be applied to the lift trap, measurements revealed a high hydraulic efficiency up to 97 %.

The lift trap is actually intended for systematic sampling during high discharges and flood peaks, considering its robust construction including a novel hydraulically operated and remotely controlled trap door. Thus, combined with other measuring methods including a Large Helley-Smith sampler, a geophone device and two fixed installed bedload traps, an important aim is the calculation of a bedload-rating curve for the complete hydrograph at the measuring site in Dellach. It should be noted that the first and so far only sampling with the hydraulic lift trap was undertaken in July 2009 at comparatively low discharge rates between 90 and 136 m³ s⁻¹. Nevertheless, the resultant comparably long time period of 15 hours required to fill the trap proved to be optimal to correlate the weight increase of the trap with the continuous, indirect recordings of the upstream geophone. Some characteristics of bedload transport initially gave rise to concern over the possible results of this correlation analysis: as displayed in distinct peaks of geophone impulses, bedload transport occurs in waves. Thus, bedload supply from the channel and the riverbanks to some degree fluctuates independently of the rate of discharge.

Another reason for concern was that more than 50 % of the trapped material was smaller than 20 mm and therefore too small to get recorded by the geophones.

However, apart from the last 20 % of filling, the proportion of small fractions turned out to be uniformly distributed. Besides, the application of a moving average of 15 minutes helped to smooth out short-term fluctuations and highlighted the longer-term trend of correlation. Considering the achieved coefficient of determination of $r^2 = 0.926$ after excluding the last 20 % of charging, the first correlation analysis between load increase and geophone impulses was very promising for further evaluations.

In general, the qualitative analysis of texture and grain-size distribution in combination with geophone data showed great potential for detailed assessment of the structural composition of bedload waves and their deposition behaviour within the trap. For this purpose, future measurements need to include far more samples from different layers of the trapped material. Also an in-depth analysis of geophone impulses and the improved calibration of the geophones, which should particularly focus on accurate determination of the threshold for recordings, would be beneficial. Because the exact deposition behaviour within the trap is hardly traceable, for this purpose calibration measurements using a LHSS directly adjacent to the geophone would be more suitable and promising.

The calculation of bedload yields was made on the basis of the correlation analysis in combination with the collective dataset of the geophones. While the calculated yield for the duration of the underlying measuring period until 80 % fill seemed to be reasonable, the extrapolated annual bedload yield was much lower than the comparable result already achieved on the basis of Large Helley-Smith measurements. This can be explained by an incomplete bedload-rating curve in the area of high discharges. Consequently, additional data from floods is essential to optimise the present results. The hydraulic lift trap is the optimal instrument for this purpose.

All demands regarding functionality and operation reliability were met, so far. At the moment only the container side-doors and the arrangement of the weighing-system exhibit possibilities for optimisation.

From a practical and economical point of view, initial higher costs for material and construction of the hydraulic lift trap are partly outweighed by more sampling possibilities through the year-round option of emptying, easier handling and lower (personnel) expenses for periodic maintenance. Moreover, once constructed, the trap is suitable for operation in ecologically sensitive environments, such as the Drau River.

The identified methodological disadvantages of the lift trap are the limited coverage of only a small part of the cross-section and the fact that the deposition behaviour within the container will never be completely traceable.

Practical drawbacks are its expensive construction and the need for well-trained personnel in handling. Besides, heavy equipment is required for emptying.

To sum up, the hydraulic lift trap in particular features high functionality; due to its robust design and enough capacity for even sampling flood peaks, it is specially designed for application in large rivers. Thereby, the trap provides the option of application several times a year.

In contrast to many other bedload measuring techniques it does not disrupt the natural and is able to work independently. Moreover, past experience has revealed an excellent hydraulic and sampling efficiency.

From a practical point of view it is comparatively easy to handle and provides the option for mounting additional measuring instruments.

References

- ATV-DVWK, Deutsche Vereinigung für Wasserwirtschaft, Abwasser und Abfall. (2000). *Report: Morphodynamic Processes in Rivers* (in German). Hennef, August 2000.
- Bengtson, H. (2010). *Drag Force for Fluid Flow Past an Immersed Object*. Bright Hub. Retrieved April 19, 2010, from <http://www.brighthub.com/engineering/civil/articles/58434.aspx>
- Bergman, N., Laronne, J.B. & Reid, I. (2007). *Benefits of design modifications to the Birkbeck bedload sampler illustrated by flash-floods in an ephemeral gravel-bed channel*. *Earth Surface Processes and Landforms*, Volume 32, 317–328.
- Buffington, J. (1999). *The legend of A. F. Shields*. *Journal of Hydraulic Engineering*, Volume 125, Issue 4, 376–387.
- Buffington, J. & Montgomery, D. (1997). *A systematic analysis of eight decades of incipient motion studies, with special reference to gravel-bedded rivers*. *Water Resour. Res.*, Volume 33, Issue 8, 1993–2029.
- Bunte K, Abt S. R., Potyondy J. P., Ryan S. E. (2004). *Measurements of coarse gravel and cobble transport using portable bedload traps*. *Journal of Hydraulic Engineering*, ASCE 130, 879–893.
- Cao, Z., Pender, G., Meng, J. (2006). *Explicit Formulation of the Shields Diagram for Incipient Motion of Sediment*. *Technical Notes*. *ASCE Journal of Hydraulic Engineering*, Volume 132, Issue 10, 1097-1099.
- Delft Hydraulics. (2006). *Manual Sediment Transport Measurements. Chapter 5: Instruments Sediment Transport*. Delft Hydraulics, the Netherlands. Retrieved February 13, 2010, from: http://www.wldelft.nl/rnd/intro/fields/morphology/pdf/H5_Measuring_instruments_sediment_transport.pdf
- Delft Hydraulics. (2010). *E-40 probe for P-EMS*. Delft Hydraulics, the Netherlands. Retrieved June 17, 2010, from: <http://www.wldelft.nl/inst/velo/pems/e40.html>
- DVWK, Deutscher Verband für Wasserwirtschaft und Kulturbau. (1992). *Bedload Measurements* (in German). Paul Parey, Hamburg und Berlin, Heft 127.
- Einstein, H. A. (1944). *Bed-load transportation in Mountain Creek*, in: Lewis J. (ed): *An improved bedload sampler: Proceedings of the Fifth Federal Interagency Sedimentation Conference, Las Vegas, Nevada, VI 1 – VI 8*. Retrieved April 22, 2010 from: <http://www.fs.fed.us/psw/publications/lewis/Lewis91.pdf>
- El Kadi Abderrezak, K. (2009). *Presentation: Bedload Sediment Transport*. Santa Fe, Argentina. Retrieved June 4, 2010, from: <http://www.sos.bangor.ac.uk/~oss062/RCEM%20Short%20Course/Kamal/Bedload/Elkadi-RCEM2009-BEDLOAD.pdf>
- Emmett WW. (1980). *A Field Calibration of the Sediment-Trapping Characteristics of the Helley-Smith Bedload Sampler*, US Geological Survey Professional Paper 1139, Washington, DC.

- Environmental Protection Agency. (2008). *Channel Processes: Bedload Transport*. Watershed Assessment of River Stability & Sediment Supply (WARSSS), US EPA. Retrieved July 30, 2010, from: <http://www.epa.gov/WARSSS/sedsource/bedload.htm>
- Flintec. (2010). *Type SB4 Beam Type Load Cell*. Data Sheet. Retrieved July 30, 2010, from: <http://www.flintec.com/c2/uploads/sb4.pdf>
- Gao P. (2008). *Transition between Two Bed-Load Transport Regimes: Saltation and Sheet Flow*. Journal of Hydraulic Engineering 134: 340-349.
- Garcia, C., Laronne, J.B. and Sala, M. (2000). *Continuous monitoring of bedload flux in a mountain gravel-bed river*, in: Habersack, H., Nachtnebel, H.P., Laronne, J.B. (eds.): The continuous measurement of bedload discharge in a large alpine gravel bed river. Journal of Hydraulic Research, Volume 39, 125-133.
- Garcia, M. H. (2008). Sedimentation engineering: processes, measurements, modeling, and practice. ASCE Manuals and Reports on Engineering Practice. No. 110, 36.
- Graf, W. (1971). *Hydraulics of Sediment Transport*. McGraw-Hill Book Company, New York.
- Habersack, H.M. & Nachtnebel, H. P. (1994). *Analysis of sediment transport developments in relation to human impacts*, in: Variability in Stream Erosion and Sediment Transport (Proceedings of the Canberra Symposium December 1994). IAHS Publications, Volume 224, 385-383.
- Habersack, H. (1996). *Lack and surplus of sediments being transported by river systems*, in: Erosion and Sediment Yield: Global and Regional Perspectives (Proceedings of the Exeter Symposium, July 1996). IAHS Publications, Volume 236, 565-573.
- Habersack, H. (1997). *Spatiotemporal variability in the bedload regime and its management in the Drau River* (in German). Dissertation at the University for Applied Life Sciences, Vienna.
- Habersack, H., Nachtnebel, H. P. and Laronne, J. B. (1998). *The Hydraulic Efficiency of a Slot Sampler: Flow Velocity Measurements in The Drau River, Austria*, in: Klingemann, P. C., Beschta, R. L., Komar, P.D., Bradly, J.B./eds.): Gravel-bed rivers in the environment. Water Resources Publications, LLC, 749-754.
- Habersack, H. (2001). *Radio-tracking gravel particles in a large braided river in New Zealand: a field test of the stochastic theory of bed load transport proposed by Einstein*. Hydrological Processes, Volume 15, Issue 3, 377 – 391.
- Habersack, H., Nachtnebel, H.P., Laronne, J.B. (2001). *The continuous measurement of bedload discharge in a large alpine gravel bed river*. Journal of Hydraulic Research, Volume 39, 125-133.
- Habersack, H., Seitz, H., Liedermann, M. (2009): *Präsentation Geschiebeleitfaden*. Kick Off Meeting. Detection – Calibration - Interpretation (in German). Working session, Vienna, November 12, 2009.
- Habersack, H. (2009). *Sediment Regime, River Morphology, Ecological Condition and Flood Protection* (in German). National River Management Plan 2009, Vienna.

- Habersack, H., Seitz, H., Liedermann, M. (2010). *Integrated Automatic Bedload Transport Monitoring*. Published online as part of U.S. Geological Survey Scientific Investigations Report 2010-5091. p. 218-235. Retrieved October 10, 2010 from <http://pubs.usgs.gov/sir/2010/5091/papers/Habersack.pdf>
- Hayward, J. A. & Sutherland, A.J. (1974). *The Torlesse stream vortex-tube sediment trap*. Journal of Hydrology, Volume 13, No.1, 41-53.
- Hjulström, F. (1935). *Studies of the morphological activity of rivers as illustrated by River Fyriers*, in: Witt, K. J. & Johannsen, R. (eds.): Geotechnische und Ingenieurbio-logische Maßnahmen zum Erosionsschutz von Rekultivierungsschichten. Tagungsunterlage B05, 5. Leipziger Deponiefachtagung. Stilllegung, Sicherung, Nachsorge und Nachnutzung von Deponien, 2009.
- Hubbell, D. W. (1964). *Apparatus and techniques for measuring bedload*, in: Lewis J. (ed): An improved bedload sampler: Proceedings of the Fifth Federal Interagency Sedimentation Conference, Las Vegas, Nevada, VI 1 – VI 8. Retrieved April 22, 2010 from: <http://www.fs.fed.us/psw/publications/lewis/Lewis91.pdf>
- Hütte, M. (2000). *Ökologie und Wasserbau: ökologische Grundlagen von Gewässerverbauung und Wasserkraftnutzung*. Parey, Berlin, Wien, 23.
- Kodama, Y. (1994). *Downstream Changes in the Lithology and Grain Size of Fluvial Gravels, the Watarase River, Japan: Evidence of the Role of Abrasion in Downstream Fining*. Journal of Sedimentary Research, Volume 64a. Abstract retrieved from AAPG database.
- Krainer, K. (1994). *Die Geologie der Hohen Tauern*. Universitätsverlag Carinthia.
- Kreisler, A. (2007). *Petrografische Untersuchung des Geschiebetransportes an der Isel und Drau*. Fächerübergreifendes Projekt an der Universität für Bodenkultur. Wien
- Kreisler, A. (2010). *Bedload measurements at the Drau River: Comparison between direct and indirect methods* (in German). Thesis at the University of Applied Life Sciences, Vienna.
- Kresser, W., (1964). Gedanken zur Geschiebe- und Schwebstoffführung der Gewässer. ÖWW, 16. Jg., H. 1/2, 6-11.
- Krenmayr, H. (1999). *Rocky Austria - Eine bunte Erdgeschichte von Österreich*. Geologische Bundesanstalt, Vienna.
- Kuhnle, R. A., Willis, J.C. & Bowie, A.J. (1988). *Measurement of bed load transport on Goodwin Creek, Northern Mississippi*, in: Habersack, H., Nachtnebel, H.P., Laronne, J.B. (eds.): *The continuous measurement of bedload discharge in a large alpine gravel bed river*. Journal of Hydraulic Research, Volume 39, 125-133
- Kuhnle, R. A. (1992). *Bedload yield and in-channel provenance in a flash-flood fluvial system*, in: Dynamics of Gravel-Bed Rivers, Billi P, Hey RD, Thorne CR, Tacconi P (eds.): Wiley, New York, 551–554.
- Laronne, J. B. & Cohen, H., (1998). *Optimization of gravel mining and estimation of reservoir sedimentation rates in the south eastern coast of the Dead Sea*, in: Habersack, H., Nachtnebel, H.P., Laronne, J.B. (eds.): *The continuous measurement of bedload discharge in a large alpine gravel bed river*. Journal of Hydraulic Research, Volume 39, 125-133.

- Laronne, J. B., Alexandrov, Y., Bergman, N., Cohen, H., Garcia, C., Habersack, H., Powell, D. M. & Reid, I. (2003). *The continuous monitoring of bed load flux in various fluvial environments. Erosion and Sediment Transport Measurement in Rivers: Technological and Methodological Advances*. Proceedings of the Oslo Workshop, June 2002. IAHS Publications, Volume 283, 134–145.
- Laronne, J. B., Reid, I., Yitshak, Y. & Frostick, L.E. (1992). *Recording bedload discharge in a semiarid channel, Nahal Yatir, Israel*, in: Habersack, H., Nachtnebel, H.P., Laronne, J.B. (eds.): The continuous measurement of bedload discharge in a large alpine gravel bed river. *Journal of Hydraulic Research*, Volume 39, 125-133.
- Laronne, J. B., Reid, I., Yitshak, Y. and Frostick, L. E. (1994). *The non-layering of gravel streambeds under ephemeral flood regimes*. *Journal of Hydrology*, Volume 159, Issues 1-4, 353-363
- Leopold L. B., Emmett W. W. (1976). *Bedload measurements, East Fork River, Wyoming*, in: Bergman, N., Laronne, J.B. & Reid, I. (eds.): Benefits of design modifications to the Birkbeck bedload sampler illustrated by flash-floods in an ephemeral gravel-bed channel. *Earth Surface Processes and Landforms*, Volume 32, 317–328.
- Lewis J. (1991). *An improved bedload sampler*, in: Proceedings of the Fifth Federal Interagency Sedimentation Conference. Fan S, Kuo Y (eds.): Volume 6, 1-8. Retrieved April 22, 2010 from <http://www.fs.fed.us/psw/publications/lewis/Lewis91.pdf>
- Malcharek, A. (2009). *Sediment Transport and Morphodynamics* (in German). Institut für Wasserbau. Lecture notes, University of Munich.
- McCann, T. (ed.) (2008). *The Geology of Central Europe: Mesozoic and Cenozoic*. Geological Society, London, Volume 2.
- McGraw-Hill Encyclopedia of Science and Technology. (2005). *Wheatstone bridge*. Answers.com. The McGraw-Hill Companies. Retrieved June 6, 2010, from <http://www.answers.com/topic/wheatstone-bridge>
- Michor, K. et al. (1993). *Gewässerbetreuungskonzept Obere Drau. Lienz-Sachsenburg, I. Zusammenfassender Bericht*, in: LIFE Final Report: Auenverbund Obere Drau. Bundeswasserbauverwaltung. Klagenfurt, Carinthia.
- Milhous, R. T. (1973). *Sediment transport in a gravel-bottomed stream*, Lewis J. (ed): An improved bedload sampler: Proceedings of the Fifth Federal Interagency Sedimentation Conference, Las Vegas, Nevada, VI 1 – VI 8. Retrieved April 22, 2010 from: <http://www.fs.fed.us/psw/publications/lewis/Lewis91.pdf>
- Muhar, S., Jungwirth, M., Unfer, G., Wiesner, C., Poppe, M., Schmutz, S., Hohensinner, S., Habersack, H. (2008). *Restoring riverine landscapes at the Drau River: successes and deficits in the context of ecological integrity*, in: Habersack, H., Pié gay, H., Rinaldi, M. (eds.): Gravel-Bed Rivers VI, From Process Understanding to River Restoration. Elsevier, 779-801.
- Mühlhofer, L. (1933). *Analysis of the suspended load and bedload transport in the Inn River near Kirchbichl* (in German). *Die Wasserwirtschaft*, No. 1-6.

- Omega Engineering Inc. (2010). *Introduction to Load Cells*. Omega Engineering Technical Reference. Retrieved July 30, 2010, from: <http://www.omega.com/prodinfo/loadcells.html>
- Patt, H., Jürging, P., Kraus, W. (2004). *Naturnaher Wasserbau. Entwicklung und Gestaltung von Fließgewässern*. Springer, Berlin, Heidelberg, 2nd edition.
- Petutschnig, W., Petutschnig J. & Egger G. (1991). *Gefährdete Augewässer im Oberen Drautal*. Carinthia II, 181./101.Jg., 79-87. Retrieved July 12, 2010, from http://www.biologiezentrum.at/pdf_frei_remote/CAR_181_101_0079-0087.pdf
- Pichler, F.(2003). *LIFE-Project Upper Drau River. Final Report* (in German). Administration of hydraulic construction, Klagenfurt. Retrieved July 20, 2010, from http://ec.europa.eu/environment/life/project/Projects/files/book/LIFE99_NAT_A_006055_Endbericht_Monitor.pdf
- Powell, M., Reid, I., Laronne, J.B. & Frostick, L. (1998). *Cross-stream variability of bedload flux in narrow and wider ephemeral channels during desert flash floods*, in: Habersack, H., Nachtnebel, H.P., Laronne, J.B. (eds.): The continuous measurement of bedload discharge in a large alpine gravel bed river. *Journal of Hydraulic Research*, Volume 39, 125-133.
- Reid, I., Layman, J.T. & Frostick, L.E. (1980). *The continuous measurement of bedload discharge*. *Journal of Hydraulic Research* 18, 243-249.
- Rickenmann, D., McArdeell, B.W. (2007). *Continuous measurement of sediment transport in the Erlenbach stream using piezoelectric bedload impact sensors*. *Earth Surface Processes and Landforms*, 32, 1362-1378, doi: 10.1002/esp. 1478
- Rickenmann, D., Turowski, J. M., Hegglin, R. and Fritschi, B. (2010). *Improving sediment transport measurements in the Erlenbach stream using a moving basket system*. Swiss Federal research Institute WSL. Presentation Poster at the Conference of the European Geosciences Union, May 2010.
- Rijn, L. C. van (2007). *Manual sediment transport measurements in rivers, estuaries and coastal seas*. Aquapublications. The Netherlands. Retrieved February 14, 2010, from http://www.coastalwiki.org/coastalwiki/Manual_Sediment_Transport_Measurements_in_Rivers,_Estuaries_and_Coastal_Seas
- Ryan, S. E., Bunte, K. & Potyondy, J.P. (2005). *Breakout Session II, Bedload-Transport Measurement: Data Needs, Uncertainty, and New Technologies*. US Geological Survey Online Publications. Retrieved June 16, 2010, from http://pubs.usgs.gov/circ/2005/1276/pdf/Breakout_SessionII.pdf
- Schober, S. (1999). *Messung des Feststofftransportes an der Oberen Drau und der Unteren Isel*. Thesis at the University for Applied Life Sciences, Vienna.
- Sear, D. A., Damon, W., Booker, D. J. and Anderson, D. G. (2000). *A Load Cell based continuous Recording Bedload Trap*. *Technical Communication*. *Earth Surface Processes and Landforms*, Volume 25, 659-672.

- Seitz, H., Kreisler, A., Habersack, H. (2009). *Bedload Measurements at Drau River and Isel River* (in German). Progress report. IWHW, May 2009.
- Sensor. (2008). *Sensor Geophones*. Voorschoten, The Netherlands. Retrieved July 26, 2010, from <http://www.geophone.com/techpapers/Geophone-brochure.pdf>
- Shields, A., (1936). *Anwendung der Ähnlichkeitsmechanik und der Turbulenzforschung auf die Geschiebebewegung*, in: Strobl, T., Zunic, F. (eds.): *Wasserbau. Aktuelle Grundlagen, Neue Entwicklungen*. Springer-Verlag, Berlin, Heidelberg, 2006, 104 pp.
- Tacconi, P. & Billi, P. (1987). *Bed load transport measurements by the vortex-tube trap on Virginio Creek, Italy*. in: Lewis J. (ed.): *An improved bedload sampler: Proceedings of the Fifth Federal Interagency Sedimentation Conference, Las Vegas, Nevada, VI 1 – VI 8*. Retrieved April 22, 2010 from <http://www.fs.fed.us/psw/publications/lewis/Lewis91.pdf>
- Tollmann, A. (1980). *Geology and Tectonics of the Eastern Alps (Middle Sector)*. International Geological Congress: 26th Session. Institute of Geology, Vienna. Retrieved July 30, 2010, from http://www.geologie.ac.at/filestore/download/AB0034_197_A.pdf
- Turowski, J. M., Badoux, A., Rickenmann, D., Fritschi, B. (2008). *Erfassung des Sedimenttransportes in Wildbächen und Gebirgsflüssen. Anwendungsmöglichkeiten von Geophonmessanlagen*. Wasser Energie Luft - 100. Jahrgang, Heft 1, Baden, Switzerland.
- University of Innsbruck. (1980). *Tyrol. Geology and Tectonics*. Institute for Geography. Universitätsverlag Wagner, Innsbruck.
- U.S. Army Corps of Engineers (COE). (1994). *Engineering and Design: Channel Stability Assessment for Flood Control Projects*. EM 1110-2-1418. U.S. Army Engineer Waterways Experiment Station, Vicksburg, MS. Retrieved June 5, 2010, from <http://140.194.76.129/publications/eng-manuals/em1110-2-1418/toc.htm>
- Vericat D, Church M, Batalla R. (2006). *Bedload bias: comparison of measurements obtained using two Helley-Smith samplers in a gravelbed river*. *Water Resources Research* 42, 1–13.
- Wilcock P. R. (1992). *Flow competence: a criticism of a classic concept*. *Earth Surface Processes and Landforms* 17, 289–298. Abstract retrieved from Wiley Interscience database.
- Yang, C.T., (1996). *Sediment Transport: Theory and Practice*. McGraw-Hill, New York, 396 pp.
- Zanke, U. (2002). *Hydromechanik der Gerinne und Küstengewässer*. Parey, Berlin, Germany.

Acknowledgement

I would like to thank Ao. Univ. Prof. DI Dr. Helmut Habersack for supervising this thesis and providing me thereby with valuable ideas and suggestions.

In this regard I am also particularly grateful to Mr Graeme Buchan, my co-supervisor at Lincoln University in Christchurch/New Zealand.

Special thanks go to my advisor, DI Hugo Seitz, whose encouragement, guidance and support from the initial to the final level enabled me to develop an understanding of the subject. Our field work at the Drau River and in Tyrol will always remain in good memory.

At this point I would also like to express my gratitude to my parents and family, who not only allowed me to go my own way, but also encouraged and supported me in my interests.

I am heartily thankful to my partner Maria for the patience, understanding and love even at busy times during the completion of the project.

Last but not least I offer my regards and blessings to my friends, colleagues and all those who supported me in any respect during my years of study.

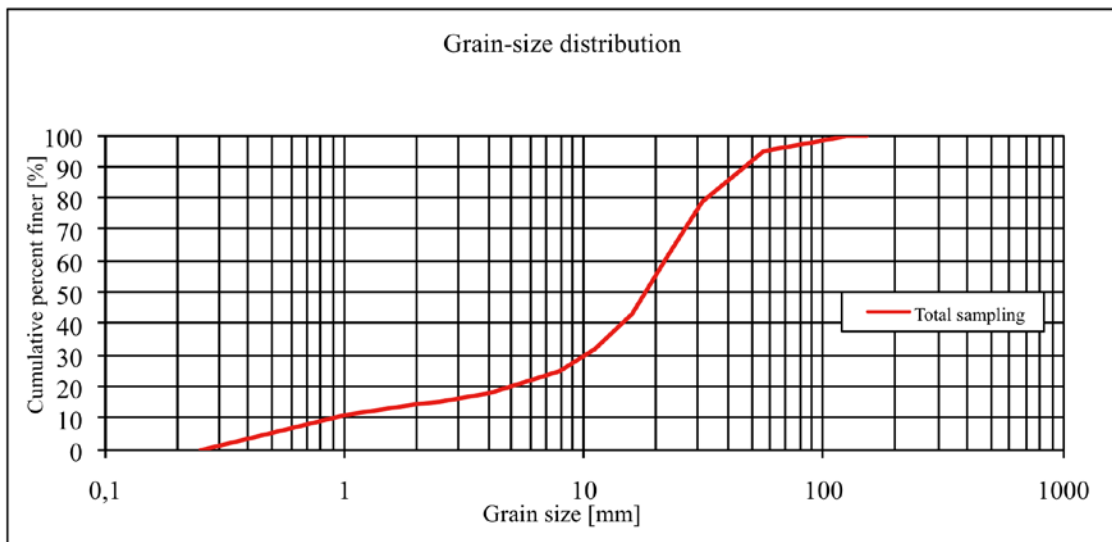
Appendix 1: Sieve analyses in detail

Sieve Analysis: total

Sampling date:	16.11.2009
Station:	Dellach Dellach Drau
Method:	Lift trap

Laboratory:	Bad Deutsch-Altenburg
Controller:	Hugo Seitz, Lukas Strahlhofer
Sieving date:	11.12.2009
Material condition:	dry
Net weight:	99,39 kg

Mesh width d [mm]	Sieve weight S [kg]	Catch+Sieve C+S [kg]	Catch C			Pass-through P [%]	Number Stones	Standard grain-size [mm]
			[kg]	[%]	[%]			
150,00	1,720	1,720	0,000	0,00	0,00	100,00		d ₁₀ = 0,87
125,00	1,720	1,720	0,000	0,00	0,00	100,00		d ₂₀ = 4,85
90,00	1,500	3,760	2,260	2,27	2,27	97,73		d ₃₀ = 10,12
63,00	1,520	3,100	1,580	1,59	3,86	96,14		d ₄₀ = 14,33
56,00	1,540	2,570	1,030	1,04	4,90	95,10		d ₅₀ = 18,09
31,50	1,690	17,590	15,900	16,00	20,90	79,10		d ₆₀ = 21,86
22,40	1,630	19,340	17,710	17,82	38,72	61,28		d ₇₀ = 26,47
16,00	1,720	19,400	17,680	17,79	56,50	43,50		d ₈₀ = 32,54
11,20	1,630	12,900	11,270	11,34	67,84	32,16		d ₉₀ = 46,62
8,00	1,650	8,760	7,110	7,15	75,00	25,00		d ₁₆ = 2,83
4,00	1,580	8,460	6,880	6,92	81,92	18,08		d ₈₄ = 37,57
2,50	1,440	4,240	2,800	2,82	84,74	15,26		d _m = 22,37
2,00	1,520	2,430	0,910	0,92	85,65	14,35		U = 25,00
1,00	1,430	4,690	3,260	3,28	88,93	11,07		C _c = 5,35
0,25	1,300	12,300	11,000	11,07	100,00	0,00		d _{max} = 125,00

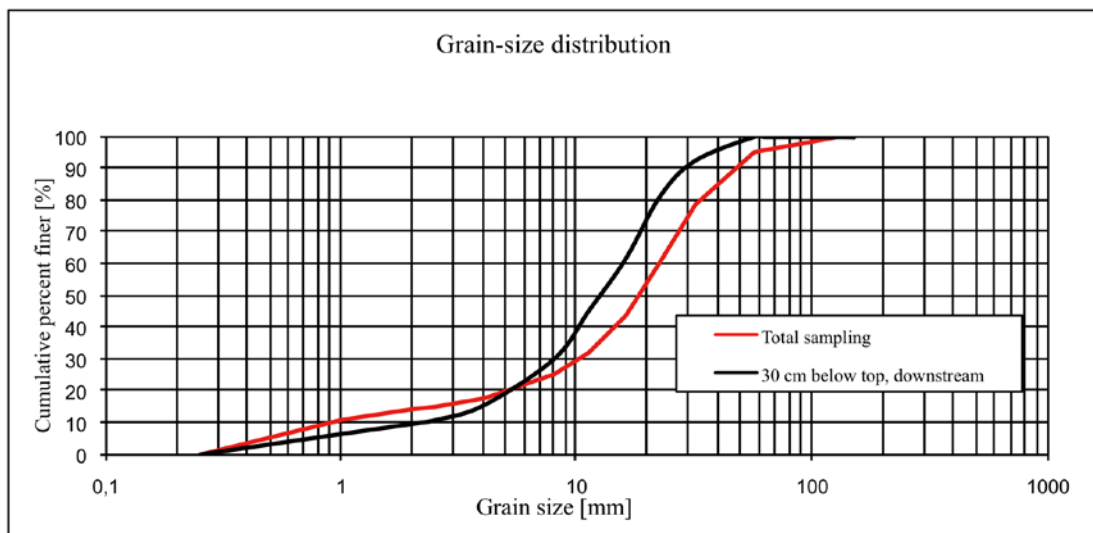


Sieve analysis: 30 cm below top, downstream

Sampling date:	16.11.2009	
Station:	Dellach	Dellach Drau
Method:	Lift trap	

Laboratory:	Bad Deutsch-Altenburg	
Controller:	Hugo Seitz, Lukas Strahlhofer	
Sieving date:	11.12.2009	
Material condition:	dry	
Net weight:	8,47 kg	

Mesh width d [mm]	Sieve weight S [kg]	Catch + Sieve C + S [kg]	Catch C			Pass-through P [%]	Number Stones	Standard grain-size [mm]
			[kg]	[%]	[%]			
150,00	1,720	1,720	0,000	0,00	0,00	100,00		d ₁₀ = 2,12
125,00	1,720	1,720	0,000	0,00	0,00	100,00		d ₂₀ = 4,95
90,00	1,500	1,500	0,000	0,00	0,00	100,00		d ₃₀ = 7,92
63,00	1,520	1,520	0,000	0,00	0,00	100,00		d ₄₀ = 9,95
56,00	1,540	1,540	0,000	0,00	0,00	100,00		d ₅₀ = 12,41
31,50	1,690	2,330	0,640	7,56	7,56	92,44		d ₆₀ = 15,48
22,40	1,630	2,580	0,950	11,22	18,77	81,23		d ₇₀ = 18,49
16,00	1,720	3,390	1,670	19,72	38,49	61,51		d ₈₀ = 21,93
11,20	1,630	3,000	1,370	16,17	54,66	45,34		d ₉₀ = 29,25
8,00	1,650	2,930	1,280	15,11	69,78	30,22		d ₁₆ = 4,10
4,00	1,580	2,830	1,250	14,76	84,53	15,47		d ₈₄ = 24,37
2,50	1,440	1,830	0,390	4,60	89,14	10,86		d _m = 14,92
2,00	1,520	1,620	0,100	1,18	90,32	9,68		U = 7,28
1,00	1,430	1,700	0,270	3,19	93,51	6,49		C _c = 1,91
0,25	1,300	1,850	0,550	6,49	100,00	0,00		d _{max} = 55,00

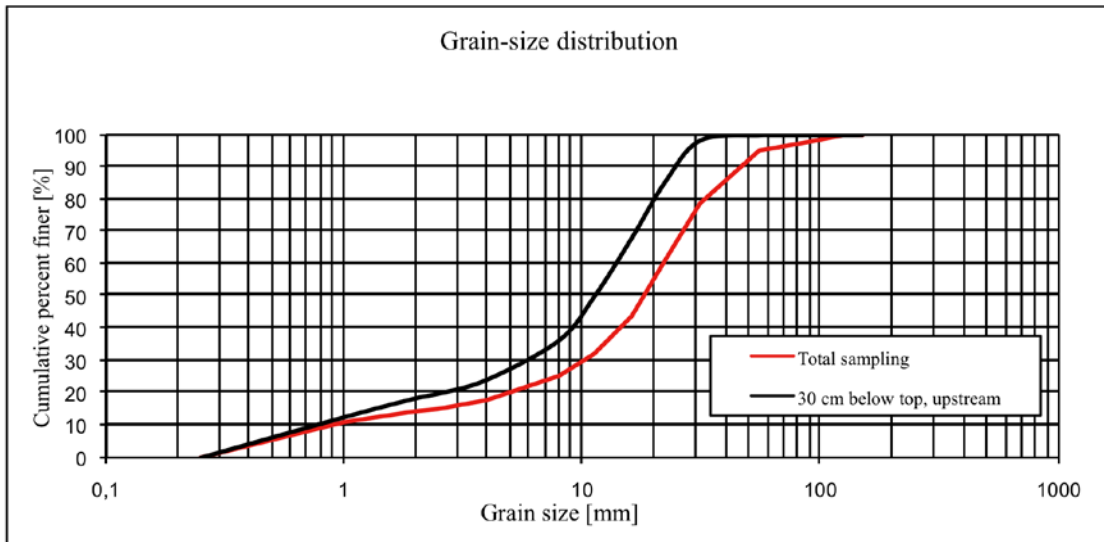


Sieve analysis: 30 cm below top, upstream

Sampling date:	16.11.2009	
Station:	Dellach	Dellach Drau
Method:	Lift trap	

Laboratory:	Bad Deutsch-Altenburg
Controller:	Hugo Seitz, Lukas Strahlhofer
Sieving date:	11.12.2009
Material condition:	dry
Net weight:	11,56 kg

Mesh width d [mm]	Sieve weight S [kg]	Catch + Sieve C + S [kg]	Catch C			Pass-through P [%]	Number Stones	Standard grain-size [mm]
			[kg]	[%]	[%]			
150,00	1,720	1,720	0,000	0,00	0,00	100,00	d ₁₀ = 0,76	
125,00	1,720	1,720	0,000	0,00	0,00	100,00	d ₂₀ = 2,53	
90,00	1,500	1,500	0,000	0,00	0,00	100,00	d ₃₀ = 5,57	
63,00	1,520	1,520	0,000	0,00	0,00	100,00	d ₄₀ = 8,78	
56,00	1,540	1,540	0,000	0,00	0,00	100,00	d ₅₀ = 11,28	
31,50	1,690	1,880	0,190	1,64	1,64	98,36	d ₆₀ = 13,78	
22,40	1,630	3,110	1,480	12,80	14,45	85,55	d ₇₀ = 16,77	
16,00	1,720	3,810	2,090	18,08	32,53	67,47	d ₈₀ = 20,20	
11,20	1,630	3,690	2,060	17,82	50,35	49,65	d ₉₀ = 25,22	
8,00	1,650	3,190	1,540	13,32	63,67	36,33	d ₁₆ = 1,50	
4,00	1,580	2,980	1,400	12,11	75,78	24,22	d ₆₄ = 21,76	
2,50	1,440	1,940	0,500	4,33	80,10	19,90	d _n = 12,41	
2,00	1,520	1,690	0,170	1,47	81,57	18,43	U = 18,24	
1,00	1,430	2,110	0,680	5,88	87,46	12,54	C _c = 2,98	
0,25	1,300	2,750	1,450	12,54	100,00	0,00	d _{max} = 45,00	

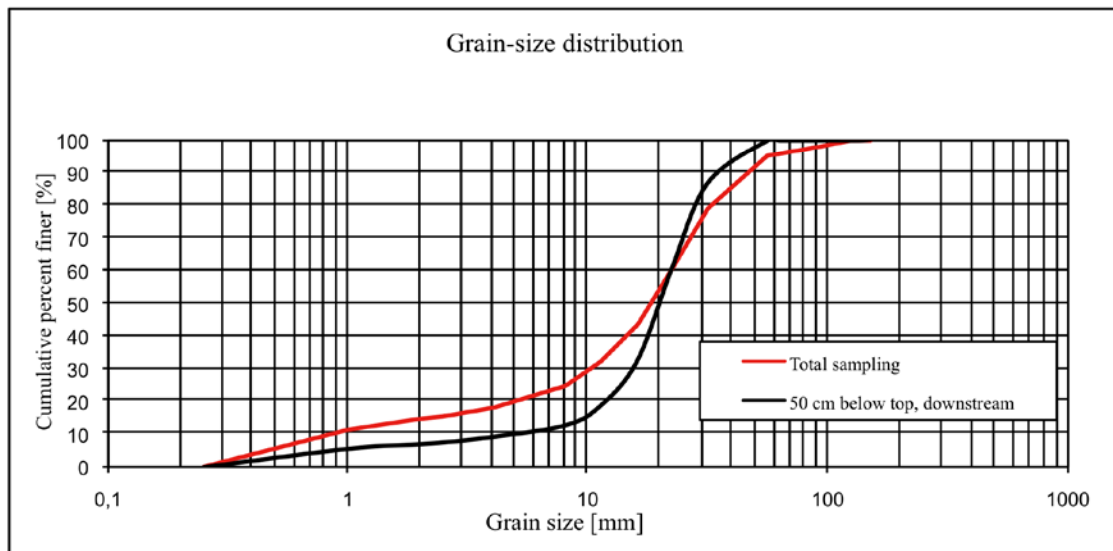


Sieve analysis: 50 cm below top, downstream

Sampling date:	16.11.2009	
Station:	Dellach	Dellach Drau
Method:	Lift trap	

Laboratory:	Bad Deutsch-Altenburg
Controller:	Hugo Seitz, Lukas Strahlhofer
Sieving date:	11.12.2009
Material condition:	dry
Net weight:	7,66 kg

Mesh width d [mm]	Sieve weight S [kg]	Catch + Sieve C + S [kg]	Catch C			Pass-through P [%]	Number Stones	Standard grain-size [mm]
			[kg]	[%]	[%]			
150,00	1,720	1,720	0,000	0,00	0,00	100,00		d ₁₀ = 4,62
125,00	1,720	1,720	0,000	0,00	0,00	100,00		d ₂₀ = 11,59
90,00	1,500	1,500	0,000	0,00	0,00	100,00		d ₃₀ = 15,00
63,00	1,520	1,520	0,000	0,00	0,00	100,00		d ₄₀ = 17,47
56,00	1,540	1,540	0,000	0,00	0,00	100,00		d ₅₀ = 19,66
31,50	1,690	2,690	1,000	13,05	13,05	86,95		d ₆₀ = 22,11
22,40	1,630	3,610	1,980	25,85	38,90	61,10		d ₇₀ = 25,19
16,00	1,720	3,910	2,190	28,59	67,49	32,51		d ₈₀ = 28,74
11,20	1,630	2,690	1,060	13,84	81,33	18,67		d ₉₀ = 36,03
8,00	1,650	2,100	0,450	5,87	87,21	12,79		d ₁₆ = 9,61
4,00	1,580	1,850	0,270	3,52	90,73	9,27		d ₈₄ = 30,30
2,50	1,440	1,570	0,130	1,70	92,43	7,57		d _m = 20,95
2,00	1,520	1,560	0,040	0,52	92,95	7,05		U = 4,79
1,00	1,430	1,540	0,110	1,44	94,39	5,61		C _c = 2,20
0,25	1,300	1,730	0,430	5,61	100,00	0,00		d _{max} = 60,00

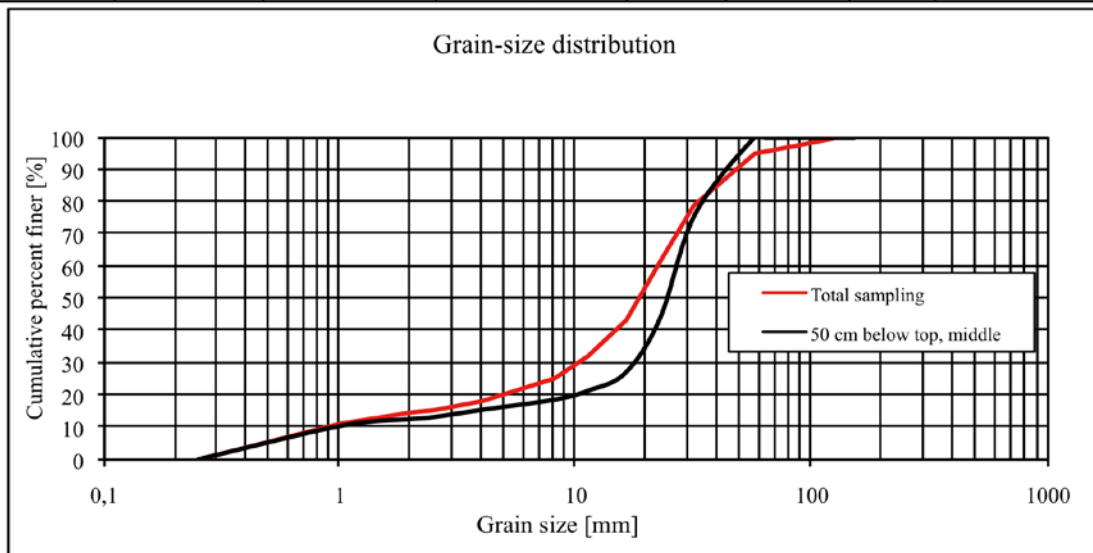


Sieve analysis: 50 cm below top, middle

Sampling date:	16.11.2009	
Station:	Dellach	Dellach Drau
Method:	Lift trap	

Laboratory:	Bad Deutsch-Altenburg
Controller:	Hugo Seitz, Lukas Strahlhofer
Sieving date:	11.12.2009
Material condition:	dry
Net weight:	9,33 kg

Mesh width d [mm]	Sieve weight S [kg]	Catch + Sieve C + S [kg]	Catch C			Pass-through P [%]	Number Stones	Standard grain-size [mm]
			[kg]	[%]	[%]			
150,00	1,720	1,720	0,000	0,00	0,00	100,00		d ₁₀ = 0,95
125,00	1,720	1,720	0,000	0,00	0,00	100,00		d ₂₀ = 9,48
90,00	1,500	1,500	0,000	0,00	0,00	100,00		d ₃₀ = 17,02
63,00	1,520	1,520	0,000	0,00	0,00	100,00		d ₄₀ = 20,76
56,00	1,540	1,540	0,000	0,00	0,00	100,00		d ₅₀ = 23,90
31,50	1,690	3,910	2,220	23,79	23,79	76,21		d ₆₀ = 26,56
22,40	1,630	4,650	3,020	32,37	56,16	43,84		d ₇₀ = 29,51
16,00	1,720	3,300	1,580	16,93	73,10	26,90		d ₈₀ = 34,52
11,20	1,630	2,140	0,510	5,47	78,56	21,44		d ₉₀ = 43,97
8,00	1,650	1,920	0,270	2,89	81,46	18,54		d ₁₆ = 4,54
4,00	1,580	1,870	0,290	3,11	84,57	15,43		d ₈₄ = 38,03
2,50	1,440	1,650	0,210	2,25	86,82	13,18		d _m = 23,78
2,00	1,520	1,580	0,060	0,64	87,46	12,54		U = 28,01
1,00	1,430	1,630	0,200	2,14	89,60	10,40		C _c = 11,50
0,25	1,300	2,270	0,970	10,40	100,00	0,00		d _{max} = 55,00

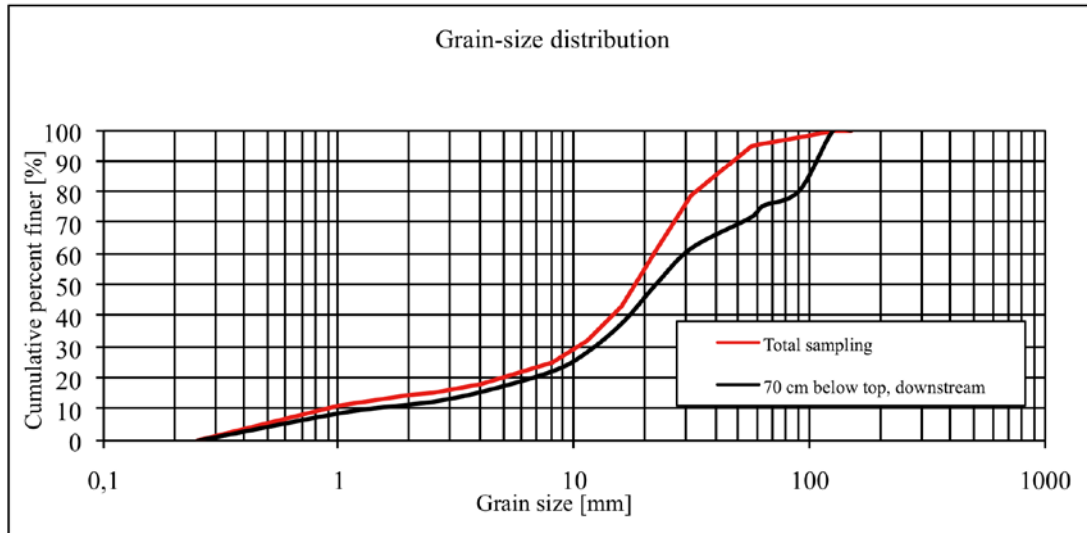


Sieve analysis: 70 cm below top, downstream

Sampling date:	16.11.2009	
Station:	Dellach	Dellach Drau
Method:	Lift trap	

Laboratory:	Bad Deutsch-Altenburg
Controller:	Hugo Seitz, Lukas Strahlhofer
Sieving date:	11.12.2009
Material condition:	dry
Net weight:	11,65 kg

Mesh width d [mm]	Sieve weight S [kg]	Catch + Sieve C + S [kg]	Catch C			Pass-through P [%]	Number Stones	Standard grain-size [mm]
			[kg]	[%]	[%]			
150,00	1,720	1,720	0,000	0,00	0,00	100,00	$d_{10} = 1,33$	
125,00	1,720	1,720	0,000	0,00	0,00	100,00	$d_{20} = 6,27$	
90,00	1,500	3,760	2,260	19,40	19,40	80,60	$d_{30} = 11,90$	
63,00	1,520	2,100	0,580	4,98	24,38	75,62	$d_{40} = 16,82$	
56,00	1,540	1,970	0,430	3,69	28,07	71,93	$d_{50} = 21,92$	
31,50	1,690	2,830	1,140	9,79	37,85	62,15	$d_{60} = 29,53$	
22,40	1,630	2,950	1,320	11,33	49,18	50,82	$d_{70} = 49,99$	
16,00	1,720	3,200	1,480	12,70	61,89	38,11	$d_{80} = 86,21$	
11,20	1,630	2,770	1,140	9,79	71,67	28,33	$d_{90} = 105,53$	
8,00	1,650	2,350	0,700	6,01	77,68	22,32	$d_{16} = 4,12$	
4,00	1,580	2,350	0,770	6,61	84,29	15,71	$d_{84} = 95,33$	
2,50	1,440	1,810	0,370	3,18	87,47	12,53	$d_m = 39,16$	
2,00	1,520	1,620	0,100	0,86	88,33	11,67	$U = 22,22$	
1,00	1,430	1,760	0,330	2,83	91,16	8,84	$C_c = 3,61$	
0,25	1,300	2,330	1,030	8,84	100,00	0,00	$d_{max} = 125,00$	

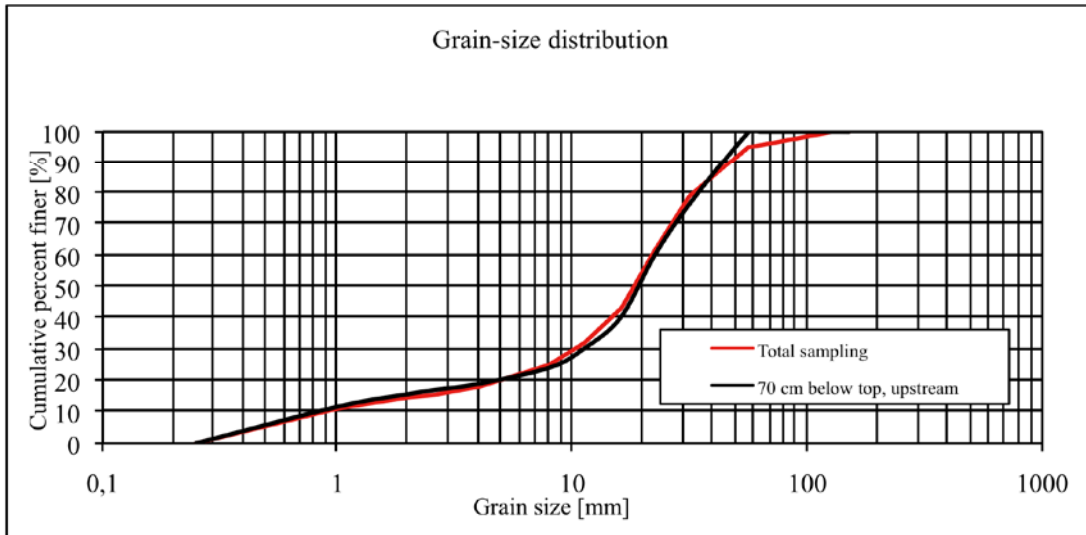


Sieve analysis: 70 cm below top, upstream

Sampling date:	16.11.2009	
Station:	Dellach	Dellach Drau
Method:	Lift trap	

Laboratory:	Bad Deutsch-Altenburg	
Controller:	Hugo Seitz, Lukas Strahlhofer	
Sieving date:	11.12.2009	
Material condition:	dry	
Net weight:	6,92	kg

Mesh width d [mm]	Sieve weight S [kg]	Catch + Sieve C + S [kg]	Catch C			Pass-through P [%]	Number Stones	Standard grain-size [mm]
			[kg]	[%]	[%]			
150,00	1,720	1,720	0,000	0,00	0,00	100,00	d ₁₀ = 0,82	
125,00	1,720	1,720	0,000	0,00	0,00	100,00	d ₂₀ = 4,52	
90,00	1,500	1,500	0,000	0,00	0,00	100,00	d ₃₀ = 10,98	
63,00	1,520	1,520	0,000	0,00	0,00	100,00	d ₄₀ = 15,82	
56,00	1,540	1,540	0,000	0,00	0,00	100,00	d ₅₀ = 18,82	
31,50	1,690	3,300	1,610	23,27	23,27	76,73	d ₆₀ = 22,25	
22,40	1,630	2,760	1,130	16,33	39,60	60,40	d ₇₀ = 27,37	
16,00	1,720	3,110	1,390	20,09	59,68	40,32	d ₈₀ = 34,15	
11,20	1,630	2,320	0,690	9,97	69,65	30,35	d ₉₀ = 43,73	
8,00	1,650	2,070	0,420	6,07	75,72	24,28	d ₁₆ = 2,10	
4,00	1,580	1,940	0,360	5,20	80,92	19,08	d ₈₄ = 37,70	
2,50	1,440	1,590	0,150	2,17	83,09	16,91	d _m = 20,92	
2,00	1,520	1,600	0,080	1,16	84,25	15,75	U = 27,24	
1,00	1,430	1,710	0,280	4,05	88,29	11,71	C _c = 6,64	
0,25	1,300	2,110	0,810	11,71	100,00	0,00	d _{max} = 65,00	

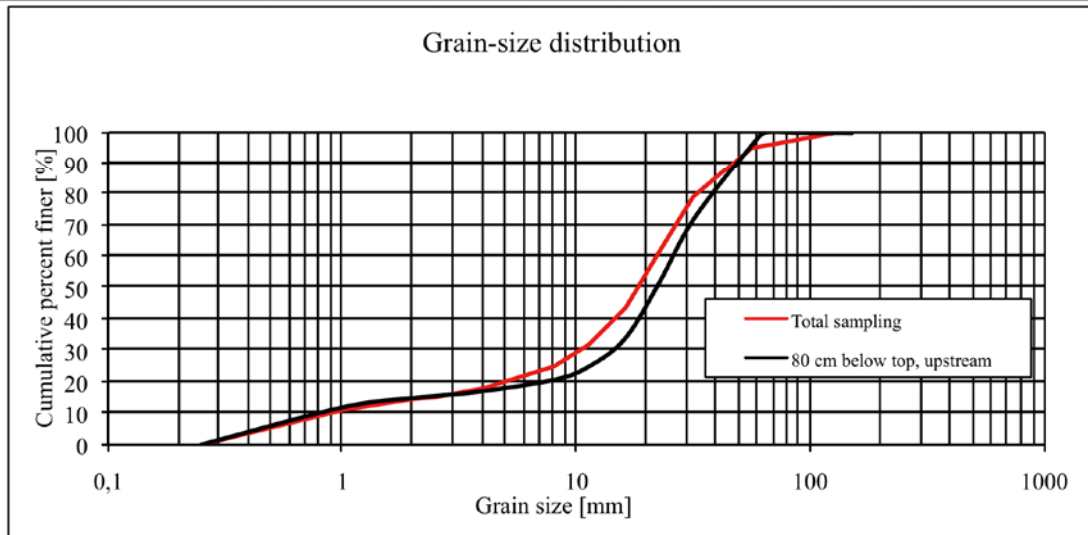


Sieve analysis: 80 cm below top, upstream

Sampling date:	16.11.2009	
Station:	Dellach	Dellach Drau
Method:	Lift trap	

Laboratory:	Bad Deutsch-Altenburg	
Controller:	Hugo Seitz, Lukas Strahlhofer	
Sieving date:	11.12.2009	
Material condition:	dry	
Net weight:	15,81	kg

Mesh width d [mm]	Sieve weight S [kg]	Catch + Sieve C + S [kg]	Catch C			Pass-through P [%]	Number Stones	Standard grain-size [mm]
			[kg]	[%]	[%]			
150,00	1,720	1,720	0,000	0,00	0,00	100,00	d ₁₀ = 0,80	
125,00	1,720	1,720	0,000	0,00	0,00	100,00	d ₂₀ = 7,02	
90,00	1,500	1,500	0,000	0,00	0,00	100,00	d ₃₀ = 13,76	
63,00	1,520	1,520	0,000	0,00	0,00	100,00	d ₄₀ = 17,99	
56,00	1,540	2,140	0,600	3,80	3,80	96,20	d ₅₀ = 21,73	
31,50	1,690	5,510	3,820	24,16	27,96	72,04	d ₆₀ = 25,77	
22,40	1,630	4,860	3,230	20,43	48,39	51,61	d ₇₀ = 30,45	
16,00	1,730	4,550	2,820	17,84	66,22	33,78	d ₈₀ = 38,07	
11,20	1,630	3,040	1,410	8,92	75,14	24,86	d ₉₀ = 48,31	
8,00	1,650	2,310	0,660	4,17	79,32	20,68	d ₁₆ = 2,90	
4,00	1,580	2,150	0,570	3,61	82,92	17,08	d ₈₄ = 41,88	
2,50	1,440	1,690	0,250	1,58	84,50	15,50	d _m = 23,78	
2,00	1,520	1,620	0,100	0,63	85,14	14,86	U = 32,12	
1,00	1,430	1,900	0,470	2,97	88,11	11,89	C _c = 9,15	
0,25	1,300	3,180	1,880	11,89	100,00	0,00	d _{max} = 75,00	

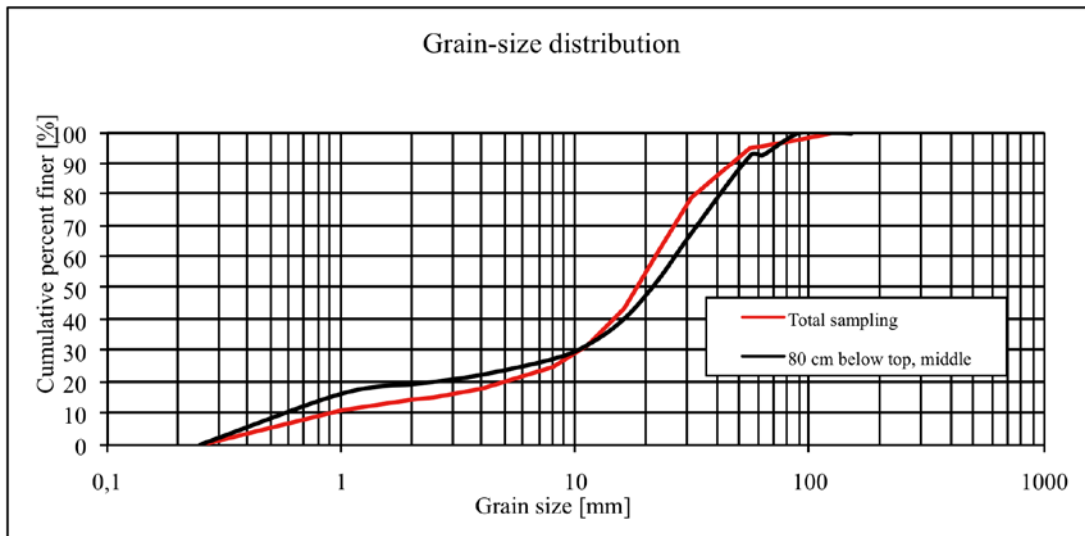


Sieve analysis: 80 cm below top, middle

Sampling date:	16.11.2009	
Station:	Dellach	Dellach Drau
Method:	Lift trap	

Laboratory:	Bad Deutsch-Altenburg	
Controller:	Hugo Seitz, Lukas Strahlhofer	
Sieving date:	11.12.2009	
Material condition:	dry	
Net weight:	14,02	kg

Mesh width d [mm]	Sieve weight S [kg]	Catch + Sieve C + S [kg]	Catch C			Pass-through P [%]	Number Stones	Standard grain-size [mm]
			[kg]	[%]	[%]			
150,00	1,720	1,720	0,000	0,00	0,00	100,00	d ₁₀ = 0,59	
125,00	1,720	1,720	0,000	0,00	0,00	100,00	d ₂₀ = 2,42	
90,00	1,500	1,500	0,000	0,00	0,00	100,00	d ₃₀ = 9,76	
63,00	1,520	2,520	1,000	7,13	7,13	92,87	d ₄₀ = 15,99	
56,00	1,540	1,540	0,000	0,00	7,13	92,87	d ₅₀ = 20,97	
31,50	1,690	5,170	3,480	24,82	31,95	68,05	d ₆₀ = 26,42	
22,40	1,630	3,820	2,190	15,62	47,57	52,43	d ₇₀ = 32,96	
16,00	1,720	3,460	1,740	12,41	59,99	40,01	d ₈₀ = 41,55	
11,20	1,630	2,780	1,150	8,20	68,19	31,81	d ₉₀ = 52,40	
8,00	1,650	2,270	0,620	4,42	72,61	27,39	d ₁₆ = 0,98	
4,00	1,580	2,280	0,700	4,99	77,60	22,40	d ₈₄ = 45,59	
2,50	1,440	1,760	0,320	2,28	79,89	20,11	d _m = 24,99	
2,00	1,520	1,630	0,110	0,78	80,67	19,33	U = 45,06	
1,00	1,430	1,860	0,430	3,07	83,74	16,26	C _c = 6,15	
0,25	1,300	3,580	2,280	16,26	100,00	0,00	d _{max} = 85,00	



Sieve analysis, 80 cm below top, downstream

Sampling date:	16.11.2009	
Station:	Dellach	Dellach Drau
Method:	Lift trap	

Laboratory:	Bad Deutsch-Altenburg	
Controller:	Hugo Seitz, Lukas Strahlhofer	
Sieving date:	11.12.2009	
Material condition:	dry	
Net weight:	13,97	kg

Mesh width d [mm]	Sieve weight S [kg]	Catch + Sieve C + S [kg]	Catch C			Pass-through P [%]	Number Stones	Standard grain-size [mm]
			[kg]	[%]	[%]			
150,00	1,720	1,720	0,000	0,00	0,00	100,00	d ₁₀ = 0,84	
125,00	1,720	1,720	0,000	0,00	0,00	100,00	d ₂₀ = 4,16	
90,00	1,500	1,500	0,000	0,00	0,00	100,00	d ₃₀ = 8,48	
63,00	1,520	1,520	0,000	0,00	0,00	100,00	d ₄₀ = 12,15	
56,00	1,540	1,540	0,000	0,00	0,00	100,00	d ₅₀ = 15,84	
31,50	1,690	3,490	1,800	12,88	12,88	87,12	d ₆₀ = 18,89	
22,40	1,630	4,040	2,410	17,25	30,14	69,86	d ₇₀ = 22,46	
16,00	1,720	4,440	2,720	19,47	49,61	50,39	d ₈₀ = 27,37	
11,20	1,630	3,510	1,880	13,46	63,06	36,94	d ₉₀ = 35,82	
8,00	1,650	2,820	1,170	8,38	71,44	28,56	d ₁₆ = 2,48	
4,00	1,580	2,850	1,270	9,09	80,53	19,47	d ₈₄ = 29,62	
2,50	1,440	1,920	0,480	3,44	83,97	16,03	d _m = 17,46	
2,00	1,520	1,670	0,150	1,07	85,04	14,96	U = 22,52	
1,00	1,430	1,920	0,490	3,51	88,55	11,45	C _c = 4,53	
0,25	1,300	2,900	1,600	11,45	100,00	0,00	d _{max} = 70,00	

